DESIGN OF ADAPTIVE PROTECTION SCHEMES FOR MICROGRIDS

A Thesis

submitted in fulfilment of the requirements for the award of the degree of

Doctor of Philosophy

in Engineering

Submitted by

Manjeet Singh
(Registration No.: 901504004)

Under the supervision of

Dr. Prasenjit Basak
(Associate Professor)

Department of Electrical and Instrumentation Engineering

THAPAR INSTITUTE OF ENGINEERING AND TECHNOLOGY
(Deemed to be University)
P. O. BOX 32, BHADSON ROAD, PATIALA, PUNJAB – 147004, INDIA

www.thapar.edu

September 2020

CERTIFICATE

This is to certify that the thesis entitled **"Design of adaptive protection schemes for microgrids"** being submitted by Mr. Manjeet Singh to the Department of Electrical & Instrumentation Engineering, Thapar Institute of Engineering & Technology (Deemed to be University), Patiala, Punjab, India for the award of the degree of **Doctor of Philosophy**, is a record of bonafide research work carried out by him under my guidance and supervision and has fulfilled the requirements for the submission of this thesis, which to my knowledge has reached the requisite standard.

The results embodied in the thesis have not been submitted in part or full to any other Institute or University for the award of any diploma or degree.

Dr. Prasenjit Basak
Associate Professor
Department of Electrical & Instrumentation Engineering,
Thapar Institute of Engineering & Technology (Deemed to be University),
Patiala, Punjab, India

ACKNOWLEDGEMENTS

I would like to extend thanks and gratitude to the many people, who so generously contributed to the work presented in this thesis. I honestly feel short of words to acknowledge all those who helped me directly and indirectly during this research work.

With due regards and great delight, I convey my heartful gratitude and indebtedness to my supervisor **Dr. Prasenjit Basak**, Associate Professor, Department of Electrical & Instrumentation Engineering, Thapar Institute of Engineering & Technology (Deemed to be University), Patiala for skilful guidance, persistent encouragement, proficient evaluation and conscientious supervision throughout this academic endeavour. He was always available to help me with utmost care, kind attention and prudent suggestions during odd hours of the job. His hard working, polite nature and methodical suggestions were a constant source of encouragement to me. It is owing to his guidance, expertise, inquisitive attitude and tireless efforts apart from his working hours that I find my vision even more broadened. I earnestly thank him from the core of my heart for being a consistent source of inspiration right through the beginning till the end.

I am very thankful to **Dr. Mukesh Singh**, Associate Professor, Department of Electrical & Instrumentation Engineering, **Dr. Parag Nijhawan**, Associate Professor, Department of Electrical & Instrumentation Engineering and **Dr. Prashant Rana**, Assistant Professor, Department of Computer Science Engineering, for being the member of Doctoral Committee and spending their valuable time in reviewing and critically examining the work.

I am also thankful to present Chairman of the Doctoral Committee **Dr. R. S. Kaler**, Senior Professor & Head, Department of Electrical & Instrumentation Engineering for the much-needed support throughout the work.

My heartfelt gratitude is due to **Dr. Rafat Siddique**, Senior Professor & Dean, Research and Sponsored Projects and Honourable Director **Dr. Prakash Gopalan** for the support, encouragement and providing the necessary facilities to carry out and complete this work on steady course.

I also wish to express my deep sense of gratitude to all the faculty and staff members, particularly **Dr. Mandeep Singh** Professor, Department of Electrical & Instrumentation Engineering, **Dr. S.K.**

Jain Professor, Department of Electrical & Instrumentation Engineering, **Ms. Manbir Kaur** Associate Professor, Department of Electrical & Instrumentation Engineering, **Dr. Souvik Ganguli**, Assistant Professor, Department of Electrical & Instrumentation Engineering and all the persons who with their encouraging and caring words, constructive criticism and suggestions have contributed directly or indirectly in a significant way towards completion of this research work. My deepest appreciations are due to the research scholars under the supervision of **Dr. Prasenjit Basak**. They have always stood by me in all difficult times and reinforced my confidence. Their never-ending support is a constant source of motivation and always keeps me going.

I bow with gratitude for my parents, who are the most precious persons in my life and without their efforts I would have not achieved this milestone.

I express my gratitude to all those, with whom I have worked, interacted and whose thoughts have helped me in furthering my grasps and understanding of the work.

Last but not the least, I bow in reverence to **ALMIGHTY GOD** who has always showered blessings on me at each and every step to complete this thesis.

Manjeet Singh

ABSTRACT

With the integration of small energy sources that can feed loads independently constitutes a microgrid. If those small energy sources or distributed generators (DGs) are of different nature like photovoltaic or wind or any other types of distributed energy source; then that microgrid is termed as hybrid microgrid. After the integration of DGs into the existing system, the conventional protection schemes may fail to provide reliable operation. The dynamic behavior of microgrid system under faulty conditions makes adaptive protection a general necessity for reliable microgrid operation. In design of adaptive protection, the grid-connected and islanded modes have immense importance including grid-connected mode without DGs in microgrid. In this thesis, a new adaptive protection scheme is proposed based on the above-mentioned modes of microgrid operation. The proposed method considers nature of DGs connected, fault location detection and fault nature identification based on quadrature and zero sequence components of fault current considering impact of X/R ratio of DGs. The proposed methodologies for adaptive protection schemes are verified in Matlab-Simulink environment and the results are found to be satisfactory while various faults are simulated at different nodes of the microgrid model. At the time of verification of effectiveness of the proposed methodologies, the time derivative of quadrature and zero-axis components of fault current are considered sufficient to instantaneously detect the fault location and fault nature in microgrid system.

Types I, III and IV wind distributed generators have a different and wide range of current sharing capacity during the fault occurrence. For the design of the proper protection scheme in a hybrid microgrid, it becomes important to study different wind distributed generators. In a hybrid microgrid consisting of single and doubly-fed induction generators and photovoltaic distributed generators, the fault current in a feeder shows different behavior which changes as per the type of distributed generators and grid/islanded connection of microgrid operation. Based on the type of wind and photovoltaic distributed generators, a provision of a new adaptive protection scheme should be the primary concern for updating the relay settings as per the change like distributed generators, a distance of the fault from the point of common coupling and nature of the loads in the microgrid system. The q0 components of fault current are used for detecting the low X/R ratio of distributed generators, modes of operation, transient reactance during the series and shunt faults in a hybrid microgrid. The novel contribution in this part of research work is the implementation

of a fuzzy-based adaptive protection scheme through analysis of the q0 components. In addition, the relay current shared by different distributed generators is derived for the q0 components in terms of the transient's component is another contribution. Considering q0 components and transient reactance, a new relation between the relay current settings and modes of operation has been identified for adaptive relaying. The effectiveness of the proposed adaptive protection scheme for the hybrid microgrid is verified through a simulation case study using Matlab–Simulink software.

In a Hybrid microgrid, the overcurrent relays sense the changes in the fault currents while the microgrid switches from the grid-connected to islanded mode of operation. Further, for the different types of distributed generator, such as PV, Wind turbines of types I, III, and IV; the variation in fault currents are detected by the relays. This leads to delays and inappropriate coordination in conventional protection schemes. In this thesis, an adaptive protection scheme with optimal settings is proposed for phase and earth fault detection. It also takes care of different nature of distributed generators (DGs), all feasible operating modes of hybrid microgrid with only q component of fault current while zero component is used to differentiate between earth and phase faults. Also, a new strategy is proposed that optimizes the coordination time of fuses as a backup to primary and backup relays with new coordination time interval constraints. A differential evolutionary algorithm is proposed for determination of optimal settings for the directional overcurrent relays.

TABLE OF CONTENTS

LIST OF FIGURES

LIST OF TABLES

LIST OF ACRONYMS

µPMU	Micro Phasor Measurement Units
AA	Adaptive Auto
AC	Alternating Current
ADAS	Advanced Distribution Automation System
AI	Artificial Intelligence
AMFA	Adaptive Modified Firefly Algorithm
ANM	Active Network Management
ANN	Artificial Neural Network
BESS	Battery Energy Storage Systems
CCT	Critical Clearing Time
CERC	Central Electricity Regulatory Commission
COA	Cuckoo Optimization Algorithm
CT	Coordination Time
DC	Direct Current
DDSE	Distributed Dynamic State Estimation
DERs	Distributed Energy Resources
DFIG	Doubly Fed Induction Generator
DGs	Distributed Generators
DICOPT	Discrete Continuous Optimizer
DOUFR	Digital Over and Under Frequency Relay
DSRF	Double Synchronous Rotating Frame
DT	Detection Time
ESS	Energy Storage System
ESUs	Energy Storage Units
FACTS	Flexible Alternating Current Transmission System
FCL	Fault Current Limiter
FPGA	Field Programmable Gate Array
FRT	Fault Ride Through
GA	Genetic Algorithm
GAMS	General Algebraic Modeling System
GHz	gigahertz

GW	gigawatts
HHT	Hilbert Huang Transform
HSA	Harmony Search Algorithm
HVDC	High Voltage Direct Current
IBDG	Inverter Based Distributed Generators
IEC	International Electrotechnical Commission
IEEE	Institute of Electrical and Electronics Engineers
IIDGs	Inverter Interfaced Distributed Generators
kVA	kilovolt-ampere
kvar	kilovar
kW	kilowatt
L1PV	Load1 of Photovoltaic DG
L1W	Load1 of Wind DG
LG	Line to Ground
LL	Line to Line
LLG	Line to Line to Ground
LLL	Line to Line to Line
LLLG	Line to Line to Line to Ground
LN	Location and Fault Nature Matrix
LOM	Loss-of-Mains
LP	Linear Programming
LPS	Lightning Protection Systems
LT	Low Tension
LV	Low Voltage
LVRT	Low Voltage Ride Through
MCPU	Microgrid Central Protection Unit
MG	Microgrid
MGCC	Microgrid Central Controller
MHW	Morphological Haar Wavelet
MINLP	Mixed Integer Nonlinear Programming
MPPT	Maximum Power Point Tracking
MV	Medium Voltage
MVA	megavolt-ampere

MW	megawatt
NITI	National Institution for Transforming India
NLPP	Non-Linear Programming Problem
NSQ	Negative Sequence
OCR	Over Current Relay
OT	Operation Time
PC	Protection Coordination
PCC	Point of Common Coupling
PCO	Protection Coordination Optimization
PI	Proportional Integral
PID	Proportional Integral Differential
PMG	Permanent Magnet Generator
PMSG	Permanent Magnet Synchronous Generator
PQ	Power Quality
PS	Plug Setting
PSERC	Punjab State Electricity Regulatory Commission
PSM	Plug Setting Multiplier
PSO	Particle Swarm Optimization
PSQ	Positive Sequence
PV	Photovoltaic
PVG	Photovoltaic & Grid
PVI	Photovoltaic Islanded
ROCOF	Rate of Change of Frequency
SCIG	Squirrel Cage Induction Generator
SG	Synchronous Generators
SIPS	System Integrity Protection Scheme
SSCB	Solid State Circuit Breakers
SSUFCLs	Solid-State Unidirectional Fault Current Limiters
TDS	Time Dial Setting
THD	Total Harmonic Distortion
TSM	Time Setting Multiplier
VSC	Voltage Source Converter
VSG	Virtual Synchronous Generators

VTDPS	Variable Tripping Time Differential Protection Scheme
WDG	Wind Distributed Generator
WECSs	Wind Energy Conversion Systems
WG	Wind & Grid
WGs	Wind Generators
WI	Wind Islanded
WiMAX	Worldwide Interoperability for Microwave Access
WPV	Wind & Photovoltaic
WPVG	Wind Photovoltaic & Grid

Chapter 1

Introduction and Literature Survey

Introduction

The continuous developments in our society are directly or indirectly dependent on the sustainability of energy. We must switch over to renewable energy resources gradually to eliminate the dependency of the current energy chain on conventional fossil fuel combustion-based energy resources and to protect the natural reserves. The continuous development of human civilization is directly or indirectly dependent on the sustainability of electrical power generation technology which is possible through proper utilization of renewable energy resources. In modern power scenario, the electrical energy is extracted from renewable energy sources which are also known as distributed energy resources (DERs) in the microgrid systems. When microgrid is integrated with conventional power system, the integration of distributed generators (DGs) into existing network needs modified control and protection strategies to be incorporated in interconnected power system to meet the high-end challenges aiming smooth operation.

To fulfil the goals set by the National Institution for Transforming India (NITI) Aayog, it is of utmost importance from Indian power system perspective that proper installation of technologies is required to extract more renewable energy from DERs. This needs advancement in microgrid technology to achieve 175 giga watts (GW) of renewable energy by 2022 [1]. Problem arises when abnormal condition persists on grid or on microgrid end, so the protection device settings that are dedicated for microgrid system must change accordingly as compared to conventional protection schemes. The integration of DGs into existing network system needs modification to the traditional protection practices to meet the high-end challenges introduced because of DGs connected downstream [2]-[3].

Problem may occur in the coordination among different protective equipment on grid side or on microgrid side. When fault occurs in a conventional power system, it is fed from generating side and feeding of fault current is said to be unidirectional. But, in case of utilities being integrated with microgrids, another situation comes forth where fault is fed from both sides in the form of flow of bidirectional currents that makes the faulty conditions more complex [4]-[5]. Microgrid can operate in different modes that are grid connected, islanded or only grid connected (conventional connections). Microgrid operation also faces challenges due to variability in nature

of DERs [6]-[7]. The main protection scheme that operates in DER integrated system should operate within the 1-3 cycles of fault current as system consists of low reactance and low inertia. For the proper distribution of electrical energy supplied to consumers, guidelines are set as recommended in [8].

At present photovoltaic (PV) and wind power plants are considered as the main DGs. But, these two kinds of DGs have totally different characteristics when they are integrated with existing utility side or operated in islanded mode. In Indian energy scenario, electrical distribution system has much potential for PV DGs, because of abundance of solar irradiance in plains. In similar manner, due to abundance of solar irradiance for PV DGs and wind speed for wind DGs along coastal line, there is vast scope of different nature of DGs to generate power in the form of PV and wind assisted hybrid microgrid catering load demands. But this will lead to complete modification of existing protection relays as wind speed and irradiance are not fixed and affect microgrid's mode of operation which will further affect the change in voltage, current, frequency, and impedance of the system.

The operation of relay is initiated based on change in voltage, current, frequency, and impedance of network system which may lead to maloperation of relays. To avoid this situation, proper new adaptive protection schemes are to be proposed that can change relay settings based on change in mode of operation. The types of faults which are normally studied for analysis of microgrid protection are line to line (LL), line to ground (LG), line to line to ground (LLG), line to line to line (LLL) and line to line to line to ground faults (LLLG). High impedance and low impedance faults are studied separately as there is variation in fault current because of DGs presence in downstream of the network as compared to other short circuit faults. In present research scenario of microgrid, the recommended protection strategies are differential protection, distance protection, voltage protection, external device protection, over current protection with symmetrical components or phase sequence components with adaptive settings. The majority of the above protection schemes for microgrid protection are dependent on the microgrid architecture and that affects the relay operation.

The main issues that arise in microgrid protection are selection of protection devices, switches, false tripping, re-synchronization, nature of faults during grid-connected mode, faults in islanded mode, anti-islanding protection and role of microgrid control architecture in protection. Main features of microgrid protection are peer to peer with plug & play concept, protection against

bi-directional feeding, sensitivity to reduction in fault current capacity, no disruption in fault detection and protection sensitivity. One of the reliable protection schemes is the adaptive protection that can promptly act according to the different configurations of microgrid operation. Inverter interfaced DGs tend to have less impact since the magnitude of the short circuit currents are low compared to conventional synchronous generators.

Adaptive protection is a continuous online protection that keeps on improvising according to modes of operation, different conditions, and requirements. In adaptive relaying, the impacts of overloading and load shedding are to be considered while designing for adaptive relay. Most of the research on microgrid protection with adaptive settings that have been reported are based on measurement of three phase voltages and currents. Further, based on change in three phase voltages and currents; positive, negative and zero sequence components of voltage and current are used to implement protection schemes. The recent research on ac microgrid protection are reported based on modification in fault current level, device discrimination, reduction in reach of impedance relays, reverse power flow, sympathetic tripping, islanding, single phase connection and selectivity.

A few research have been reported for protection strategies using static components that are dq components of fault current, but zero component was neglected corresponding to earth faults [6] - [10]. To study plug and play model of microgrid structures, DGs could be connected at any location of existing power system. So, impedance and voltages are found as variable at each location. To minimize this impact, steady state components such as q0 are measured for fault detection. These two components q and 0 are found to be enough to identify fault, its location and nature of DGs.

Based on Indian domestic load scenario and as per Punjab State Electricity Regulatory Commission's (PSERC) guidelines on "Conditions of Supply"; the number of microgrid structures are designed with the integration of synchronous generator (with low X/R ratio), PV and wind DG to existing grid [8]. An adaptive protection scheme may be proposed based on q0 components omitting 'd' component of fault current to protect a microgrid with optimum adaptive protection coordination settings. Most of the research have been reported for series faults where lightly loading of phases including the condition of single phasing are not considered for adaptive protection.

1.1. Literature survey

Throughout the world, research are going on for advancements in microgrid technology. India's NITI Aayog has also set a target to achieve 175 GW of renewable energy-based generation capacity by 2020 [1]. The issue of protection is also getting priority in the microgrid research. Whenever a protective device (relay and circuit breaker) is present near any fault in the power system, it acts to remove the fault keeping the healthy part of the circuit working uninterruptedly. This activity must be provided to the protective device with the discrimination features accordingly [2]. When a large number of converter-based DERs are connected in microgrid, the fault currents are of only two to three times the full load current or even less, depending on the control methods of converter [3]. In general, three methods are used as discrimination features for relays; such as time, comparison and magnitude. Conventional protection techniques for distribution system are provided based on radial and ring-main nature of distribution network, mainly consisting of fuses and reclosers in addition to the relays [4]-[5].

1.1.1. Microgrid protection

The challenges in the microgrid technologies are in microgrid structure planning; setting the type of DGs, availability of DERs to get maximum benefit of the renewable energy. So, there is need of proper planning, proper study on potential of DERs to meet integration and protection related challenges [6]. The adaptive protection scheme is the latest trend in microgrid protection. It can be set for centralized or decentralized control approaches with different communication architectures required for each. The centralized control architecture is the conventional method used for adaptive protection where a central controller coordinates with protection settings. If central controller fails there is total loss of adaptive protection and therefore, redundancy is must in central controller [7].

The DG connected utility side grid must have protection methods that can make DGs to stop supplying power to the utility grid if the voltage or frequency at point of common coupling (PCC) between the customer and the utility are beyond specified limits or if there is a fault on utility or microgrid side [8]. Based on capital investment and long-term operation of DGs, cost of energy is calculated for optimal designing of microgrid [9]. For proper distribution of electrical energy among consumers conditions are set for suppliers as referred in [10]. The adaptive method, proposed in [11], uses online and offline methods which could also be done through online method

for load flow and type of fault and also using communication link between all sources to check system faults promptly without using any iteration. Depending on the severity of faults, particular zone should be isolated from rest of the network based on the method of discrimination and completely blocking the faulty part of the power system [12].

Main concern for conventional relaying is bi-directional feeding by utility and DGs. In conventional methods, only grid-connected mode is present, but in microgrid architecture; grid connected, DG connected and both connected modes are present. The conventional overcurrent (OC) protection devices are usually set to operate at two to ten times the full load current because of high X/R (reactance/resistance) ratio [13]. The very first step of microgrid protection is to isolate the system from utility during disturbance and protection of microgrid loads. Deciding factors that affect microgrid protection are mode of operation, presence of downstream DGs, bidirectional nature of fault current, in-feed of fault current, inverter interfacing, location and nature of fault. Due to drastic reduction of fault current level (with low X/R ratio), the time-current coordination of OC protective devices is disturbed, whereas fuses and reclosers cannot detect directional constraints for which adaptive methods are proposed for use in online and offline methods based on communication link among all sources to check system faults [11], [14].

The use of adaptive protection scheme increases the reliability of microgrid system. Extensive communication-based adaptive protection can work based on fault current coefficient and DGs impact factor [15]-[16]. A knowledge-based wide-area differential current protection scheme was proposed to meet the dynamics of the microgrid [17]. However, real time implementation of this scheme may not be realistic in actual power system as it is going to be very much expensive and complex. Since measurement at tee connected sources and loads are required. Advanced metering infrastructure networks which can operate as per IEEE standard 802.16 based Worldwide Interoperability for Microwave Access (WiMAX) wireless networks are cost effective, need less maintenance and considered as must in smart grids [18]. Microgrid management center-based protection and reconfiguration during changing condition is also presented in [19] where adaptive protection method based on information exchange among different protection devices is used.

Most of the communication-based protection schemes presented are based on International Electrotechnical Commission (IEC) standard IEC 61850. An IEC 61850 and IEC 61850-7-420 switched based ethernet network has been used as a viable implementation model for fault current

impact coefficient based adaptive protection system as referred in [20]-[21]. A less sensitive adaptive hybrid microgrid protection system, based on traditional differential microgrid protection scheme using communication via microgrid central protection unit (MCPU) is implemented in [22]. During change in operation mode, load flow changes as impedance changes and traditional settings of relays are adaptively selected. The DGs impact on these settings of under reach is compensated as referred in [23]-[24]. Measurement of fault currents are possible based on three-phase voltage and current measurements [24]. Magnitude and directions of positive-sequence component are used for location detection in [25]. A new fuzzy rule-based protection scheme using s-transforms and time–frequency contours is proposed in [26]. In this approach, phase wise and zero sequence differential features are estimated.

A new OC protection scheme with a synchro phasor-based frequency selective technique for low inertia microgrid is proposed in [27]. Here, three-phase root mean square (r.m.s.) currents as well as the frequency are required to be measured. Depending on the accessibility of protection device settings or PV control parameters, the proposed method modifies the existing characteristic curve of OC devices or limits the output current of PV sources, respectively. The proposed strategy does not change the structure of existing distribution network protection system and can also be implemented in the old and non-programmable relays. Phase wise current measurement is must in this approach [28]. The proposed method uses the detail signal of Morphological Haar Wavelet (MHW) obtained after prediction lifting for fault detection and faulty phase selection. Accordingly, current retrieved from both ends of the feeder are processed through MHW after prediction lifting scheme to obtain the detail signals. The detail signal difference and their norms are calculated to obtain a primary protection scheme for the feeder [29]. This is complex and requires three-phase current measurements.

Hilbert Huang Transform (HHT) technique is used to process non-stationary signal (differential current) whose spectral energy content is computed and the difference in energy content of time–frequency contour of signals is indicated to find the faulty condition in grid-connected and islanded mode microgrid operation with PV and wind energy as DGs [30]. It is a time-consuming process and requires three-phase measurements. The proposed scheme pre-processes the fault current and voltage signals using discrete fourier transform and estimates the most affected sensitive features at both ends of the respective feeder [31] which needs measurement of three-phase currents and voltages at all ends for fault detection. The microgrid

primary and back-up protections are taken into consideration at each level for grid-connected and island modes. The plug and play characteristics, time constraints of low-voltage ride through and unbalanced faults are considered for DGs which again needs measurement of three-phase voltages and currents [32].

The study presented in [33] is a novel microgrid protection scheme based on HHT and machine learning techniques. The method needs measurement of three phase voltages and currents for successful operation. An adaptive directional OC relaying technique based on the positive-sequence and negative-sequence superimposed currents is proposed for microgrid protection which needs superimposition of three-phase sequence components [34]. Protection scheme measure the changes as per the change in phase voltages and currents [35]. An adaptive OC protection scheme based on the integration of technical and economic advantages of fuses and relays is set for microgrid structure. Fuse relay based adaptive OC protection is only for feeders not for DG and load side [36].

The distributed dynamic state estimation (DDSE) based protection scheme is used as setting-less component protection with real-time measurements and dynamic models of the component which is complex and time consuming [37]. In this reference, the multi-ring structure microgrid is protected by a proposed multi-function monitor. The proposed method used is based on three-phase voltage and current measurements from both ends of the line for the determination of fault and its location [38]. Second-order derivative of line current during faulty condition is utilized to extract wavelet features for extracting energy content to identify fault in low-voltage DC microgrids [39]. For a given synchronous machine direct and quadrature axes current components are obtained from stator flux linkages are shown below as referred in [40].

X_d is calculated from maximum armature terminal voltage per phase and minimum armature current per phase whereas, X_q is calculated from minimum armature terminal voltage per phase and maximum armature current per phase. It could be concluded that the quadrature axes current component corresponding to X_q is greater than direct axes current component corresponding to X_d during transient conditions [41]. In general, for the study of voltages and currents in DG integrated microgrids, transformation of AC three-phase to static components dq0 that are independent of time is done using Park's transformation as referred in [42]. Also, a nature (type of DG) governing constant is proposed to derive the role of different generation in adaptive protection study of microgrid, whereas the authors in [43] have worked about data sharing through

wireless based WiMAX for adaptive protection. The impact of communication delay and relay hierarchy are also discussed in this reference.

Also, in [44], Prims- Aided Dijkstra's algorithm is used for fault detection which runs after isolation from utility grid for which there is delay in fault location detection. If the microgrid is not islanded then Prims-Aided algorithm will not be successful in fault detection, hence reliability of system will be affected. A time-domain signal processing tool is used to get accurate and reliable signal component extraction based on MHW to detect faults in microgrid [45]. Feed currents retrieved from both ends are processed using MHW to obtain the detail signals. These are used to obtain a primary protection scheme for the feeder and same scheme was investigated for backup protection in islanded and grid-connected mode of operation for radial and looped system for various disturbances which is a time consuming and complex process.

The voltage and current characteristics for different faults are studied for Types I, III and IV wind generators operated in islanded and grid connected modes. For this system, a reliable protection schemes with different relay settings are proposed based on three-phase voltage and current characteristics [46]. A technique using differential current is proposed for accurate fault detection and its distance calculation, only for PV (DC) microgrid [47]– [48]. A directional distance element scheme based on dq components only in terms of sequence components is proposed for the fault current sensing within a PV power plant under different mode of controls. Considering synchronous generators with low X/R ratio and PV based generators (low inertia), adaptive protection schemes are proposed. It is observed that more is the number of variables considered, more complex is the circuitry [49] - [50]. An adaptive protection scheme for Type-III doubly fed induction generator (DFIG) based wind DGs, using machine learning, is proposed for microgrid protection [51].

Micro phasor measurement units (μPMU) are used for voltage and current measurement in protection scheme proposed in [52]. Collector line (35 kV) protection of DFIG based wind DGs is proposed in [53]. Considering coordination standard IEC 60255-151:2009, using different time setting multiplier (TSM) and plug setting multiplier (*PSM*) values for different faults, a new protection coordination strategy is proposed for off-shore wind DFIG based DGs [54].

A study carried out at 35 kV using IEC 61850 goose wide area protection scheme is proposed for DFIG based microgrid [55]. System integrity protection scheme (SIPS) which uses communication channel, is implemented for distribution system as reported in [56]. Based on

change in I_d and I_q components of fault current on stator and rotor side, differential protection scheme is proposed only for the protection of type – III DFIG [57]. Frequency based protection coordination scheme is proposed for DFIG based wind DGs and PV DGs feeding load together. In this work, most of the load is shared by the utility that minimizes the dependency on renewable energy or proper protection study [58].

Low voltage ride through (LVRT) capability is studied based on I_d and I_q components of current of type - III wind DGs without I_0 component being taken into consideration [59]. Based on communication channel, centralized protection coordinator and several distributed protection relays are operated using change in sub-synchronous impedances during fault condition as compared to steady state [60]. Adaptive distance relaying is proposed based on positive and negative sequence impedances only for earth faults [61]. A new distance protection is proposed for wind based DGs based on sequence impedances for offshore plants [62]. For protection coordination, the multi-agent with primary, backup and bus protection layers based on a variable tripping time differential protection scheme (VTDPS) is proposed for microgrid protection. This scheme is capable of operating in both grid-connected and islanded condition where the three-phase current and voltage are measured in offline mode [63].

In PV microgrid design, inverter control is provided using double synchronous rotating frame (DSRF) for the more flexible fault-ride-through (FRT) control. The inner-loop current control uses the regulators under a DSRF and the outer-loop voltage control regulates the dc-link voltage to realize maximum power point tracking (MPPT) as reported in [48]. Type I wind generator based on squirrel cage induction generator (SCIG), converters of DFIGs (type III and IV) are modeled as referred in [64].

Different network topologies are considered with the optimal relaying action using mixed integer nonlinear programming [65]. But they did not consider the impact of the different nature of DGs, low inertia and transient reactance in the protection scheme which are investigated in this research work as a contribution. So, the protection scheme based on symmetrical components as discussed in [66] is proposed for wind DGs.

Fault model of inverter interfaced distributed generators (IIDGs) is considered based on positive and negative sequence components of voltage and current [67]. A stochastic model, based on three phase voltages and currents to simulate the challenges existing in current protection schemes, is designed for microgrids. It has been investigated for reliability performance of a

weather dependent microgrid in an abnormal operating condition [68]. In [69]; six variable-based voltage–current behaviour is investigated for faults that occur in grid-connected mode of wind energy systems. Microgrid central controller (MGCC) uses change in three phase voltages and currents to trip relay in centralized adaptive protection based on ModBus [70]. If MGCC fails then no backup protection can be provided which is a drawback of the scheme. Generally, μPMU are used for measurement to implement protection scheme using voltage and current measurement [71]. An adaptive protection scheme proposed in [72] involves three phase dependent feeder currents and voltages.

A harbour grid is designed with facility of battery charging for modern vessels with capability to supply onshore power [73]. The rate of change of frequency (ROCOF) based protection for the performance enhancement of loss-of-mains (LOM) with multi-generator power islands in presence of virtual synchronous generators (VSG), synchronous generators (SG) and inverter interfaced PV DGs is proposed in [74]. Based on non-synchronized low voltage measurement using voltage sequence components, a protection scheme is proposed in [75]. An adaptive overcurrent protection scheme with IEC 61850 communications system is proposed which adapts the settings during islanding operation [76].

For wind power plants, a distance protection scheme with adaptive boundaries is proposed for line protection [77]. An artificial intelligence (AI) based adaptive auto (AA) reclosing algorithm is proposed for DFIG-based wind power plant [78]-[79]. An advanced distribution automation system (ADAS) method is used for changing adaptive relay setting for distribution systems with wind generators (WGs) [80]. In similar manner, an adaptive distance protection scheme for shunt- flexible alternating current transmission system (FACTS) compensated line wind power plant is proposed as reported in [81]. In most of the topologies that are proposed till date, the three different types of wind generators are simulated but the faults are sensed based on measurement of three - phase voltages and currents [82]. Also, a zone partitioning protection strategy for DC systems incorporating offshore wind farm is proposed based on dc components of current [83]. A new approach for voltage source converter of high voltage direct current (HVDC) system using μ synthesis analysis based on three phase voltage components is proposed [84]. A new model based on negative sequence quantities on the wind turbine control is proposed to simplify protection model [85]. In [86], using dq components of current; a new method for managing the responses of multiple digital relays employed in interconnected permanent-magnet

generator (PMG) based wind energy conversion systems (WECSs) with battery storage is proposed.

An optimization-based design of protective devices under varying PV penetration levels and under different PV interface connections is proposed such that proper coordination is achieved for the entire feeder under all operating conditions, corresponding to both fuse-clearing and fuse-saving schemes [87]. An adaptive offline and online protection technique based on voltage profile as a pre-fault index for current waveform to efficiently modify the protection settings before the fault occurrence is proposed in [88]. Unlike the existing classifier-based approaches involving single classifier, the ensemble-based approach is insensitive to the biasness of individual classifier and dimension/size of dataset [89]. A proposed multistage morphological fault detector analyzes sudden change in fault current magnitude as referred in [90], in which a complex technique is discussed. The PV based DGs in grid connected mode are investigated for voltage-current behaviour during faults in [91].

In [92], frequency-based relay protection for an isolated microgrid is proposed, where voltage source converter (VSC) power source provides output with variable frequency current during the short circuit on transmission line and change in frequency decides how far is the fault from relay. In [93], for LVRT under grid faults and grid support service; the capability of three mainstreams single-phase transformer-less PV inverters is explored. Setting up of lightning and surge protection in large-scale PV plants is new to PV protection. In [94], methods for assessing the external lightning protection and earthing designs that may be installed in large-scale solar applications are discussed. Fundamental design principles of external lightning protection systems (L.P.S) and earthing systems for largescale PV systems are also discussed. An adaptive scheme for overcurrent relays based on negative and positive sequence components superimposed is implemented in [95].

Low harmonics components are extracted by digital relay to detect faults in inverter fed DGs [96]. Harmonic amplification factor is used for islanding detection referred in [97]. OC based relays with same settings in looped microgrid fault are set to detect fault by indirect measurement of impedances. The DERs closest to fault will inject more current and with the help of V_d and V_q, the faulty part can be detected [98]. Voltage angle and magnitude-based classifier based on sequence components during faulty condition, as well as only voltage angle based on positive sequence components are implemented in [99] for internal protection of inverter trip. For a

distribution system, the tie line and branch switch provide the flexibility to load restoration (after isolating fault) during fault. In [100], an optimal relay setting for overcurrent relay are proposed considering change from N−1 and N−1−1 states.

Digital relay-based protection scheme which is independent of microgrid operational mode with adaptive settings based on negative sequence (NSQ) and positive sequence (PSQ) is implemented in [101]. The importance of ultrafast solid-state circuit breakers (SSCB) for converter-based ac-dc microgrid is demonstrated as reported in [102]. In [103], linear programming with artificial neural network (ANN) approach is used for different operation states in the identification of faulty and non-faulty conditions. The role of different over current relays is discussed for proper coordination of primary and backup relays through *PSM* and TSM in [104]. In [105], how overcurrent and differential frequency relays can be used for proper coordination protection of permanent magnet synchronous generator (PMSG) based DGs is discussed. Based on above literature survey different strategies that are used to sense fault measurement are as follow:

a. Three phase measurement of voltage and current.

b. dq component measurement of voltage and current.

1.1.2. Microgrid protection optimization

Considering PV DGs installation at any location of feeder and level of penetration, the characteristic curve of overcurrent devices is modified with second strategy limiting the output current of PV sources [28]. With the change in impedance of network, µPMUs sends signal to update overcurrent relay (OCR) settings using communication channel [52]. In [58], a digital over and under frequency relay (DOUFR) is proposed which operates for over and under frequency in coordination with digital proportional integral differential (PID) controller. For proper protection coordination settings considering multi-agent with primary, backup, and bus protection layers based on a VTDPS is proposed for microgrid protection capable of operating in both grid-connected and islanded mode [63]. Taking care of all possible network topologies for proper protection coordination is designed with the optimal relay settings with N−1 contingency [65].

Optimal coordination among directional overcurrent relays is a constrained non-linear programming problem (NLPP), Cuckoo Optimization Algorithm (COA) is used as an optimization

tool [106] and linear programming (LP) are combined as a new hybrid COA-LP optimization algorithm in order to optimize the coordination protection of directional overcurrent relays in microgrids and find the optimum value of fault current limiter (FCL) at the PCC. It gives an idea about proper protection coordination among dc and ac side of PV generator with inverter protection [107]. New regulations in electrical power distribution require the DG to remain connected during the faults, referred to as LVRT or FRT. Similarly, energy storage system (ESS) can also be part of grid support functions with LVRT functionality [108]. Based on COA, an optimization tool is developed with LP to get optimal coordination protection settings for relays and FCL present at PCC. An integrated control and protection system with a three-layer hierarchical protection system consisting of different operation modes is proposed in [109]. The main focus on line-line faults in PV arrays that may be caused by short-circuit faults or double ground faults is given in [110].

Optimally sizing of FCL and accordingly settings for directional overcurrent relays are proposed in [111], where problem has been formulated as a constrained NLP problem and is solved using the genetic algorithm (GA) with the static penalty constraint-handling technique. Protection coordination problem has been taken care of based on minimum power loss [112]. Considering dual settings for directional overcurrent relay (DOR) a scheme is proposed which is capable of properly operating in forward and reverse direction coordinating through communication channel [113].

For better power quality (PQ) and proper protection coordination (PC) in presence of DERs optimal sizing of solid-state unidirectional fault current limiters (SSUFCLs) is proposed [114]. Harmonic current injection capability of IIDGs is used to implement harmonic DOR [115]. Superconducting FCLs are used to provide FRT capability with proper protection coordination [116].

An optimal protection scheme based on differential evolution algorithm considering different operating modes of microgrid along with different types of phase fault is proposed [117]. Adaptive modified firefly algorithm (AMFA) is used to get optimum plug setting (PS) and TSM parameters [118]. Using fuzzy decision-making tool with the help of multi-objective particle swarm optimization algorithm is used to obtain optimal coordination settings [119]. Optimal sizing of the supercapacitors is done based on two-level optimization scheme along with optimizing its controller parameters [120].

Depending upon protective relay blocking, generator rescheduling and load shedding a new protection coordination scheme is proposed for minimizing power loss in [121] for wind DGs. Virtual inertia is controlled depending on change in frequency during different modes by optimal proportional integral (PI) controller using particle swarm optimization (PSO) to minimize protection coordination time interval [122]. A non-standard tripping characteristic curve with modified settings for current multiplier finalized by GA is proposed in [123]. Definite time grading relay using negative sequence resistance for islanded IBDGs is proposed using voltage frequency control [124].

More emphasis should be given on real time techniques or on to current transformer based zero sequence detection, differential current or voltage methods as mentioned in [125]. In case of high impedance fault there is possibility of directional elements failure. That will impact the detection in location of fault. To minimize this effect, zero sequence directional elements are used [126]. A new adaptive distance protection is proposed [127] depending upon DGs connected, based on a fault characteristic analysis of the distribution system with DG, that can automatically calculate the settings according to the operation mode and the output power of DG without any need for communication. In [128], based on the primary and backup protection relays, pickup currents are calculated using Thevenin's and Norton's equivalent model for DGs.

IEEE 802.16 is a standard with main focus on frequency range 23.5 to 43.5 GHz [129] which is issued to provide guidelines to manufacturers and operators for minimizing interference in fixed broadband wireless systems. It covers frequencies in the range of 10 to 66 Giga Hertz (GHz). In [130], a core logic processor extracts the information received, performs the analysis and executes the control action by sending a control command back to the automation system. IEC 61850 standard includes a number of possible communication profiles and the services defined are mapped to the same [131]. IEC 6087-5-104 standard provides information on a communication profile for sending basic telecontrol messages between a central telecontrol station and telecontrol outstations [132].

An IEC 61850-7-420 switched based ethernet network has been used for communicating fault current impact coefficient based adaptive protection system [133]. Communication channel-based distance adaptive protection scheme is proposed in [134] which uses short-circuit current producing capability of DG. Adaptive distance protection is more effective in microgrid system with source impedance variation which is helpful during change of mode from grid connected to

islanded mode and vice-versa [135]. Local measurements are more suitable for the microgrid system using distance protection so that a DG is inter-connected between the relay and fault which can be easily detected. With adaptive capability it becomes more useful in inverter interfaced microgrids. [136].

A given frequency relay is made adaptive, so that it can change its settings with the change of operational mode of microgrid [137]. In grid connected mode, the no detection region is narrower with ± 2.5% variation of frequency, while for islanded mode the non-detection zone has ±5% variation. A new protection strategy [138], that selects different fault detection methods in both modes of microgrid operation, is made adaptive according to type of fault. A new protection scheme with nonintrusive approach is used in ring networks with the help of additional signal processing based on the submarine multi-function monitor protection units [139]. Field programmable gate array (FPGA) [140], is used for faster and fault detection in microgrid protection. Modern FPGA is fast enough to reduce fault detection time. Comparison between the real time measured process variable and trip threshold is used as the main logic for the change in relay settings.

The dq component wavelet-packet-transform [141], based digital multi relay protection scheme is implemented. Responses of the dq transform are successfully coordinated by employing the wavelet-packet-transform second-level high frequency sub-bands without any pre-set time delays, adaptive features and relay to relay communication. In [142], two relay group settings are used, one group for the steady state operation and other group is for transient state. An adaptive overcurrent protection scheme is proposed in [143] using critical clearing time (CCT) for a microgrid which properly works during fault in any mode of operation. Adaptive current fast tripping protection strategy is using equipment's posterior circuit's equivalent electromotive force timely in real time [144] to set the setting for relay operation depending upon mode of operation, type and location of fault.

Optimal relay coordination method is proposed in [145], which takes care of DGs inter-connected and change of mode of operation. In [146], different time-current characteristics are set as variables in optimization problem in which the main constraints are time setting multiplier and nature of pickup setting. The coordination problem is formulated as a mixed integer nonlinear programming (MINLP) and solved with discrete continuous optimizer (DICOPT) solver in general algebraic modeling system (GAMS). Protection scheme based on directional overcurrent relays is

proposed for synchronous based DGs interconnected in microgrid that is capable of efficiently operating in both modes of microgrid operation [147]. The relay coordination problem is formulated as a MINLP and optimal settings for a given relay are set using PSO algorithm. In [148], for optimum selection of settings during protection coordination, two phase nonlinear-linear programming optimization model is presented using GAMS software in conjunction with a developed Matlab code.

Due to large number of coordination constraints related to the different network topologies, an optimal solution to the directional overcurrent relay coordination problem is given in [149]. In [150], directional overcurrent relay coordination is proposed based on harmony search algorithm (HSA) where better results have shown as compared to GA and LP problems. Relay settings for proper protective relay coordination of microgrid are proposed using modified particle swarm optimization algorithm in [151]. Hybrid PSO algorithm is used in [152], so that the protection system has an appropriate operation satisfying coordination constraints for both modes of operation in microgrid. A differential zone protection scheme [153] which works on comparison of current measurements from several devices on the borders of the zones is proposed. The decision variables in optimization are the locations of sensors and relays on network and are represented by a protection device matrix.

Graph theory is used in [154], in which various branches of a feeder are identified with the constraints for using particle swarm optimization algorithm to optimize the location of protective equipment. In this algorithm; the location, type and direction of relays are optimized simultaneously. A new scheme [155] is has been introduced not merely on the flexibility of automatic relay setting group adjustment, but also on the determination of optimal time dial setting (*TDS*) and pickup setting values for the DOCRs. A new strategy of digital protection methodology [156] for the microgrid using PSO is implemented for parallel feeder protection with the directional feature, TMS and *PSM* which are also optimized using PSO.

In [157], dual setting directional over-current relays are proposed for protecting meshed distribution systems with DGs. The dual setting relays are equipped with two inverse time-current characteristics whose settings are dependent on fault direction. The relay settings can be adapted in a flexible manner with OC relays and directional relays combined together. This new scheme needs two sets of relay settings; one for grid connected and other for islanded mode. In [158], a scheme has been proposed using extensive communication based adaptive protection based on

fault current coefficient and DGs impact factor. In [159], active network management (ANM) functionality is utilized for efficient islanding detection in medium-voltage (MV) and low-voltage (LV) DG network based on reactive power unbalance.

1.1.3. Fault current limiters in distributed generation

FCLs play important role in providing fault ride through capability to a given system. Fault current limiters (FCLs) can be resistive, inductive and non-inductive. Briefly they are classified as superconducting and nonsuperconducting FCLs [160]-[166]. Nonsuperconducting FCL is the emerging technology in FCLs to minimize the use of switches and resistances for the minimization of power losses [167]-[169].

Fault recovery and disconnecting switch issues are reduced with implementation of nonsuperconducting FCLs [166]-[169]. But proper and less expensive protection coordination still remains issue for FCLs based technologies. These are also effective for offshore wind DGs but still no research has been reported for the implementation of FCLs in Hybrid nature of microgrids where low X/R ratio and low inertia impacts the fault current of DGs. Optimal placement is also an issue in FCLs usage. A new FCL based protection scheme is proposed for fault current limiting using a capacitor [168]. But for protection of load side, the implementation of FCLs becomes expensive as compared to use of numerical relay backed by fuses. FCLs do not work in single phasing or one phase lightly loaded faults, open conductor and high impedance faults.

A new approach with an event-based protection strategy for dc hybrid microgrid under different loading is proposed in [170] where less data is transferred as compared with other data-based protection methods. Here, each and every protection unit autonomously identifies the type of event based on current derivative identification method considering inductive line impedance (artificial). Number of existing protection schemes are analyzed and classified including communication infrastructures [171]. New strategic devices are proposed for hybrid AC/DC microgrids. A review on technical challenges faced by the conventional protection schemes and the need of adaptive protection scheme is emphasized [172].

Analyzing the fault current characteristics of dc lines, the protection zones for hybrid microgrid are found as distributed. The protection scheme for dc line using main protection with local and remote backup relays is proposed [173]. For the reduction in sensitivity of existing microgrid protection schemes because of intermittent weather; a protection scheme is proposed

considering stochastic modeling for weather intermittency with probability distribution function [174]. The coverability is used to propose the joint probabilistic model on variation of solar irradiance and wind speed.

Most of the FCL are meant for conventional synchronous generators that are ideal sources but distributed generators are dynamic in nature. So, there is necessity of an adaptive protection scheme that can operate as per dynamicity in hybrid microgrids due to different operation modes and availability of wind and irradiance. Storn and Price introduced the population based stochastic algorithm in 1995 [175]. It is simple and fast in implementation with the ability of finding out global best available values [176].

DGs source capacity is considered as SCR (short circuit ratio) which can provide an estimated guide to set the voltage level at the point of common coupling [177]. Sensitivity and selectivity are the two main problems that persist in microgrid protection during different modes of operation. Travelling wave based, an accurate and improved fault location technique is implemented without any uncertainty in the line parameters and errors introduced due to data time synchronization [178]. Based on considerable number of parameters, that include voltage magnitude, angle and current sequence components measured using distributed non-synchronized monitoring devices present at secondary substations; new protection scheme is proposed in [179].

So, the main concern of protection engineer is how to set different sensitivity and selectivity aspects to keep microgrid performance reliable during abnormal condition for any mode of microgrid operation [180]. Based on above literature it can be concluded that while dealing with optimization of directional overcurrent relay coordination, time of operation is affected by current and voltage with respect to time and there must also exist some effects of fault current limiter which in turn are going to affect fault current coefficients and DGs' impact factor, which will finally modify the time of operation. Considering sensitivity and selectivity with dependency on minimum number of parameters, the research objectives are set based on the outcomes of literature survey as discussed in the next section.

1.2. Outcomes of literature survey: Gaps in research

Based on the literature survey of microgrid protection with main emphasis given on adaptive protection, it could be concluded that there is vast area for research on adaptive protection to be explored. Optimization techniques considering minimum number of variables for adaptive

Table 1.1. Comparison of existing protection technologies for microgrid protection

Reference	Communication		Controller		Mode of operation	Speed	Variables
	Wireless	Wired	Centralized	Decentralized			
[19]	-	✔	✔	-	Islanded & Grid connected	Fast	More
[24]	-	✔	-	✔	Grid connected	Fast	Less
[34]	-	✔	✔	-	Islanded & Grid connected	Fast	More
[36]	-	✔	✔	-	Islanded & Grid connected	Fast	More
[44]	-	-	✔	-	Grid connected	Slow	More
[49]	-	-	✔	-	Grid connected	Fast	More
[51]	-	✔	✔	-	Grid connected	Fast	More
[52]	-	✔	✔	-	Grid connected	Fast	Less
[61]	-	-	-	-	Grid connected	Fast	More
[76]	-	✔	✔	-	Islanded & Grid connected	Fast	More
[97]	-	✔	✔	-	Islanded & Grid connected	Fast	More
[118]	-	-	-	-	Grid connected	Fast	More
[120]	-	-	✔	✔	Islanded & Grid connected	Fast	More
[127]	-	-	-	-	Grid connected	Slow	More
[144]	-	✔	✔	-	Grid connected	Slow	Less

protection coordination also needed to be explored. Comparison among existing protection technologies is done in Table 1.1. and Table 1.2. Gaps are categorized depending upon nature of DGs, area to be protected, nature of fault and type of protection required.

Table 1.2. Comparison of existing protection technologies for wind and PV based microgrid

Reference	Generation type	Variables
[47]	PV	3
[90]	PV	3
[91]	PV	3
[99]	PV	3
[46]	Wind	3
[53]	Wind	3
[60]	Wind	3
[69]	Wind	3
[77]	Wind	3
[81]	Wind	3
[85]	Wind	3
[86]	Wind	3
[106]	Wind	3
[121]	Wind	3
[174]	Hybrid	3

Adaptive protection for islands within islanded mode (for 'n' system case) of operation must also be taken into account. Adaptive protection scheme considering ring main connections for microgrid also needed to be studied. The gaps in research are identified for determination of the research objectives based on current research scenario. Relation among different combination of settings of adaptive relay for different conditions can also be considered in microgrid research. Protection of double fed induction generator (DFIG) and PV from utility sags and swells arising within the microgrid is also found as a matter of concern. The need of study on adaptive protection scheme for single phase and three phase microgrid system is also found significant. The research

on PV and wind DG based hybrid microgrids in plains and coastal region of rural India aiming reduction in number of variables for adaptive protection during different modes of operation are found as need of hour.

Based on the gaps found while doing literature survey in the last section, it can be said that the large change in fault current from grid connected to islanded mode of operation necessitates adaptive protection scheme for effective microgrid protection. So, the relay settings can be adapted in a flexible manner with OC relays and directional relays combined together. This new scheme needs two sets of relay settings, one for grid connected and other for islanded mode. DGs' impact factor depends on the impedance between the DGs and relays, within radial distribution. So, in case of fault current coefficients and DGs impact factors, a case can be studied on effect of fault current coefficients for faults on DGs considering impact of ring main connection on DGs impact factor. Also, in adaptive protection scheme, DGs protection settings can be adjusted according to change across transformer operation while implementing differential protection.

It can also be concluded that optimization of directional overcurrent relay coordination and time of operation is affected by current and voltage with respect to time. There also, some effects of fault current limiter exist which in turn can change fault current coefficients and DGs' impact factors, finally modifying the time of operation. So, the relay sensitivity can also be considered with dependency on minimum number of parameters to provide optimized adaptive protection in microgrids. Hence, the research objectives are set as appended in the next Section.

1.3. Objectives of research work

From the findings of the above literature survey on the adaptive protection of microgrid, the following objectives are proposed in the present research proposal: -

1. Study and selection of microgrid structures.
2. Modeling and simulation of adaptive relaying based protection schemes for microgrids.
3. Design of optimum adaptive microgrid protection schemes for relay coordination.

1.4. Layout of thesis

To describe the research work for achieving the objectives as mentioned in Section 1.3, the thesis has been organized into six chapters. An outline of the thesis is appended as follow:

Chapter 1

Chapter 1 covers the introduction and literature survey on microgrid protection. It also describes the brief idea about different protection strategies that are used to sense the fault using different measurement techniques. The status of microgrid protection coordination and its optimization for reliable operation of microgrid is also summarised in this chapter. Use of fault current limiters (FCLs) to provide fault ride through capability to microgrid operation is also discussed. Based on extensive literature survey gaps in research are identified from which the main objectives of this research work are proposed.

Chapter 2

Chapter 2 presents the brief idea about the need of developing and designing of new microgrid structures based on available DERs potential in plains and coastal areas of India as per the Govt. of India directives including the needs to develop different strategies as a developed nation in energy sector. Different components, control methods and modes, problems faced and standards used in microgrid design, parameters of microgrid design, cost of energy and proposed microgrid structures are also discussed. Depending upon potential of different DERs throughout India, different nature of DGs are proposed and designed that have surplus capacity for generation of electrical power to meet the demands of rural and agriculture sector. This chapter covers the first objective of this research work. Behavior of voltage, current and frequency is also studied for different modes of microgrid operation.

Chapter 3

Chapter 3 describes the dynamic behaviour of microgrid system under faulty conditions which makes adaptive protection as a general necessity for reliable microgrid operation. The problems faced in design of adaptive protection, the grid-connected and islanded modes of microgrid operation including grid-connected mode without DGs in microgrid are also analyzed. In this study, a new adaptive protection scheme is proposed based on the above-mentioned modes of microgrid operation. This chapter covers the second objective of this research work. It also covers the proposed adaptive protection technique, impact of low X/R ratio of DGs connected, fault location detection and fault nature identification based on quadrature and zero sequence components of fault current. The proposed methodology for adaptive protection scheme is verified

in Matlab-Simulink environment and the results are found to be satisfactory while various faults are simulated at different nodes of the microgrid model.

Chapter 4

In Chapter 4, extended work on second objective of this research work is carried out. The design of adaptive protection scheme in a hybrid microgrid consisting of single and doubly fed wind- induction generators including photovoltaic generators is described. Also, study on fault current behavior in a feeder with different distributed generators and grid/islanded mode of operation are considered. The novel contribution of this research work is reflected in the implementation of a fuzzy logic based adaptive protection scheme in microgrid through analysis of q0 components of fault current. Importance of transient reactance in low X/R ratio in distributed generators, modes of operation, transient reactance during series and shunt faults are also analyzed.

Chapter 5

Chapter 5 covers the third and last objective of this research work where protection coordination optimization (PCO) problem is treated as one of the main objectives with coordination-time minimization for relays. Moreover, the changes in fault currents are sensed by the relays for different types of resources, such as PV and wind turbine types I, III and IV etc. In this research work an adaptive protection scheme with optimal settings is proposed for phase and earth faults. It also takes care of different nature of DGs, all feasible operating modes of hybrid microgrid with only q component of fault current. A new strategy is proposed that optimizes the use of fuses as a backup to primary and backup relays with the help of differential evolutionary algorithms.

Chapter 6

In Chapter 6, the brief summary of research work is discussed as conclusions of the dissertation. The future scope of this research work is also discussed in this chapter.

Chapter 2

Study and Selection of Microgrid Structures

Introduction

As per geographical scenario in different countries, the microgrid structure may vary depending upon the availability of DGs at a particular place. It is observed that in India there is good scope for microgrid implementation based on synchronous generators with low X/R ratio, such as small diesel generators independent of environment factors like irradiance and wind speed, PV DGs, wind DGs and combined PV and wind DGs. When the DGs are integrated to existing power system, they can feed loads individually depending on their capability to share the load in a simple microgrid structure involving DGs and loads [2]-[3]. The DGs that are normally used now a days are mostly PV and wind based. Other DGs that can be used in microgrids are [4]-[5] (a) Microturbine, Geo thermal energy, Biomass energy, Ocean energy including energy storage etc.

As per observation from literature survey, the microgrid structure may vary not only depending upon the type of available resources, but also depending upon the specific type of control and protection mechanisms to be implemented in microgrid for its smooth operation. In this research, the microgrid structure has been proposed keeping in mind the introduction of adaptive protection scheme based on dq0 components of fault current. So, apart from standard approach for different types of DGs, catering scattered load demand, provision of PCC, grid connected and islanded mode of operation; the adaptive protection scheme has been presented as a key component in the design of microgrid structure in this research.

In microgrid planning and design, the main purpose is the selection of different components of DERs and electrical network. In the microgrid design architecture, number of standards and protocols are considered because of involvement of different types of DERs, control and protection models. Mostly used standards in microgrid design are the IEEE Std 1547-2018 and IEEE Std 2030.9-2019 [181]-[182] which have been followed in the present research.

2.1. Components of microgrid structure

In general, microgrid structure consists of utility grid, distributed generators, point of common coupling (PCC) and loads including the control and protection systems [4]-[5]. The

MGCC plays important role for implementation of control and protection systems in microgrid structure. A typical hybrid microgrid structure is shown in Figure 2.1. IEC 61850 standard recommends communication link for data excahnge among MGCC, grid, main bus, adaptive protection, DGs, BESS and load end etc. The MGCC and adaptive protection exchange data when three phase currents are transformed into *dq0* components. Depending on the variation in dq0 components of fault current, the relays in adaptive protection initiate circuit breakers for opening and closing. The adaptive protection can adapt itself as per change in microgrid mode of operation and as per nature of DGs for fault isolation which is throughly explained in next Chapters. The main structure of microgrid includes following general elements.

a) Intermittent DERs or DGs.

b) Dispatchable micro sources.

c) Energy storage units (ESUs).

d) Distribution system (Transformer & Feeders).

e) Connected loads.

f) Communication and control system.

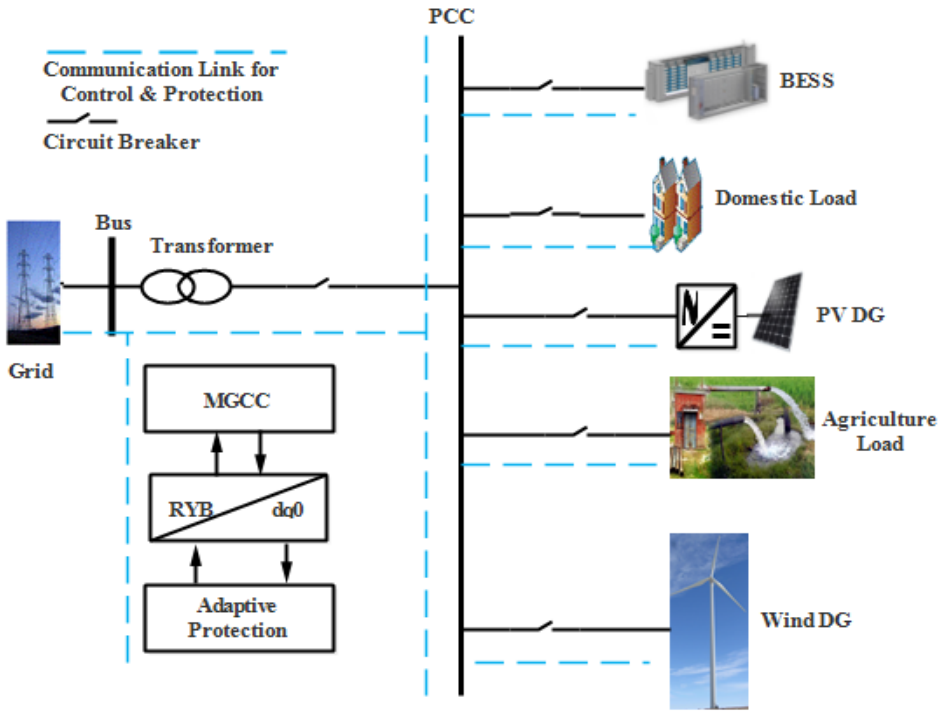

Fig. 2.1. *Block diagram of microgrid structure*

g) Protection system.

h) Point of common coupling (PCC)

Moreover, the Figure 2.1. provides general idea about a microgrid structure which can operate in grid connected/ islanded mode through transformer and PCC controlled by MGCC including wind DG, PV DG and energy storage feeding resistive and inductive loads. The dotted line shown in the Figure 2.1. indicates the communication link for control and protection. In India, to achieve 100 percent rural electrification, renewable energy-based localized distributed generation plants are becoming effective as they will minimize the distribution losses.

In the design of microgrid structure for rural areas in India or for any other country, a new approach has been followed in this research. The low/medium voltage DGs are designed as per the scattered load demand (200 kW to 1.5 MW). Main emphasis is given on operation of low X/R ratio based synchronous generators, PV and wind DGs operating in grid connected and islanded modes for designing the efficient and reliable adaptive protection scheme for loads connected in microgrid structures. The operation of relays may be intermittent as those can see different impedances and bidirectional current feed due to change in microgrid mode from grid connected to islanded and vice-versa.

The selectivity and sensitivity are the main issues faced by the relays during different modes of microgrid operation and the proposed adaptive protection will provide the solution to these issues which exist in microgrid structures.

2.1.1. Selection of microgrid structure

To establish the concept of reliable and feasible microgrid structure, its selection should be based on the IEEE Std. 2030.9-2019. As per this standard, the basic microgrid structure is formed in the proposed research work and same is validated in Matlab/Simulink software environment. The proposed approach of simulation for the selection of microgrid structure can assess the performance of the system in design level, hence may be helpful to reduce the research and development cost.

The first objective of this research work is to select a reliable structure so that proposed adaptive protection scheme could be easily implemented in a microgrid. The step by step procedure has been followed while designing microgrid as per IEEE Std. 2030.9-2019. It starts with voltage level selection as per the requirement of end user to minimize distribution losses.

Microgrid structure selection procedure is shown in Figure 2.2. and also discussed in the following section.

a) Select the voltage levels at which DGs should work depending upon the load requirement.

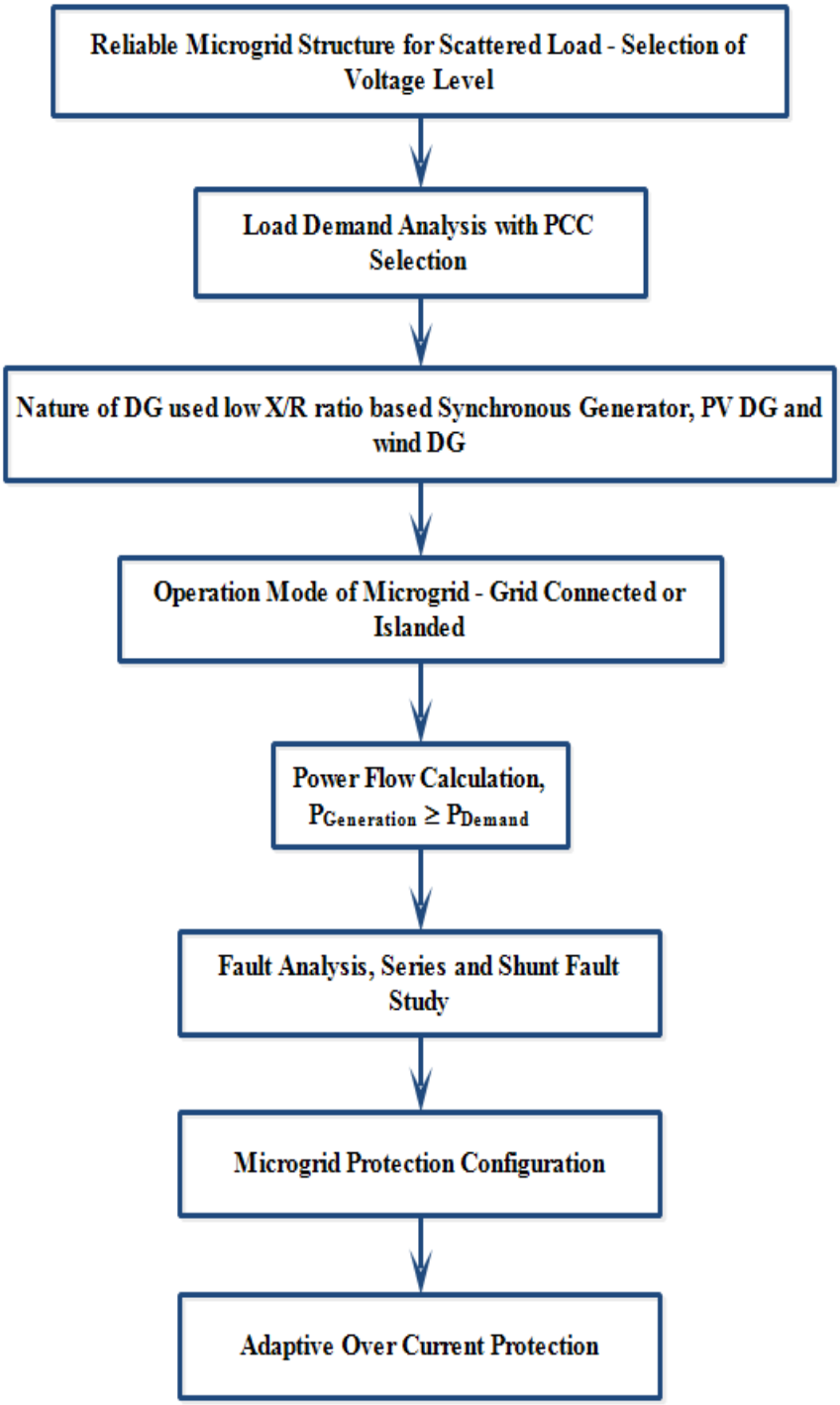

Fig. 2.2. *Flowchart of microgrid structure with adaptive protection*

b) Check the load demand is met with the proper selection of PCC.

c) Analyse the different nature of DGs that are going to feed the load.

d) Select among the grid connected and islanded mode operation of microgrid.

e) After selection of mode of operation recheck whether load demand is fulfilled in present mode of operation or not.

f) Study the different faults and the magnitude of fault current fed by different nature of DGs.

g) Analyse feasible protection configuration.

h) Design adaptive over current protection for reliable operation of microgrid.

2.1.2. Challenges in the selection of microgrid structure

The main concern while designing the microgrid is the availability of DERs in that geographical location with proximity of load as most of the microgrids consist of low and medium voltage DGs. So, to avoid transmission losses and capital cost, the DGs are installed nearest to the load's location. Now, depending on type of load requirement, microgrid could be ac or dc, the load and DGs may be single phase or three-phase. The basic requirement of microgrid design is recommended in [6] from the power system reliability perspective, though more work on standards and procedures is needed for integration of DGs. The challenges in microgrid structuring are given below.

a) The voltage regulation

b) Reactive power capability.

c) Low and high voltage ride-through capacity.

d) Inertia-response of different DGs.

e) Control of the MW ramp rate or curtailment of MW output.

f) Frequency control.

2.2. Parameters in microgrid design

With reference to the standards [181]-[182] recommended for microgrid design, various parameters are identified that generally decide the different architectures involved for reliable and economical design of microgrid structure. The parameters are identified as follow [7]-[8].

a) Nature of supply in microgrid (AC or DC).

b) Nature of DERs used (PV, wind, diesel generator, fuel cell etc.).

c) Voltage level of DERs and load (Low or Medium).

d) Distance of distribution lines connecting DERs to load end (few kilometers).

e) Feeder connection (Radial, Ring, Radial-Ring).

f) Nature of loads connected (R, L, RL, R-L-C etc.).

g) Protective relaying.

h) Voltage level and frequency at PCC.

i) Fault current at PCC.

2.3. Distribution guidelines in India as a reference for selection of proposed microgrid

At present, Indian electrical energy system is found mostly based on thermal and hydro energy and at some places, DERs are available solely based on PV DGs feeding the distribution system. Considering global trend towards on and off-shore wind DGs, Indian DERs' usage could be equally distributed among wind and PV DGs. This study is carried out for proper selection of DGs and the microgrid structure from Indian rural and domestic perspective. The Punjab State Electricity Regulatory Commission (PSERC) in compliance to Indian Electricity Act 2003 has issued guidelines under "Conditions of Supply" to licensee (supplier) for giving supply to consumers, following should be considered for electrical energy distribution [10].

a) Low Tension (LT) ac supply is defined at 50 cycles, 230 – 440 V.
b) For a single-phase supply, voltage between phase and neutral connections should be 230 V for general load not exceeding 7 kW and motive load not exceeding 2 brake horse power (BHP) like induction motor load.

c) Three phase 400 volts between phases (line to line) connections for motive load more than 2 brake horse power (BHP) for induction motors with general load exceeding 7 kW but not exceeding 100 kW. Supply given to loads above 7 kW should be three-phase with neutral.
d) Motive load supply for agricultural sector with load up to 100 kW and supply to street lighting should be from three-phase LT.

The proposed microgrid models are designed while maintaining above guidelines in terms of operating frequency, LT supply, three phase supply to the loads above 7 kW and motive loads.

2.4. Proposed microgrid models

As per the guidelines given in "Conditions of Supply", the proposed microgrid models are designed while maintaining the guidelines in terms of operating frequency which is set at 50 Hz. The LT supply is three phase and 400 to 440 V (line voltage) and three phase supply to 200 kW load. The need of maintaining guidelines mentioned in "Conditions of Supply" is for keeping power quality intact, no harm to domestic and agrarian load, optimum use of electricity and no impact on existing power system network structure.

With reference to [10], "The supply voltage and classification of consumers", the DGs are to be reliable and economical; generation should be three-phase with minimum voltage level 230 V and maximum voltage level be 440 V at frequency of 50 Hz. This is to be considered because India is an agriculture dominated nation with most of the loads available in rural India as three-phase motive load. It is considered under the low tension AC (LT) supply operating at 50 Hz within voltage limits from 220 V to 440 V.

Three phase supply is considered because of saving in conductor materials as well as cost. The three-phase distribution system is economical with better efficiency due to less line losses. In addition, three phase supply can generate self-revolving magnetic field for the three phase induction motors, efficient and reliable as compared to single phase system. So, all the microgrid models are proposed with three phase supply, well equipped with over current adaptive protection scheme for efficient and reliable operation which have been thoroughly discussed in the following chapters.

2.4.1. Microgrid based on low X/R ratio

Based on the above-mentioned aspects, the microgrid is designed for Indian rural areas. The proposed microgrid is modelled according to typical small Indian rural village whose load is mostly inductive having range of 200-400 kW and whose feeders can operate at 415 V. The Location of DGs and load with respect to utility grid resembles a microgrid for rural area of India which has domestic and automotive load. The schematic diagram and single line diagram of the proposed microgrid model is shown in Figure 2.3. (a) and (b). The Low X/R ratio based synchronous generator shown has been modelled based on the relations (2.1) – (2.4) as:

$$E_d = -R_a I_d \ + \psi_q P\theta + \ P\psi_d \qquad (2.1)$$

$$E_q = -R_a I_q \ + \psi_d P\theta + \ P\psi_q \qquad (2.2)$$

where $\theta = \ \omega_r t$, ψ_d and ψ_q are the direct and quadrature axes flux linkages of rotor, I_d and I_q are direct and quadrature axis currents, E_d and E_q are the direct and quadrature axes voltages of the

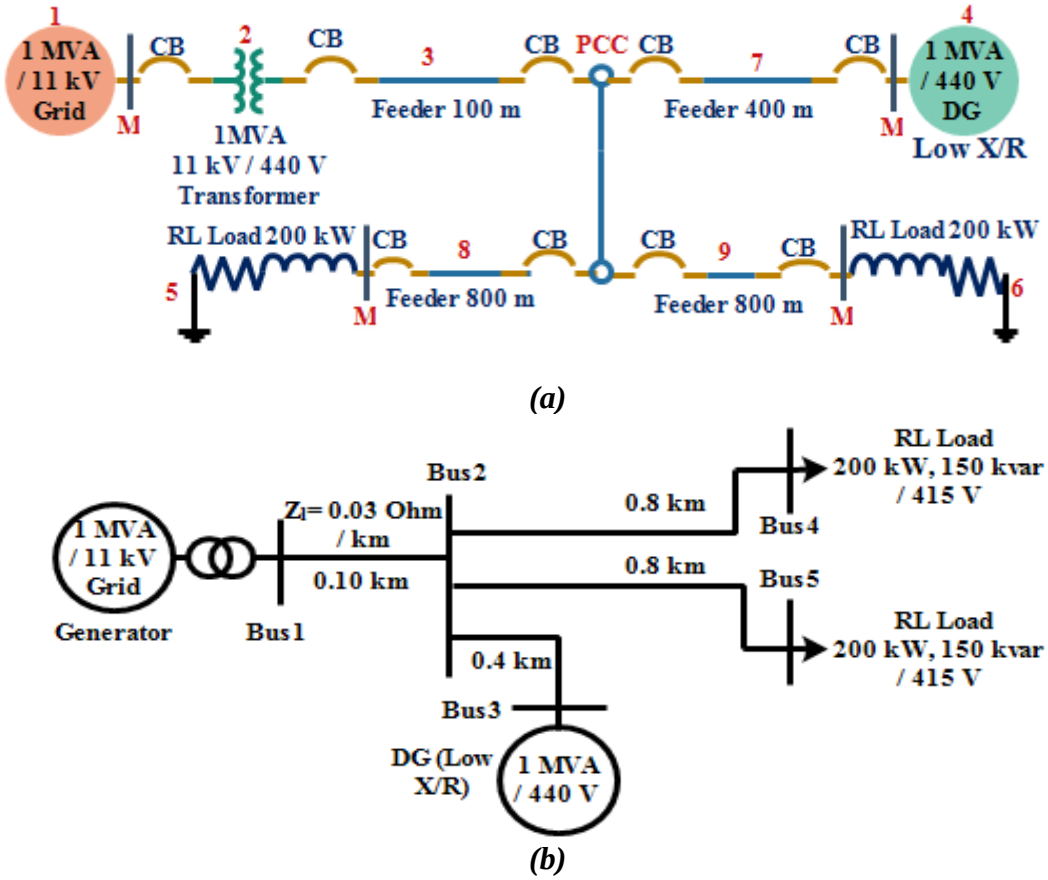

Fig. 2.3. (a) *Block diagram of microgrid system,* ***(b)*** *Single line diagram of microgrid system.*

stator axes of synchronous machine, R_a is armature resistance. *P* is first order derivative *(d/dt).* θ is angular displacement and ω_r is rotor speed. Real and reactive powers are given as:

$$P_t = E_d i_d + E_q i_q \quad (2.3)$$

$$Q_t = E_q i_d - E_d i_q \quad (2.4)$$

P_t and Q_t are the real and reactive powers at the terminals of synchronous machine. The brief discussion of mathematical model for low X/R synchronous generator with proposed adaptive protection scheme implementation is discussed in Chapter 3. In the microgrid system designed, the X/R ratio of utility grid system is kept 7 and X/R ratio of synchronous generator acting as DG is considered with low X/R ratio of 5.

Three-phase AC system of 1 MVA and 11 kV (per phase voltage 6.4 kV) utility side with step-down transformer of 1 MVA, 11 kV/440 V (R is 0.89 %, X is 5.1 % and X/R is 5.7) operating at 50 Hz and 0.8 lagging power factor are connected before point of common coupling (PCC). So, considering that effect of low X/R ratio, a synchronous generator with low X/R ratio is treated as DER which is connected at PCC through feeder of 500 m (R + jX = (0.04 + j 0.3) Ω/km) distribution line capable of supplying 800 kW load at 0.8 lagging power factor. Two loads of 200 kW each are connected to DER at 1.2 km and distance between PCC and DG is considered as 500 m. The above system is modelled using Matlab/Simulink as a five-bus system having one slack bus, one generator bus and two load buses.

2.4.2. Microgrid based on photovoltaic (PV) DG

The PV fault current is determined by several factors such as *β, γ, K, P_0'* and *Q_0'* [48] etc. Different possible microgrid structures are designed and simulated as per the requirements of rural India. Here, A PV based microgrid is designed and simulated. PV control provided based on inverter control - using double synchronous rotating frame (DSRF) for the more flexible fault-ride-through (FRT) control. The inner-loop current control uses the regulators under a DSRF, and the outer-loop voltage control regulates the dc-link voltage to realize maximum power point tracking (MPPT) that is used in [48]. During faulty conditions, depending on the design and operating mode, the inverter may change to FRT mode. FRT mode is neglected to study maximum current share. Here, PV controller is designed based on equations given as (2.5) and (2.6). The PV fault current is determined by several factors such as *β, γ, K, $P_0^{'}$* and *$Q_0^{'}$*.

$$I_{dq}^{+} = \frac{2}{3\gamma E_m}\sqrt{\left(\frac{P_0'}{1-K\beta^2}\right)^2 + \left(\frac{Q_0'}{1+K\beta^2}\right)^2} \quad (2.5)$$

$$I_{dq}^{-} = \frac{2\beta}{3\gamma E_m}K\sqrt{\left(\frac{P_0'}{1-K\beta^2}\right)^2 + \left(\frac{Q_0'}{1+K\beta^2}\right)^2} \quad (2.6)$$

where I_{dq}^{+} and I_{dq}^{-} are dq axis currents corresponding to positive and negative sequence, γ is the coefficient of the positive-sequence voltage sag, β is E_{dq}^{-}/E_{dq}^{+} where E_{dq}^{-} and E_{dq}^{+} are dq axis voltages corresponding to positive and negative sequence components, P_0' and Q_0' are the average values of real and reactive power supplied by PV unit. K is the control factor and with $K=0$ injection of three-phase symmetrical currents under unbalanced voltage conditions takes place; for $K=-1$, elimination of reactive power oscillations and for $K=1$ elimination of active power oscillations, E_m is the pre-fault voltage amplitude at the point of common coupling (PCC). The schematic diagram of proposed microgrid model is shown in Figure 2.4. The proposed PV DG based microgrid is thoroughly discussed with wind DG in next Chapters.

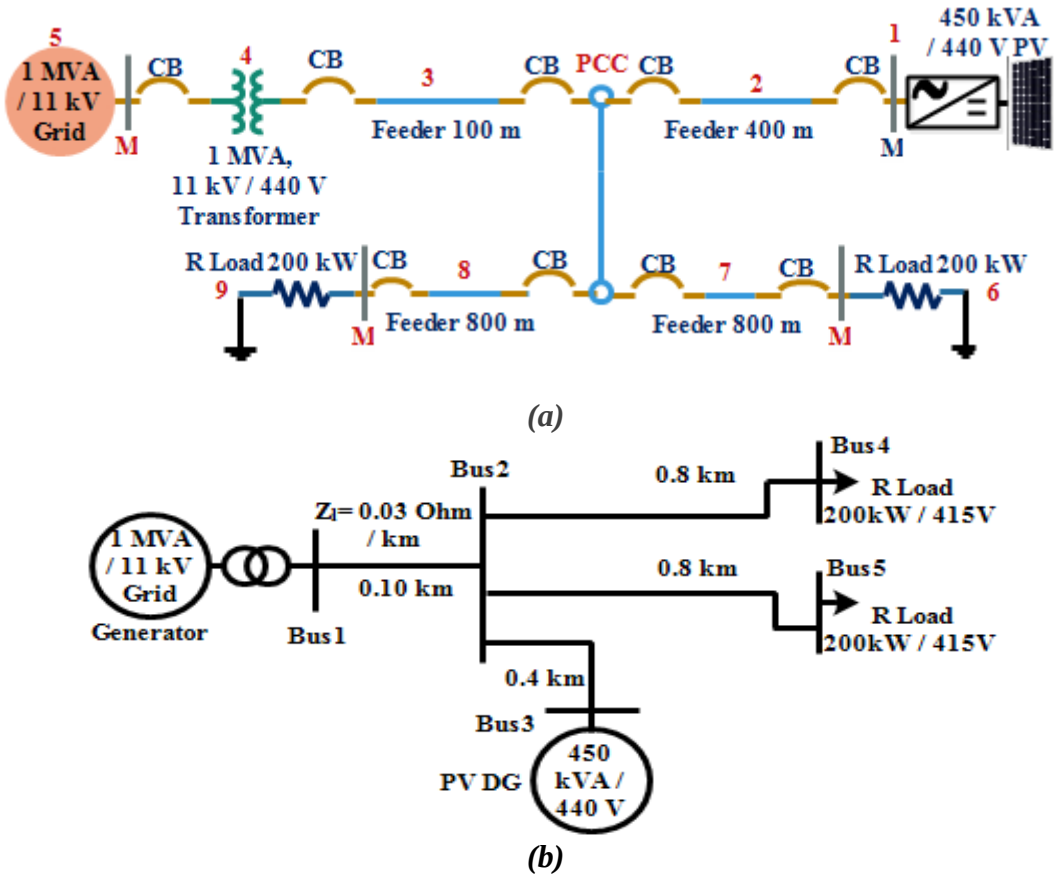

Fig. 2.4. (a) *Block diagram of PV microgrid system,* ***(b)*** *Single line diagram of PV microgrid system.*

In the Figure 2.4, three-phase-three-bus AC system of 1 MVA and 11 kV (per phase voltage 6.4 kV) utility side with stepdown transformer of 1 MVA, 11 kV/440 V operating at 50 Hz and 0.8 lagging power factor are connected before point of common coupling (PCC). PV based distributed generator which is connected at PCC through feeder of 500 m distribution line, capable of supplying 400 kW load at 0.8 lagging power factor. Two loads of 200 kW each are connected to DER at a distance of 1.2 km and distance between PCC and DG is 500 m. The above system is modelled using Matlab/Simulink as a three-bus system having one slack bus, one generator bus and two load bus as shown in Figure 2.4. (a) and (b).

2.4.3. Microgrid based on wind DG

The schematic diagram of the proposed microgrid model is shown in Figure 2.5. (a) and

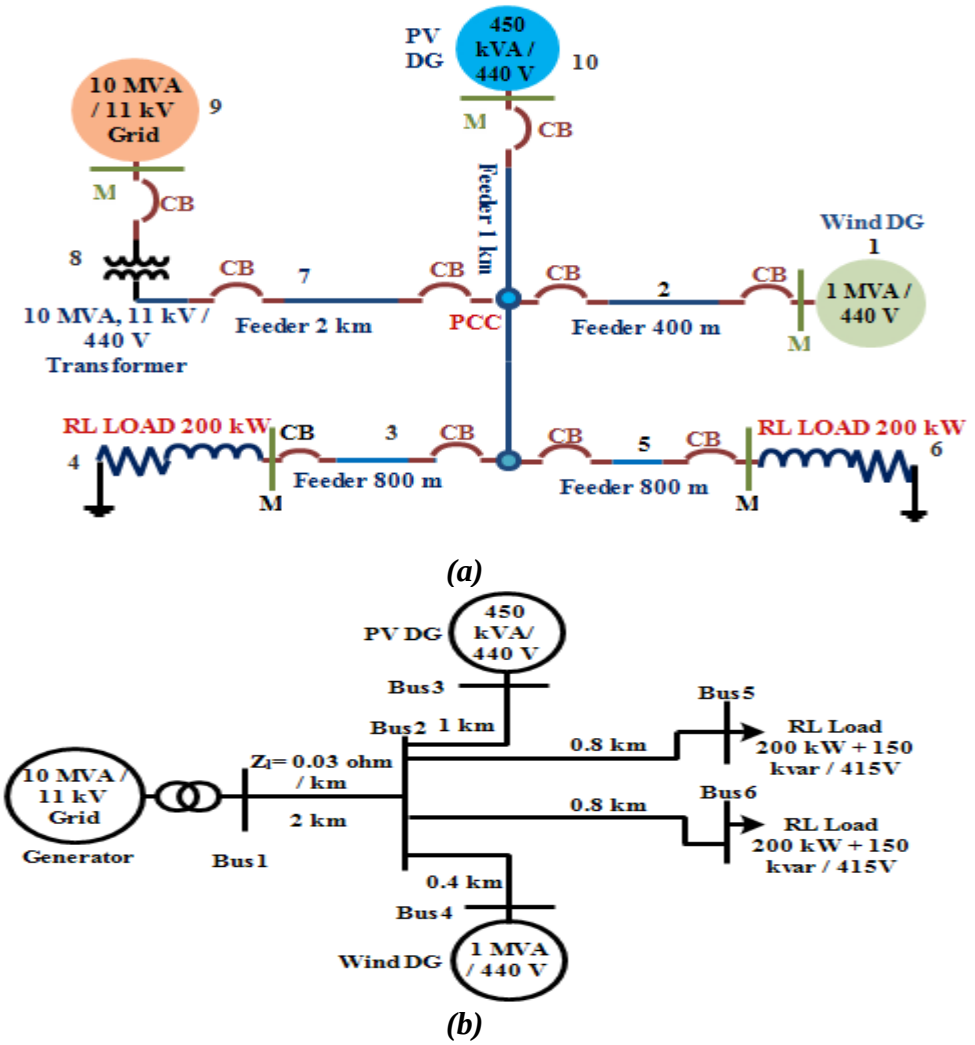

Fig. 2.5. (a) *Block diagram of wind-PV microgrid system,* ***(b)*** *single line diagram of wind-PV microgrid system.*

(b). The layout of a three-phase AC microgrid system equipped with 450 kVA / 440 V photovoltaic (PV) system, type I wind energy (WE) system of 1 MVA /440 V; all are interconnected with utility grid of 1 MVA and 11 kV (per phase voltage 6.4 kV) through a step-down transformer of 1 MVA, 11 kV/440 V, 50 Hz at point of common coupling (PCC). For hybrid microgrid, PV DG is modelled as discussed in Section 2.4.2. Type I wind turbine model designed is based on relations (2.7) given below [177]:

$$P_m = \frac{1}{2}\rho\pi R^2 C_p(\beta,\lambda)v^3 \quad (2.7)$$

Where, P_m is mechanical power output fed to run singly fed induction generator in terms of torque, ρ is density of air, R is rotor radius of wind turbine, v is the wind speed which is kept constant, C_p is power coefficient of the wind turbine, λ is tip speed ratio and β is pitch angle. Fault ride through mode of PV-Wind DGs is not considered to check maximum fault current in hybrid mode.

The entire system has resistive load of 400 kW and reactive load of 300 kvar. As mentioned above, hybrid microgrid system is shown in Figure 2.5. (a)-(b) and described as three-phase AC system of 10 MVA and 11 kV utility with step-down transformer of 10 MVA, 11 kV/440 V operating at 50 Hz, connected before point of common coupling (PCC).

2.4.4. Hybrid microgrid based on PV and wind DGs

For hybrid microgrid, PV DG is modeled as discussed in Section 2.4.2. Converters of DFIGs (type III and IV) are modeled according to [64] as relations (2.7) – (2.10):

$$V_s = R_s I_s + j\omega_1 L_{s\lambda} I_s + j\omega_1 L_m(I_s + I_r + I_{Rm}) \quad (2.8)$$

$$\frac{V_r}{s} = \frac{R_r}{s} I_r + j\omega_1 L_{r\lambda} I_r + j\omega_1 L_m(I_s + I_r + I_{Rm}) \quad (2.9)$$

$$0 = R_m I_{Rm} + j\omega_1 L_m(I_s + I_r + I_{Rm}) \quad (2.10)$$

V_s is stator voltage; R_s is stator resistance; V_r is rotor voltage; R_r is rotor resistance; I_s is stator current; R_m is magnetizing resistance; I_r is rotor current; $L_{s\lambda}$ is stator leakage inductance; I_{Rm} is magnetizing resistance current; $L_{r\lambda}$ is rotor leakage inductance; ω_1 is stator frequency; L_m is magnetizing inductance; s is slip (0.3 to -0.3).

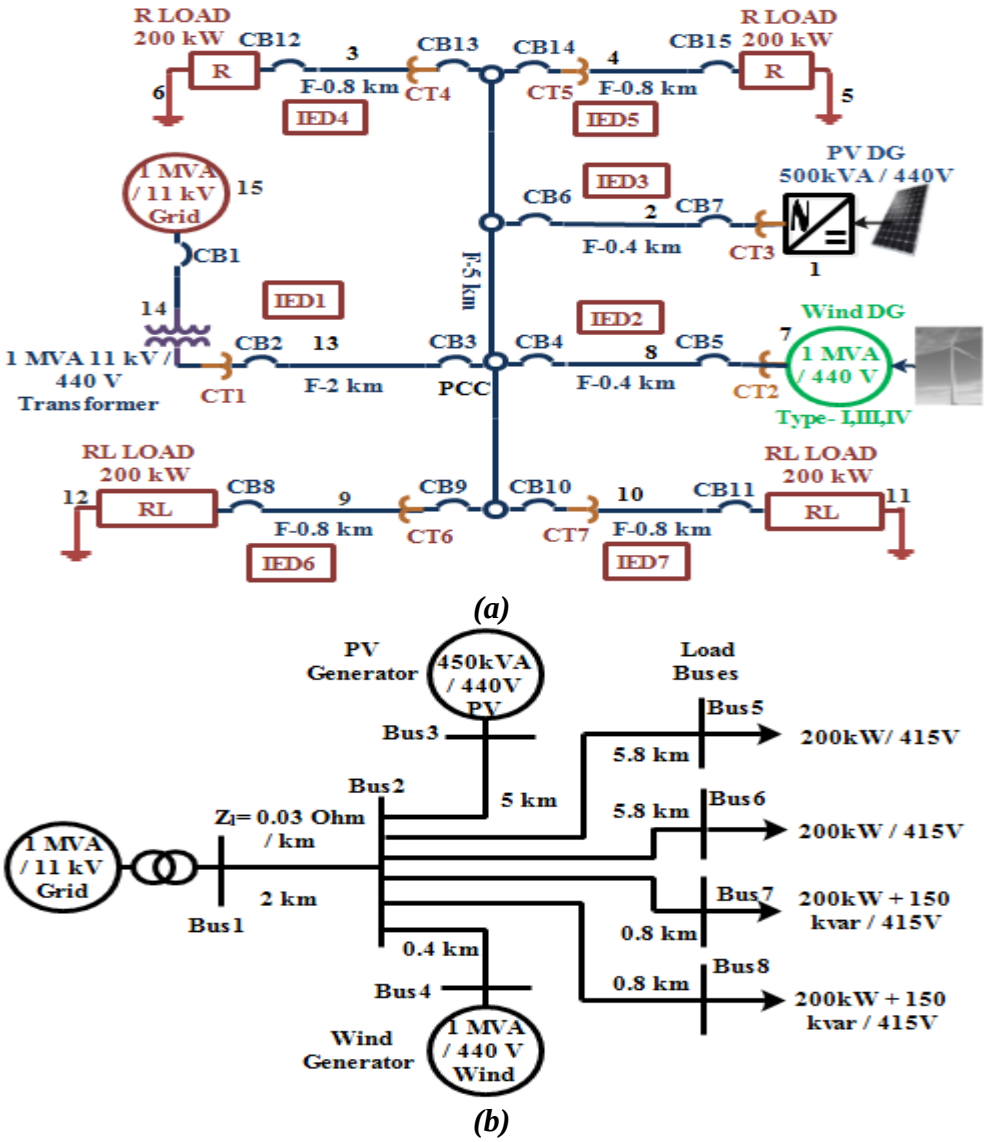

Fig. 2.6. (a) *Block diagram of wind-PV hybrid microgrid* ***(b)****Single line diagram of wind-PV hybrid microgrid.*

The proposed hybrid microgrid is self-sufficient to feed the loads connected to it irrespective of the utility grid's availability. The locations of CBs (fifteen circuit breakers marked as CB1 to CB15), CTs (seven current transformers marked as CT1 to CT7) and intelligent electronic device (IEDs) (IED 1 to IED7) are shown in Figure 2.6. (a)-(b). The equipment connected at PCC through feeder of 400 m distribution line and PV based distributed generator of 450 kVA /440 V is also feeding PCC via 0.4 km distribution line. Two loads of 200 kW each are connected to wind based DER at a distance of 1.2 km and the distance between PCC and wind-based DG is considered as 400 m. Interconnection of wind-PV based hybrid system based distributed generators (DGs), load and utility resembles a hybrid microgrid.

Considering the effect of low X/R ratio, wind energy based double fed induction generators (type III and IV) with rating of 1 MVA/440 V with low X/R ratio is shown in Figure 2.6. (a)-(b). The Figure 2.6. (a)-(b) shows the layout of a three-phase AC microgrid system equipped with 450 kVA/440 V photovoltaic (PV) system, wind energy (WE) system of 1 MVA/440 V; all are interconnected with utility grid of 1 MVA and 11 kV (per phase voltage 6.4 kV) through a step-down transformer of 1 MVA, 11 kV/440 V, 50 Hz at point of common coupling (PCC). The entire system has resistive load of 800 kW and reactive load of 300 kvar. For protection studies faults are simulated at node 9 near RL load (node 12), at node 2 near PV DG, at node 8 near Wind DG, at node 3 near R load (node 6) and at node 15. The proposed microgrid models are well equipped with over current adaptive protection scheme which is thoroughly discussed in next chapters for efficient and reliable hybrid microgrid operation.

2.5. Simulation of microgrid characteristics

Steady state behavior of designed low X/R ratio based microgrid system are studied in terms of dq components. The *dq* components are static components and show steady state behaviour. Three-phase to *dq* component transformation is performed based on equations (2.11) – (2.12) as per [42]. The following study is carried out on microgrid system shown in Figure 2.3. (a). These components have beeen thoroughly discussed in concluding Chapters.

$$\left[I_{dq0}\right] = [K_\theta] \times [I_{RYB}] \qquad (2.11)$$

$$\left[V_{dq0}\right] = [K_\theta] \times [V_{RYB}] \qquad (2.12)$$

2.5.1. Voltage and current characteristics – Grid connected mode

The results are shown for grid connected mode of operation with utility grid of high X/R ratio and synchronous generator as DG with low X/R ratio. Those are feeding load together as shown in Figures 2.7. to 2.11. This study is carried out by simulating microgrid using Matlab/Simulink. The grid is shown operating at 11 kV (in terms of V_{dq}) and 30 A (in terms of I_{dq}). It is important to check whether the designed microgrids have ability to operate the grid connected and islanded modes. This feature is simulated to check availability of utility side grid and DG to feed the load which is based on comparison of current fed at PCC.

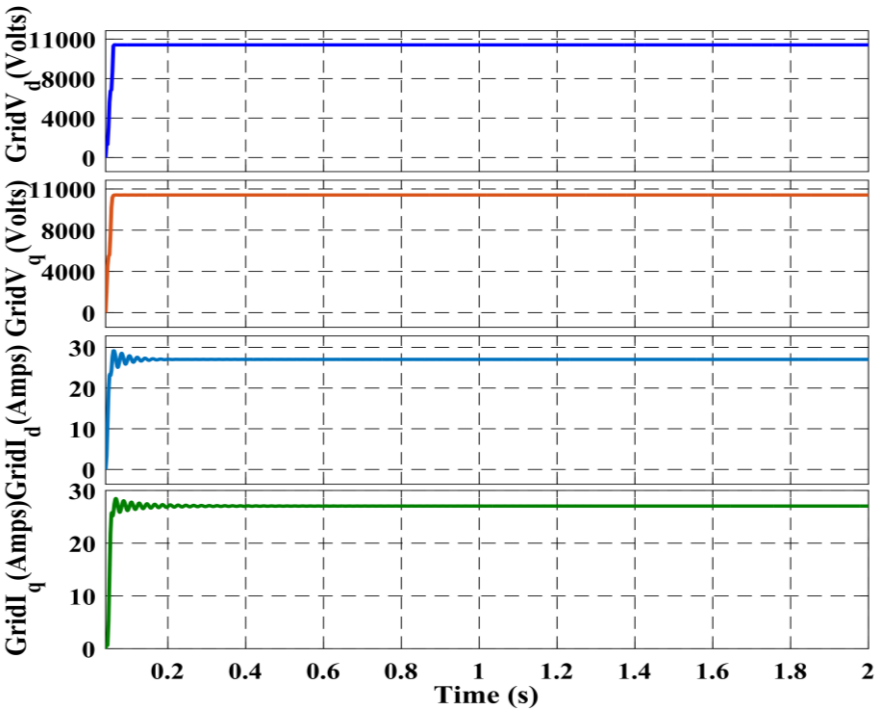

Fig. 2.7. *Grid side voltages and current in terms of their dq components*

The Figure 2.7. shows grid voltages (grid V_d and V_q ,11 kV) and currents (grid I_d and I_q, 27 A) at utility grid end in terms of *dq0* components. The voltage and currents of low voltage DG in terms of *dq* components are shown in Figure 2.8. The voltage (DG V_d and V_q ,440 V) generated by

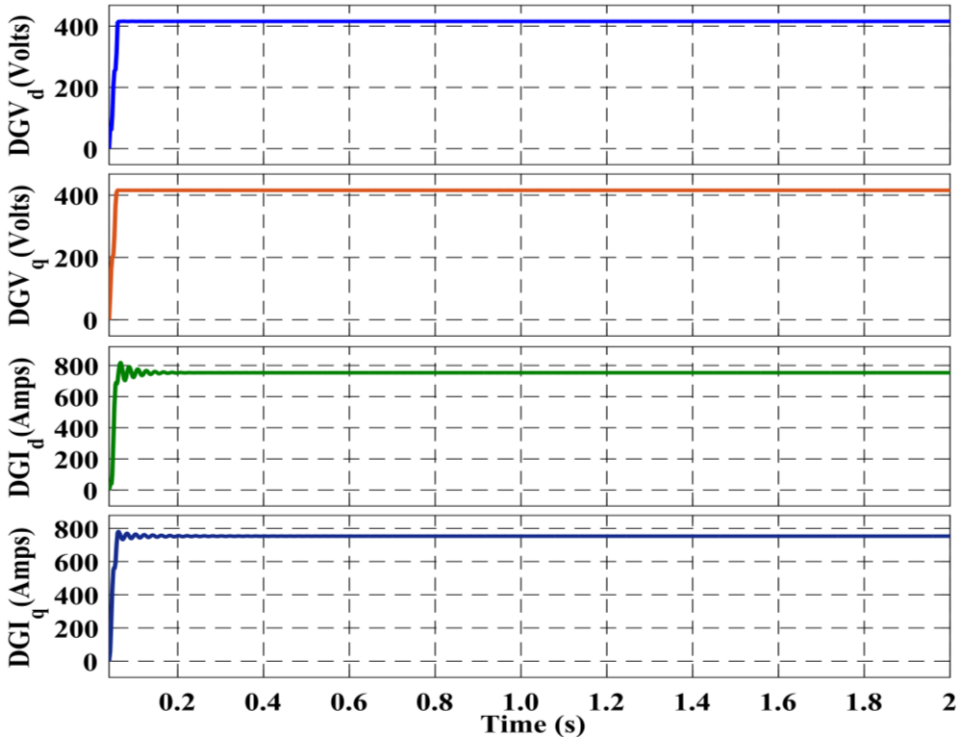

Fig. 2.8. *DG side voltages and current in terms of their dq components*

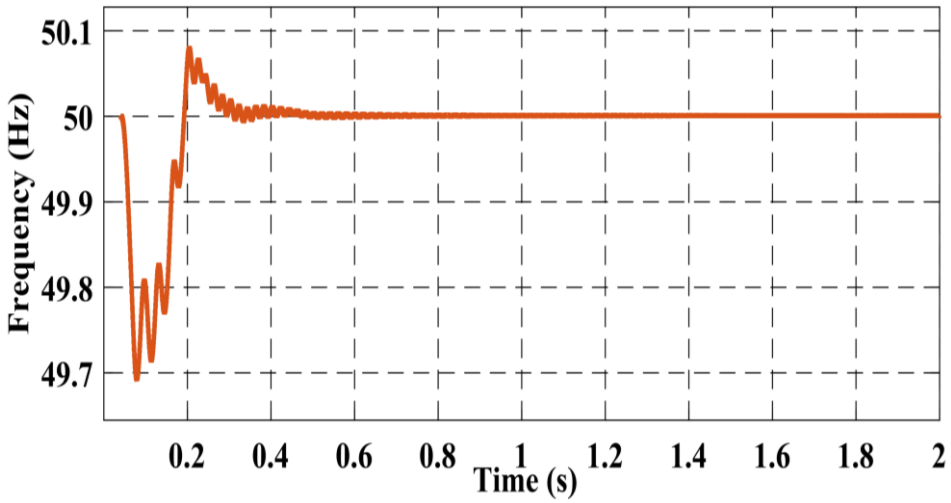

Fig. 2.9. *Frequency measured at point of common coupling*

DG is 440 V and current is 780 A (DG I_d and I_q, 780A). If current fed from utility side grid is small and DG is sharing most of the infeed at PCC, it is grid connected mode. Figure 2.9. shows the frequency at point of common coupling. During integration of DG having low X/R ratio, there is small drop in frequency in the range of 0.37 Hz (50. 08 Hz – 49.7 Hz). The DG gives maximum in-feed at PCC for the implementation of plug and play model of microgrid. Figure 2.10. shows

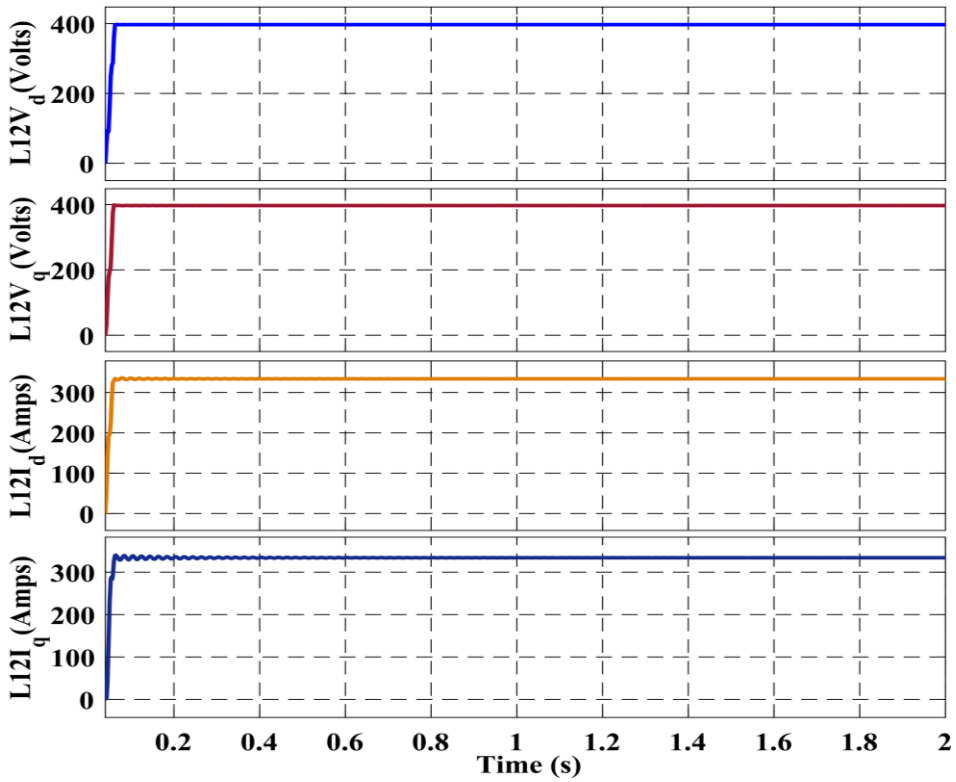

Fig. 2.10. *Load 1,2 side voltages and current in terms of their dq components*

the Load 1 and 2 voltages in terms of $L12V_d$ and $L12V_q$, which are nearly 415 V and currents in terms of dq components as $L12I_d$ and $L12I_q$, which are nearly 340A. Load 1 and 2 are of same rating and connected in parallel. They are fed at 415 V and 340 A each. When only DG is feeding at PCC, it is considered as islanded mode of operation. If grid is connected to the DGs and load, then intelligent relays must be able to see the different current feeding from different directions; else it may lead to mal-operation of relay during fault. In similar manner, during islanded operation, when grid is absent and only DGs are feeding load, the intelligent relays must also sense change in current share as only DGs are feeding. Figure 2.11.(a) shows the availability of DG and

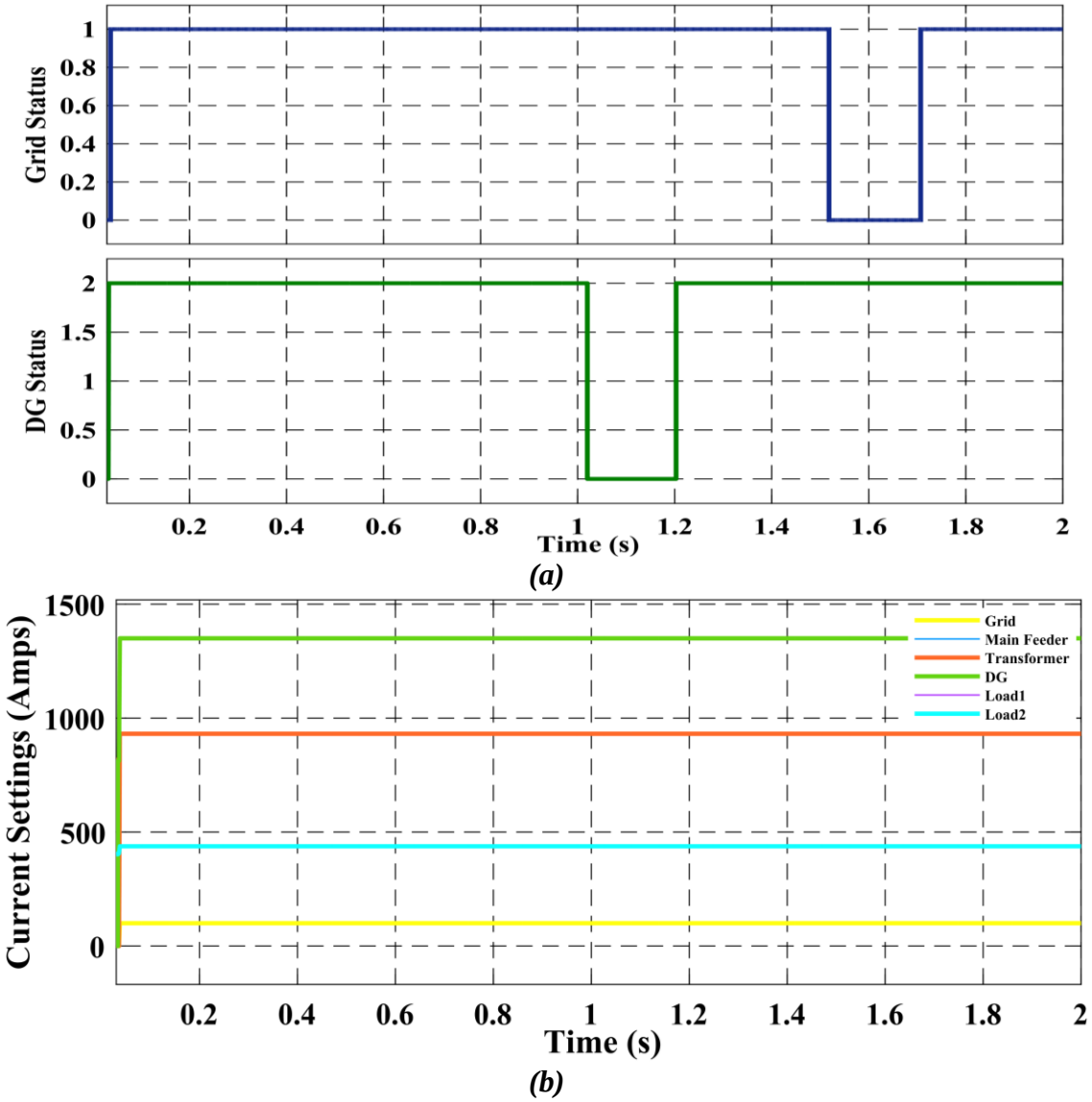

Fig. 2.11. (a) *Status of grid and DG feeding load 1 & 2 using dq components of current,* ***(b)*** *Relay settings of grid, DG and load 1 & 2 using dq components of current during normal operation*

grid in grid connected and islanded mode of operation. So, in both the cases different current infeed are to be detected by the relays for which the intelligent relays must possess the ability to detect this change in mode of operation and change the current settings as per the mode of operation.

A simple approach using change in *dq0* component of infeed current is used to check the availability of grid and DGs in microgrid mode of operation. If grid is available, then its $Grid_{status}$ is high and 1 is assigned as its status. If grid is not available, then its status is low and 0 is assigned as its status. If DG is available, then its DG_{status} is high and 1 is assigned as its status; if DG is not available, then its status is low and 0 is assigned as its status. When grid is available its status is 1 and during the interval of 1.5 to 1.7 s it is not available and its status falls to zero during the interval of 0.2 seconds. When DG is available, its status is set to 2. During the interval of 1.0 to 1.2 s it is not available and its status falls to zero during this interval of 0.2 seconds. The following ranges of different parameters are considered.

Grid range – 100 A (yellow), Transformer range – 950 A (brown), Main feeder range – 950 A (blue), DG range – 1400 A (green), DG feeder range – 1400 A (green), Load1 range – 480 A (purple) and Load2 range – 480 A (c-green).

Figure 2.11.(b) shows the settings of conventional relays which are shown as pickup current range, considering maximum 15-25 % overloading and above these current values, the steady state of utility side grid, DG and load 1-2 is lost. In this case there is no change in mode of operation, grid and DG remains in the system. During grid connected mode of operation, intelligent relays present at different locations at utility grid side, DG side, Load1 side and at Load2 side; sense no change in available currents. Due to this, the setting of all the relays which are present at different locations, remain same as conventional relays. If during microgrid operation, somehow either grid or DG are disconnected and fault occurs, this may lead to maloperation of relays present at all the locations. For only the grid feeding the load, different magnitude of current is present in the system. If the grid and DG both are present in the system then different current magnitudes are present which necessitates the need of adaptive protection scheme in microgrid structures.

2.5.2. Voltage and current characteristics – Islanded mode

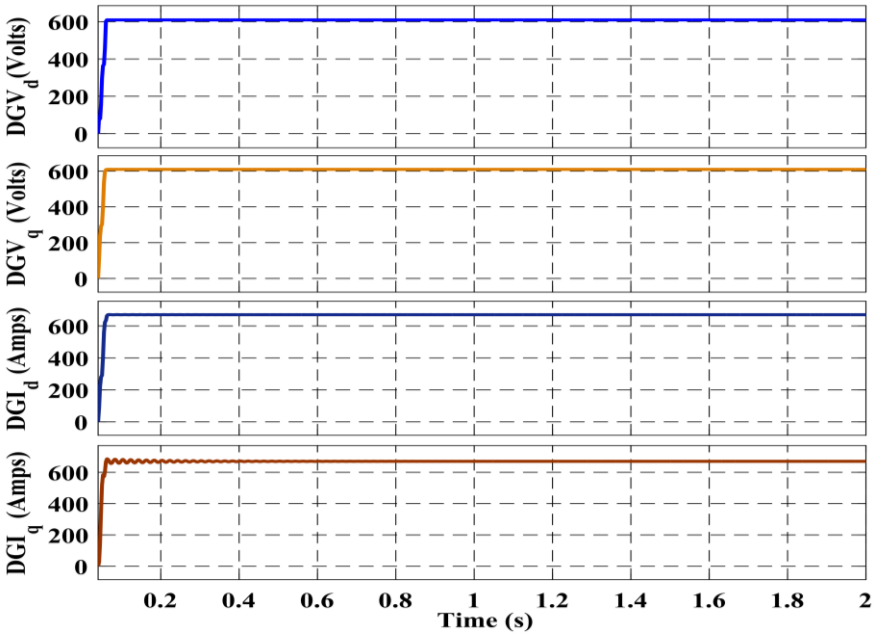

Fig. 2.12. *DG side voltages and current in terms of their dq components during islanded mode*

In this case, only DG is feeding the loads 1 and 2 at PCC as islanded mode of operation. The voltage and currents of low voltage DG in terms of *dq* components are shown. Voltage generated by DG is 600 V and current is 680 A. Figure 2.12. shows DG voltages (DG V_d and DG V_q) and currents (DG I_d and DG I_q) in terms of *dq* components. Figure 2.13. shows the voltage and currents of Load 1 and 2 in terms of *dq* components. Load 1 and 2 are of same wattage capacity

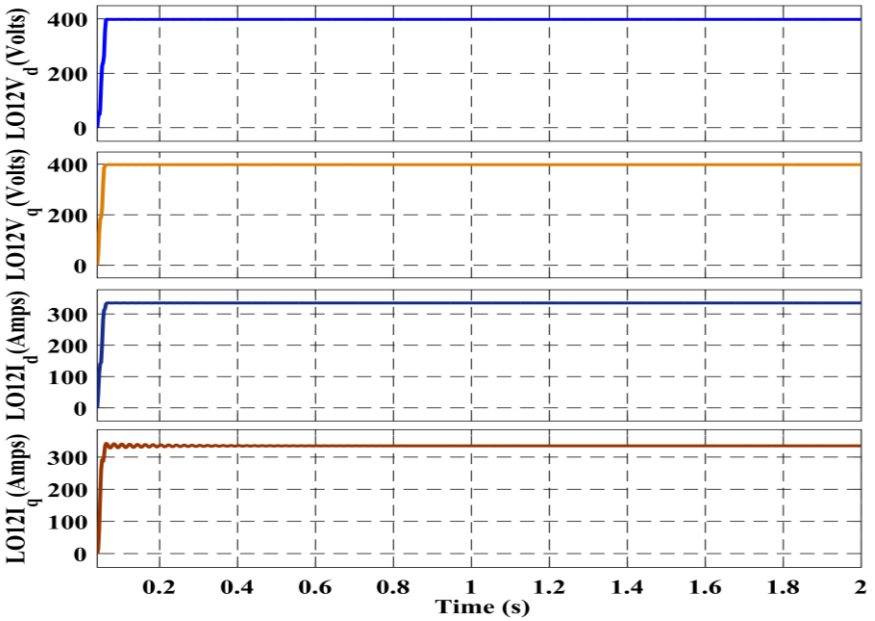

Fig. 2.13. *Load 1 & 2 side voltages and current in terms of their dq components during islanded mode*

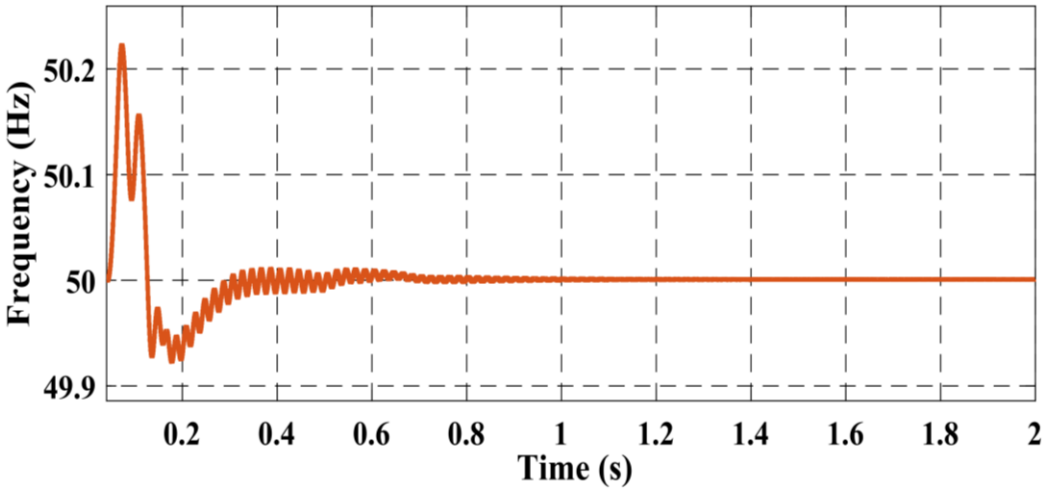

Fig. 2.14. *Frequency measured at point of common coupling during islanded mode*

and being connected in parallel they are fed at 415 V ($LO12V_d$ and $LO12V_q$) and 340 A ($LO12I_d$ and $LO12I_q$) each. During islanded mode of DG having low X/R ratio, there is small increase in frequency as speed of DG is increased to feed to load with higher voltage generation. It is of the frequency range with increase up to 50.235 Hz and drop up to 49.94 Hz. Figure 2.14 shows the frequency at point of common coupling. Total variation in frequency (Hz) at PCC is 0.295 Hz which is in the maximum allowable limit for keeping power quality standards. The voltages and currents of utility side grid and transformer are not considered as grid is not feeding the load except only DG is feeding. So, during islanded mode of operation, no feeding from grid side is observed and only DG and load sides are studied. As discussed earlier in the islanded mode of operation, only DG remains present and feeds connected loads. Steady state behaviour of designed microgrid system with only DG feeding the loads in terms of *dq* components is studied to check the feasibility of islanded mode of microgrid operation.

The following study is carried out on microgrid system shown in Figure 2.3. (a) but without utility side grid. The results are shown for islanded mode of operation with synchronous generator as DG with low X/R ratio feeding the loads as shown in Figures 2.12. to 2.15. The results as shown in Figure 2.12. - 2.15 validates the feasibility and availability of proposed microgrid in any mode of microgrid operation. The relay settings of conventional relays are shown as the pickup current range. For different conventional relays maximum 15-25 % overloading is considered. Above these current values, the steady state of DG, load 1 and load 2 is lost. In this case, there is no change in mode of operation; only DG remains in the system for feeding the Loads 1 and 2. Pickup current ranges are as follow:

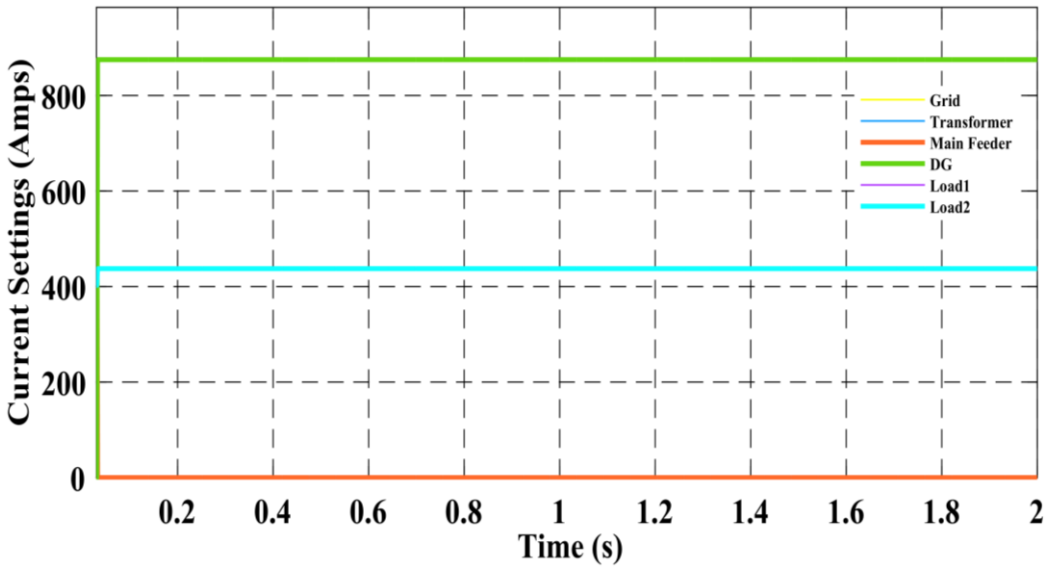

Fig. 2.15. *Relay settings of grid, DG and load 1 & 2 using dq components of current during islanded mode*

DG range – 880 A (green), DG feeder range – 880 A (green), Load1 range – 440 A (purple) and Load2 range – 440 A (c-green).

Figure 2.15 shows the conventional relay settings of DG, Load1 and Load 2. During islanded mode of operation, the intelligent relays present at different locations at DG side, Load1 side and at Load2 side sense no change in available currents. Due to this, setting of all the relays present at different locations remain same like existing conventional relays. Figure 2.15 shows pickup currents set as per existing islanded microgrid system.

Comparing relay settings for grid connected and islanded mode of microgrid operation, the drastic change is observed in pickup currents of same DG and Loads connected in the system. In grid connected mode, the DG pickup current range is 1400 A and in islanded mode it is 880 A; for loads it remains nearly same. But this will lead to maloperation of certain conventional relays present in the system during grid connected and islanding condition.

If, in any circumstance, either grid or DG fails and fault occurs, then relay may lead to maloperation. This necessitates the need of adaptive relaying for efficient, reliable and economical operation of microgrid structures [11]. An adaptive relay has that intelligence which changes the settings as per change in microgrid modes of operation.

2.5.3. Voltage and current characteristics – Utility grid and islanded mode

Voltage and current characteristics of grid connected and islanded mode individually throughout the microgrid operation have been studied earlier. It is also of utmost importance to study the grid connected and islanded modes of microgrid operation both during a specific time.

2.5.3.1. Voltage and current characteristics of grid and DG sides at PCC

Further a study is also carried out on newly designed microgrid to compare the voltage and current of utility grid, DGs and Load1-2 during intentional islanding, only grid and grid connected mode. Grid connected mode is considered from 0.0 to 2 seconds, only grid mode is simulated at 2 to 2.2 seconds and islanded modes is simulated at 3.5 to 3.7 seconds. The voltages, currents and frequency during different modes of operation are compared and shown in Figure 2.16 to Figure 2.18. In Figure 2.16, from 0.0 to 2 seconds, the grid connected mode is considered. The utility grid voltage near PCC in *d* and *q* components of voltage is found nearly 11 kV (Grid V_d and V_q, 11 kV). For same duration, the DG side *d* and *q* components of voltage is found as 440 V (DG V_d and V_q ,440 V). For the duration of 2.0 to 2.2 seconds, only grid connected mode is considered. The utility side grid voltage near PCC in *d* and *q* components of voltage is observed approximately 11 kV with drop of 100 V. For same duration, the DG side voltage near PCC in *d* and *q* components is observed as 480 V with increase in potential of 40 V due to presence of grid.

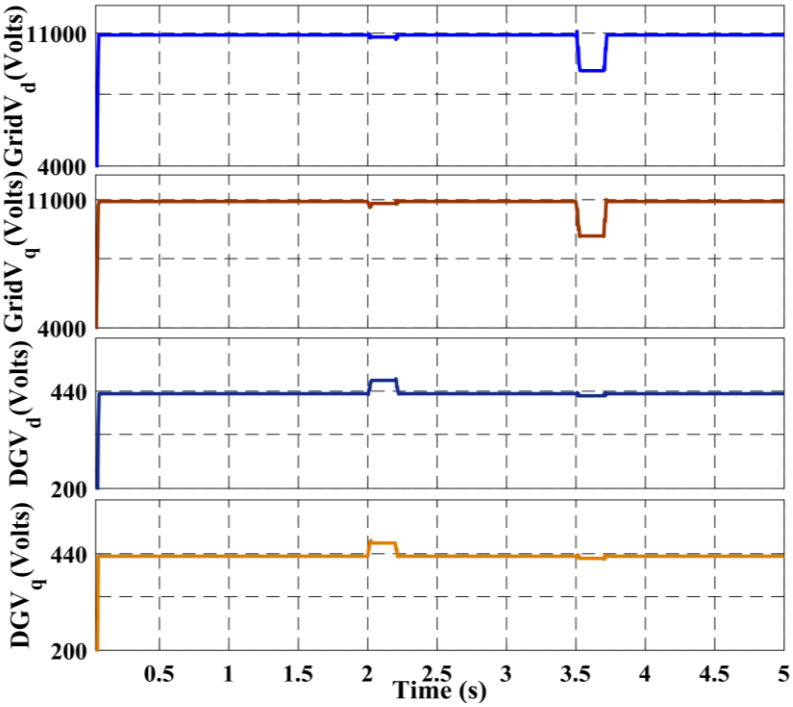

Fig. 2.16. *Voltages of grid & DG in terms of their dq components switching from grid connected to islanded mode of operation*

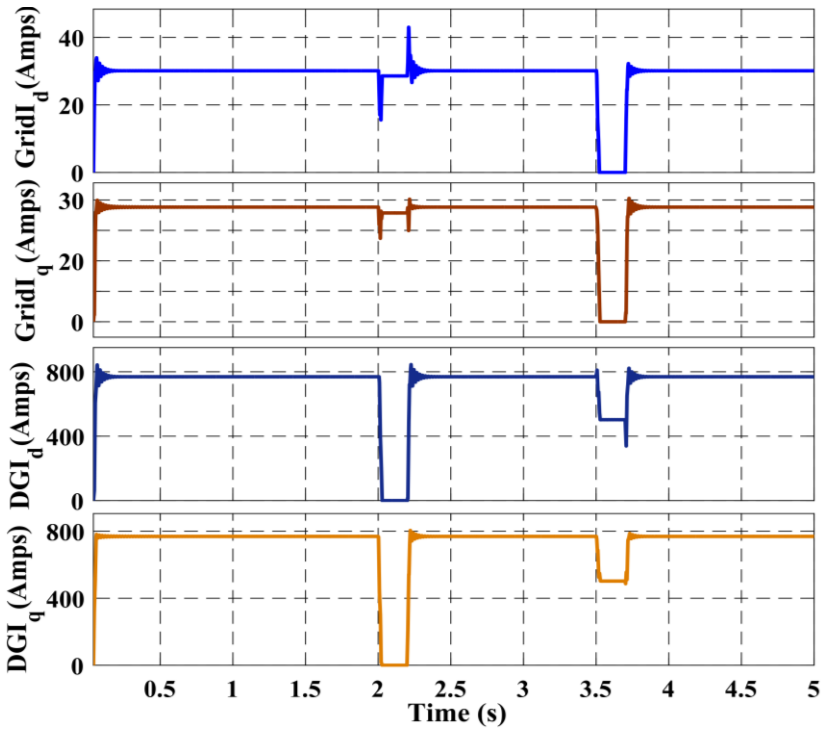

Fig. 2.17. *Currents of grid & DG in terms of their dq components switching from grid connected to islanded mode of operation*

For the duration of 2.2 to 3.5 seconds, again grid connected mode is present with changes as discussed for 0.0 to 2.0 seconds. For the duration of 3.5 to 3.7 seconds, during islanded mode, the utility side grid voltage near PCC is observed in *d* and *q* components of voltage has a drop of 2 kV. For same duration, the DG side voltage near PCC in *d* and *q* components of voltage is observed as 440 V with drop in potential of 10 V. For the duration of 3.7 to 5.0 seconds, again grid connected mode is restored with the same magnitudes of all the parameters as observed for 0.0 to 2.0 seconds.

From the results shown in Figure 2.17, for the duration of 0.0 to 2 seconds during grid connected mode; the utility side grid current (Grid I_d and I_q, 27 A) at PCC in *d* and *q* components of current is found as almost 30 A. For same duration, the DG side current (DG I_d and I_q) at PCC in *d* and *q* components of current is near to 780 A. For the duration of 2.0 to 2.2 seconds, during only grid connected mode, the utility grid current at PCC in *d* and *q* components of current is near 30 A. For, same duration, the DG side current (DG I_d and I_q) at PCC in d and *q* components of current falls to 0 A. During reconnection of DG the sudden increase in grid side current 30 A is observed at 2.2 seconds.

For the duration of 2.2 to 3.5 seconds, again grid connected mode is appeared with changes in current as discussed for 0.0 to 2.0 seconds. For the duration of 3.5 to 3.7 seconds during islanded

mode, the utility grid current at PCC in *d* and *q* components of current drops to 0 A and for same duration DG current at PCC in *d* and *q* components of current falls to 600 A. For the duration of 3.7 to 5.0 seconds, again grid connected mode has appeared with similar changes in current as discussed for 0.0 to 2.0 seconds. With the above comparison of voltages and currents in terms of *dq* components for both utility side grid and DG, it has been revealed that *d* and *q* components of current and voltage show nearly same change but while changing from steady state to transient state, more change is observed in *q* components of both voltage and current.

2.5.3.2. Voltage and current characteristics of Load1 and Load2 sides at PCC

During voltage comparison for the duration of 0.0 to 2 seconds, in the grid connected mode, the voltage of Loads 1 and 2 near PCC in *d* and *q* components of voltage ($LO12V_d$ and $LO12V_q$) is found approximately 415 V as shown in Figure 2.18. For the duration of 2.0 to 2.2 seconds, in grid connected mode, the voltage of Load 1-2 near PCC in *d* and *q* components of voltage is found near 400 V with drop of nearly 15 V each for both loads. For the duration of 2.2 to 3.5 seconds again grid connected mode is present with similar changes as discussed for 0.0 to 2.0 seconds. For the duration of 3.5 to 3.7 seconds, during islanded mode, the Load 1-2 side voltage near PCC in *d* and *q* components of voltage is 360 V and has a drop of 40 V each for both loads. For the duration

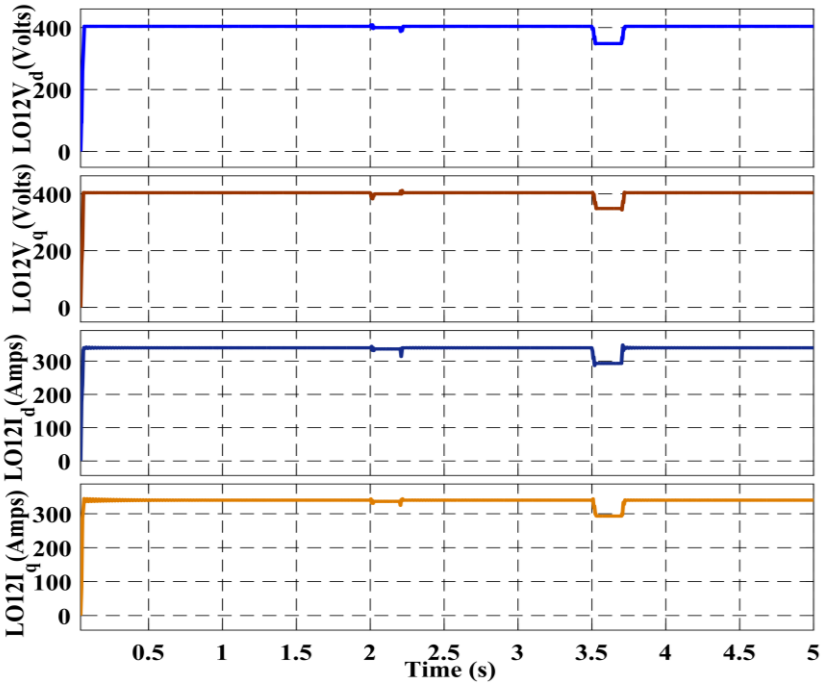

Fig. 2.18. *Voltages & currents of Load1-2 in terms of their dq components switching from grid connected to islanded mode of operation*

of 3.7 to 5.0 seconds, again grid connected mode is appeared with changes as discussed for 0.0 to 2.0 or 2.2 to 3.5 seconds.

For current comparison in the duration of 0.0 to 2 seconds during grid connected mode, the Load 1-2 side current at PCC in *d* and *q* components of current ($LO12I_d$ and $LO12I_q$) is near 350 A. For the duration of 2.0 to 2.2 seconds, in only grid connected mode, the Load 1-2 side current at PCC in *d* and *q* components of current is observed as 320 A with drop of nearly 30 A each for both loads. For the duration of 2.2 to 3.5 seconds, again grid connected mode is appeared with similar changes as discussed for 0.0 to 2.0 seconds. For the duration of 3.5 to 3.7 seconds, in islanded mode, the Load 1-2 side current at PCC in *d* and *q* components of current is 295 A and shows a drop of 55 A each for both loads. For the duration of 3.7 to 5.0 seconds again grid connected mode is present with similar changes as discussed for 0.0 to 2.0 or 2.2 to 3.5 seconds.

2.5.4. Frequency at PCC

During frequency comparison shown in Figure 2.19, in the duration from 0.0 to 2 seconds, the grid connected mode frequency (Hz) at PCC is observed approximately 50 Hz. Initial frequency fluctuations are observed due to integration of generators with different X/R ratio. For the duration of 2.0 to 2.2 seconds, only grid connected mode frequency at PCC is found near to 50 Hz with initial drop of approximately 0.2 Hz and rise of 0.2 Hz. For the duration of 2.2 to 3.5 seconds, again grid connected mode has been occurred with similar kind of changes as discussed for 0.0 to 2.0 seconds. For the duration of 3.5 to 3.7 seconds during islanded mode, the frequency at PCC is observed nearly 50 Hz with rise of 0.25 Hz and drop of 0.2 Hz. For the duration of 3.7

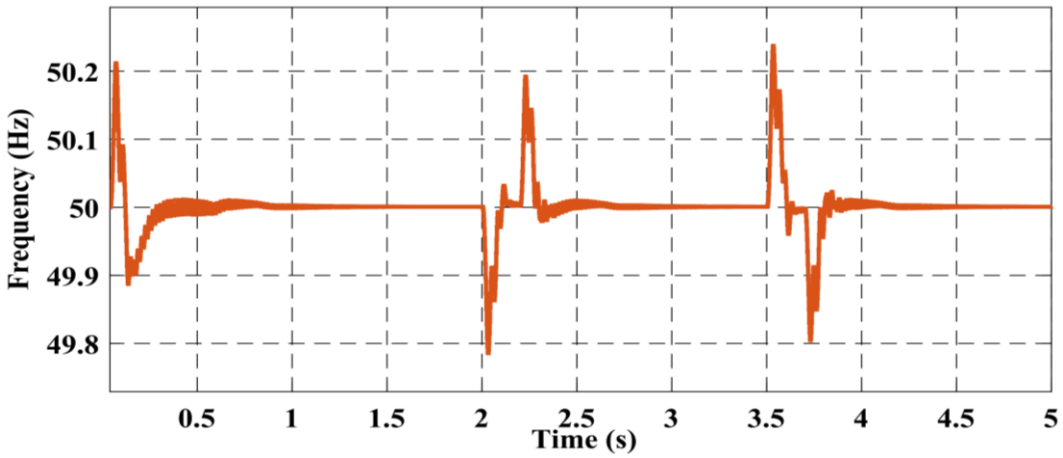

Fig. 2.19. *Frequency at PCC during switching from grid connected to islanded mode of operation*

to 5.0 seconds again grid connected mode is present with changes as discussed for 0.0 to 2.0 or 2.2 to 3.5 seconds. The above Sections 2.5.3.1.-2.5.3.2. show that with change in mode of operation in microgrid structure, there is identifiable change of voltage and current. Change in *dq* component of voltage and current varies whether grid is connected or disconnected. Also, the change in *dq* component of voltage and current during connection and disconnection of DG is different from grid connected case. This shows that during different modes of operation, the voltage and current magnitudes are different. If any fault occurs during different modes of operation at same location, the voltages and currents can be different for each mode because of which the relay will not operate properly to sense the fault current. This necessitates the need of an adaptive relay which can change its settings depending on mode of operation for efficient and reliable operation of microgrids.

2.6. Conventional protection schemes

When a large number converter based distributed energy resources (DERs) are connected in microgrid, the fault currents of only 2–3 times the full load current (or even less depending on control method of converter) are mentioned in [2]. The conventional OC protection devices are usually set to operate at 2–10 times the full load current. Hence, due to this drastic reduction of fault level, the time-current coordination of OC protective devices is disturbed; the high-set instantaneous OC devices with extremely inverse characteristics like fuses are most likely to be affected. So there is a need of real time fault location techniques to locate faults accurately. But these techniques are costlier as compared to current transformer (CT) based zero sequence detection, differential current and/or voltage methods. More emphasis should be given on real time techniques or on to CT based zero sequence detection, differential current or voltage methods. Conventional protection techniques for distribution systems are based on radial nature of distribution network, mainly consisting of fuses and reclosers, also in some cases, relays, has been designed for the system to be radial. When the DGs are connected to system than that part of system can't be treated purely as a radial or as a ring main network. So radial or ring main network coordination can't work properly. Coordination of microgrid system depends on size (medium/low voltage), type (supply), and location of DGs in microgrid.

2.7. Converter protection

Inverter interfaced based DGs tend to have less impact since the magnitude of the short circuit currents are low compared to conventional synchronous generators. They are modeled as controlled voltage sources. FCLs have been proposed as a means for mitigating the impact of conventional synchronous generators on protection coordination. IIDGs have highly variable characteristics they alter the grid structure and jeopardize safe and reliable operation. IIDGs have high non linear and varying characteristics. It is a big challenge to calculate the fault contribution of IIDGs and also inertia is not present. It is accepted that the fault contribution of IIDGs is about 1.5 to 2 times its rated current. They can also aggravate transient disturbances occurring in microgrids or their host utility grids.

In the comparison of results for voltages and currents in *dq* components in different modes of microgrid operation, it has been observed that there occur detectable changes in *d* and *q* components. With these changes in current magnitudes at different locations, the relay settings must also change their pickup currents in different mode of microgrid operation [11]. This necessitates the importance and need of adaptive relaying again for the efficient protection system.

Chapter Summary

The DERs play important role in global energy scenario. To fulfil the increasing load demand, different nature of DGs are installed. To properly utilize renewable energy sources, different microgrid structures are to be designed. In the present research work, the microgrid structures are designed within set of guidelines and available standards based on Indian renewable energy scenario. In this simulation approach, the designed microgrid structures are facilitated with new adaptive protection scheme which reduces the research and development cost before the development of real time system. Based on the simulation studies it is also found that the dq components of voltage and current can identify the changes in mode of operation of microgrid. In further studies presented in the next chapters; the LL, LLG and LLL faults are simulated at DG side nodes, grid side nodes and at Load1-2 side nodes to validate static dq component based proposed adaptive protection scheme for different microgrid structures with reduced number of variables.

Chapter 3

Adaptive Protection Methodology Using q0 Components of Fault Current in Microgrid

Introduction

The integration of DGs in microgrids needs modification in protection schemes as compared to the traditional practices in power system to meet the high-end challenges introduced. It is revealed that during change in microgrid's mode of operation, the relays must also modify the pickup current settings [15]. When fault appears on grid or on microgrid end, the protection device settings in microgrid system should change for effective adaptive protection. Whenever a protective device is present near the fault, it should act to keep the other parts of the circuit working which must show the discrimination property. In general, three factors are used in discrimination such as time, comparison and magnitude.

In the published literature, the conventional protection techniques for distribution systems are proposed based on radial nature of distribution network which are mainly consisting of fuses and reclosers, in some cases relays have been designed for the system to be radial [3], [11]-[16]. But, when the DGs, as a source of microgrid, are connected to power system then that part of system cannot be treated as a purely radial or as a ring main network. So, radial or ring main network coordination cannot work properly for such system which needs a suitable adaptive protection. Hence, the protection coordination of microgrid system must adapt the changes as per the operating mode and the DGs present in the system [17]-[25]. The adaptive feature also depends on size (medium/low voltage), type of supply and location of DGs in microgrid. In the previous chapter, the *dq0* components of fault current has been proposed as an identifiable character for detection and removal of fault. In this chapter, the adaptive protection methodology for fault location and nature detection using *q0* components of fault current in microgrid has been proposed and verified.

3.1. Problem statement

From the comprehensive literature survey, it is revealed that there is need of a novel adaptive protection scheme which was not studied earlier in the existing literatures [26]-[31]. The proposed method considers the impact of nature of DGs, distance among the fault, relay, grid and DG. In addition, an algorithm based on *dq0* system is derived for fault location, nature and fault

identification in microgrid system. Since I_d and I_q components are independent of each other, any variation of either of the two has a distinct role in fault detection.

The quadrature axes current component corresponding to quadrature axes reactance (X_q) is normally greater than the direct axes current component corresponding to direct axes reactance (X_d) during transient conditions. Microgrid system has low X/R ratio as compared to existing power system so any change in X or R of DGs or line can play an important detectable role in fault detection. The *d*-axis reactance is more as compared to *q*-axis reactance. So, during transient conditions, change in I_d component will be less as compared to I_q component of fault current. As per above clarification, variation in *q*-component can only detect phase faults, and zero (0) component can ensure ground faults; so, it is interesting to propose that *q0* components will be sufficient for sensing all kinds of faults in adaptive protection of microgrid replacing the conventional detection method using *dq0*.

It is also realized that the number of variables for fault detection is reduced by one variable which will further ensure improved speed of operation of relay and a smaller number of protection channels reducing the overall cost and size of protection system [32]-[39]. So, *q0* components can play important role is fault detection in low X/R ratio microgrids. For given synchronous machine direct and quadrature axes current components are obtained from stator and flux linkages as referred in [40].

3.2. Static components (*dq0*)

To study the behavior of fault current in terms of static *dq0* components, it is required that these components should relate different power system parameters like voltage, current, real and reactive power etc. An approach is demonstrated below to corelate *dq0* components of fault currents and other power system parameters such as stator flux linkages, rotor flux linkages etc.

3.2.1. Stator flux linkages

$$\psi_d = -L_d I_d \ + L_{afd} I_{fd} + L_{akd} I_{kd} \qquad (3.1)$$

$$\psi_q = -L_q I_q \ + L_{akq} I_{kq} \qquad (3.2)$$

Stator flux linkages for synchronous machine are given as shown in equations (3.1) and (3.2). Where ψ_d and ψ_q are the direct and quadrature axes flux linkages of stator. L_d , L_q and L_{afd} are

inductances of direct, quadrature and field (mutual) axes. I_d, $I_q$and I_{fd} are direct, quadrature and field axes currents. L_{akd} , L_{akq} are mutual direct and quadrature axes inductances, I_{kd} and I_{kq} are direct and quadrature axes currents of rotor.

3.2.2. Rotor flux linkages

$$\psi_{kd} = -\frac{3}{2}L_{akd}I_d \ + L_{kkd}I_{kd} + L_{fkd}I_{fd} \tag{3.3}$$

$$\psi_{kq} = -\frac{3}{2}L_{akq}I_q \ + L_{kkq}I_{kq} \tag{3.4}$$

Rotor flux linkages for synchronous machine are given as shown in equations (3.3) and (3.4). Where ψ_{kd} and $\psi_{kq}$are the direct and quadrature axes flux linkages of rotor. L_{kkd} , L_{kkq} and L_{fkd} are inductances of direct, quadrature and field (mutual) axes for rotor and stator currents are given as (3.5) and (3.6):

$$I_d = \frac{-E_d \ + \psi_q P\Theta + \ P\psi_d}{R_a} \tag{3.5}$$

$$I_q = \frac{-E_q \ + \psi_d P\Theta + \ P\psi_q}{R_a} \tag{3.6}$$

$\Theta = \ \omega_r t$

E_d and E_q are the direct and quadrature axes voltages of the stator axes of synchronous machine R_a is armature resistance. *P* is first order derivative *(d/dt).* Θ is angular displacement and ω_r is rotor speed. Real and reactive powers are gives us:

$$e_d \ = \ \frac{P_t - e_q i_q}{i_d} \tag{3.7}$$

$$e_q \ = \ \frac{Q_t + e_d i_q}{i_d} \tag{3.8}$$

P_t and Q_t are the real and reactive powers at the terminals of synchronous machine. From relation (3.7) and (3.8) real and reactive power during transients can also be easily calculated or studied using dq components. During transient conditions derivative components Θ, $P\psi_d$ and $P\psi_q$ as

shown in relations (3.5) and (3.6) cannot be neglected [40].Where $P\psi_d$ and $P\psi_q$ are speed voltages (due to flux change in space) and transformer voltages (due to flux change in time).

E_d is the voltage induced by flux ψ_q and E_q is the voltage induced by flux ψ_d. From the above relations it clear that *d* axis flux linkage is more than *q* axis flux linkage due to presence of field flux linkage component. So, *d* axis has more reactance as compared to *q* axis. Stator voltages for *d* and *q* axis show that the derivative change in *d* axis and *q* axis flux will play important role during transient conditions.

Also, from [41]

$$X_d = \frac{Maximum\ armature\ terminal\ voltage\ per\ phase}{Minimum\ armture\ current\ per\ phase}$$

$$X_q = \frac{Minimum\ armature\ terminal\ voltage\ per\ phase}{Maximum\ armture\ current\ per\ phase}$$

It could be concluded that the quadrature axes current component corresponding to X_q is going to be greater than direct axes current component corresponding to X_d during transient conditions. The main objective of *dq0* component analysis for faulty condition is variable reduction in fault detection as previous methods use V_{abc} and I_{abc} rms values (six variables) for fault detection and identification. In case of *dq0* components we need only three variables, and no need of rms values. *dq0* components can easily replace sequence components as they only have differed in magnitudes. I_d and I_q components are independent of each other.

The main objective of *dq0* component analysis for faulty condition is the use of reduced number of variables in fault detection as previous methods use V_{abc} and I_{abc} rms values (six variables) for fault detection and identification. In case of *dq0* components only three variables are required, and no need of rms values. *dq0* components can easily replace sequence components as they only have differed in magnitudes. Also, I_d and I_q components are independent of each other ensuring reliability in new protection methodology. Three different combinations of *dq0* components can be used for fault detection and identification that are *dq*, *d0* and *q0*. Zero component of fault current shows same behavior as that of zero sequence component which is helpful in ground fault detection as zero component flows only when ground path is available for three-phase currents to flow. So, only *dq* base technique cannot be used for proper fault detection.

3.3. Principles of fault detection

During faulty conditions of different nature in microgrid systems, priority should be given to fault location and identification of fault nature. So, those effects of the fault in particular area and severity could be easily available beforehand. Whether it is utility grid, transformer, distribution line, DGs or load, in three phase systems, it is quite difficult to identify location of fault and nature of fault, based on three phase fault currents flowing during the abnormal condition. In case of LL and LG faults, nearly same I_{dq} currents are there, they have to be differentiated using zero sequence currents for the identification of nature of faults. LG and LLG faults also behave in nearly same manner as far as the three-phase fault currents are considered. They are again to be differentiated based on amount of zero sequence currents flowing in both of the cases.

Main problem arises when three-phase faults such as LLL, LLLG occur and fault currents flow in the microgrid system causing nearly equal voltage drop in the lines but using I_0 components they could be differentiated accordingly. In case of fault location identification in microgrid systems, impedances are less as distances among distribution lines are small with low X/R ratio of low-rated DGs. So, fault location becomes difficult based on voltage and current measurement in three-phase microgrid system and also positive-sequence component of fault current is having problem of uncertain magnitude and direction for upper branch faults [25].

To resolve these issues, a new approach can be followed using *dq0* transformations of three phase systems, where three phases are resolved into *d*-direct axis, *q*-quadrature axis and *0*-zero axis components. Three-phase currents and voltages are resolved into *dq0* components. Zero components play important role in the study of abnormal conditions as it provides information about the abnormal conditions and three-phase system could be easily recovered. In general, transformation of AC three-phase to *dq0* system is done using Park's as given below [42], following relations (3.9) – (3.10).

$$[I_{RYB}] = [K_\theta]^{-1} \times \left[I_{dq0}\right] \quad (3.9)$$

$$[V_{RYB}] = [K_\theta]^{-1} \times \left[V_{dq0}\right] \quad (3.10)$$

I_{dq0}, V_{dq0}, I_{RYB} and V_{RYB} are respective *dq0* and three phase currents and voltages. I_{RYB} and V_{RYB} are instantaneous quantities, function of time, represented in matrix form. K_θ represents *dq0*

transformation matrix, where θ represents angular displacement of *dq0* system. K_θ matrix is given as:

$$[K_\theta] = 2/3\begin{bmatrix} sin\theta & sin\,(\theta - \frac{2\pi}{3}) & sin\,(\theta + \frac{2\pi}{3}) \\ cos\theta & cos\,(\theta - \frac{2\pi}{3}) & cos\,(\theta + \frac{2\pi}{3}) \\ \frac{1}{2} & \frac{1}{2} & \frac{1}{2} \end{bmatrix}$$

Total power either in three phase form or in *dq0* form must be equal.

The system is modelled using Matlab/Simulink as a three-bus system having one slack bus, one generator bus and one load bus as shown in Figure 2.2.(a) of Chapter 2. Different faults are simulated at fifth second of simulation time and removed at eighth second, on different locations or different nodes to see their impacts on either side of PCC to study the behavior of microgrid system during different faults. Line-line (LL), line-ground (LG), line-line-ground (LLG), line-line-line (LLL), line-line-line-ground (LLLG) faults are simulated at six different nodes. For adaptive protection to be simpler and effective, availability of utility, as well DG is modelled as status signal. If status signal for grid or DG is 1 or 0 it represents their availability or unavailability, respectively. According to status signal availability, mode of operation is set as grid connected, islanded and only grid connected. Grid status is 1 for grid-connected and only grid-connected mode and 0 in islanded mode with DG status as 1. DG status is 0 in only grid-connected mode. These status values are set according to current sharing at PCC. The fault current components are measured using Simulink measurement blocks (M) presented at utility, DG and load ends and so on as shown in Figure 2.2.(a)

3.4. Proposed methodology for fault detection, location and identification

To minimize the impact of low fault currents, a new adaptive protection methodology is proposed based on *dq0* components considering equation (3.11) and (3.12). This also helps in location detection and fault nature identification.

3.4.1. Proposed methodology

In case of low/medium voltage microgrids, low fault currents especially present in converter interfaced and low rating DGs having low X/R ratio, it is crucial to determine the

location of fault and its nature for proper relaying operation and coordination among protection devices.

Adaptive protection scheme could be made more reliable and simpler using dq0 transformation scheme for locating, determining and differentiating faults. The relations for tripping action and mode of operation detection are implemented based on equations (3.11) and (3.12) as referred in [15].

$$I_{relay} = \left(I_{fG} \times Grid_{Status}\right) + \sum_{k=1}^{n}\left(k_i \times I_{fDGi} \times DGi_{Status}\right) \quad (3.11)$$

$$Also, I_{fDGi} = I_{rated}^{DGi} \times G \quad (3.12)$$

Where I_{relay} is the current, according to which relay is to be set for operation when set value is crossed during abnormal condition. n is the total number of DGs in the microgrid, I_{fG} is the current share of utility grid during abnormal conditions. The operating mode of utility grid decides whether the microgrid is operating in grid connected mode with DGs, without DGs but connected with grid and islanded mode.

The status value of operating mode is 1, when grid is connected and 0 when disconnected which is set as per their current share at PCC of microgrid system. k_i is the impact factor of i^{th} DG on the fault current of the relay *r*, I_{fDGi} is the maximum fault current contribution of i^{th} DG, I_{rated}^{DGi} is the rated current of i^{th} DG and *G* is current coefficient, whose value depends on nature of DG, Its values lies in the range of 1 p.u. (100 %) to 4 p.u. (400%) for inverter interfaced DGs (IIDGs) and for rotating machines it is 5 p.u. (500%) or more than 1000 percent as mentioned in [42]. So *G* is different for IIDGs and rotating machines, where current coefficient of rotating machine is high as compared to IIDGs. Range of k_i is dependent upon impedance between relay and fault point, DGi_{Status} range value is dependent on whether they are in operation or not. DGi_{Status} is 1 for DG in operation and 0 for not in operation. In a given system, value of k_i could be calculated depending on the distance between the relays and DGs as mentioned in [15].

DGs impact factor depends on the impedance between the DGs and relays, within radial distribution. In general, fault current is dependent on fault impedance, source impedance, load impedance and feeder line impedance or the actual impedance existing between them during abnormal condition. Also, in adaptive protection scheme, protection settings of DGs can be adjusted according to change across transformer operation while implementing differential

Table 3.1 Status and adaptive relay setting

Grid (status)	DG (status)	Action Adaptive Relay Settings
0	0	No Operation Mode
0	1	Islanded Mode
1	0	Only Grid Connected Mode
1	1	Grid Connected Mode

protection. It becomes important to identify location of fault from the perspective of DGs and utility grids location from fault point.

Relations (3.11) and (3.12) are used to identify the nature of DGs connected which is not done in [15]. Same relations are also used to find availability of fault currents from DGs and grid during faulty condition. Adaptive relay setting is also updated using relations (3.11) and (3.12). Relations (3.11) and (3.12) are also recommended to be used to minimize the fault location area by updating available zones in the microgrid structure. Constant G is obtained to determine the nature of DGs connected and fault share of DGs. Adaptive relay settings are updated according to status set as shown in the following Table 3.1.

3.4.2. Location detection and fault identification

The equations (3.11) and (3.12) play distinctive roles in locating the fault and its identification. Location detection and fault identification algorithms are based on offline calculations that are compared to determine any unbalanced condition with a set of fixed values based on steady state and transient state of the given microgrid system. In fault location and type detection algorithm, first step is to check the status of different available nodes. If given node is available, its status will be 1 else 0. In the microgrid, as mentioned in Figure 2.2.(a) there are 9 nodes representing five different components of given microgrid system.

Status of utility grid and DGs are generally considered, as they are the main sources for fault currents. In second step, depending on the three-phase root mean square values (r.m.s.) of currents, status is set. In third step, according to the status of utility grid and DG in the microgrid system node detection algorithm is activated, that gives the different nodes available in the microgrid system. That also indicates the modes of operation for microgrid initially. Depending

on the activated zone detection algorithm, the fault is cleared in microgrid operation. According to assigned mode of operation in previous steps, three different algorithms can run in parallel for determination of fault location in fourth step. When the fault location algorithm is activated according to mode of operation, in addition fault location algorithm also runs in parallel along with fault identification algorithm.

As trip current is dependent on these relations or in other way trip time setting of relay is dependent on these relations in fault location process three phase fault currents are transformed into *dq0* components using relations (3.9) and (3.10), keeping θ zero for simplicity and their r.m.s. values are compared with given set of steady state values. Instantaneous values of fault current are compared in the form of I_d, I_q and I_0. Depending on the location or node of fault for utility grid, transformer, main feeder and DG, changes in I_0 and V_0 as *dq0* components are sufficient to identify the location or the node facing abnormal condition.

Independent fault location in case of loads can be easily identified using only I_q and I_0 components. In case of fault nature identification for utility grid, transformer, main feeder line and DG, it is done using six variables, which are I_{dq0} and V_{dq0}. Different logics implemented in algorithm for fault nature identification are discussed as follow.

3.4.3. Adaptive protection

Adaptive protection used for different modes of operation is discussed as per the proposed algorithm shown in Figure below. The adaptive protection scheme for microgrid system is also designed as dependent on status of utility grid and DG. In the case studied, three modes of operation of microgrid are considered, those are utility connected, islanded and only grid connected. So, in this case status of utility grid and DG decides the operation of relay under different modes of operation mentioned above. Set of values for adaptive relaying action is based on pre-observed steady state values.

Decision on selecting particular set of values for relaying operation is based on mode of operation. Proper relay coordination among the different primary and secondary relays is dependent on the set of values. Different status and mode of operation can be updated using a proper communication channel based on IEEE 802.16/WiMAX as mentioned in [22]. Adaptive protection used for different modes of operation is discussed as per the proposed algorithm shown in Figure – 3.1. Depending upon the availability of utility and DG in microgrid system status are

set to high (1) and low (0). If either of the utility or DG is available in the microgrid system, then their respective status is set to 1 (high). If either of them is not available, then the status of the respective source is set to 0 (low). If both are available, then the status of both utility and DG is 1. If both are unavailable, then the status of both utility and DG is 0.

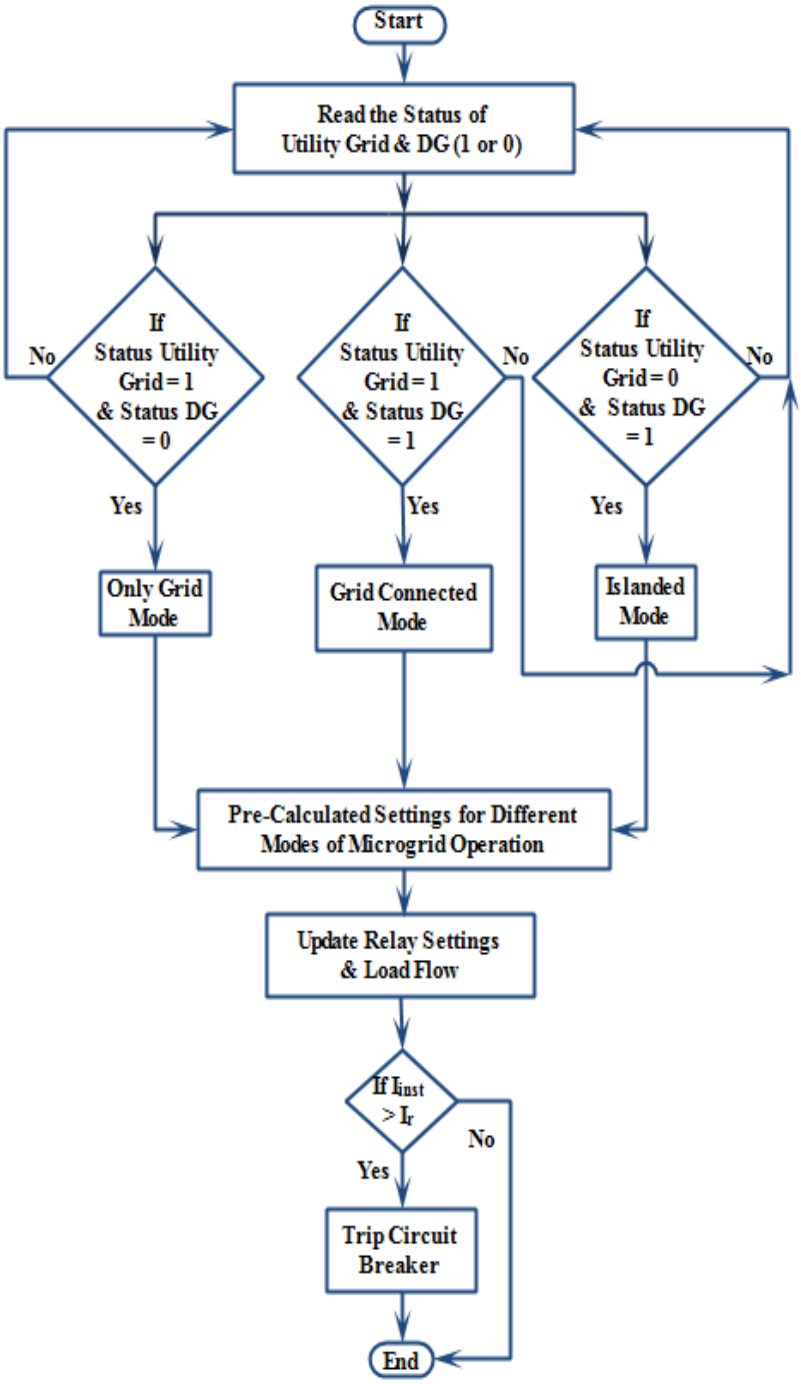

Fig. 3.1. *Algorithm for adaptive protection scheme*

Settings corresponding to the available current shared by utility and DG are updated for adaptive relaying. If status of utility and DG is 1 then available current setting are according to the share of current by both sources. If utility is not available, then current settings of relay corresponds only to DG current share. If DG is not available, then current settings of relay corresponds only to utility current share. If status for utility and DG is 0 then no action. During fault if the fault current available exceeds 1.25 p.u. value of rated current relay will have sent trip action to circuit breakers depending on the availability of utility and DG in microgrid system, which in turn depends on the status of utility and DG.

3.4.3.1. Implementation of proposed methodology

As discussed, earlier status signals for the availability of utility grid and DG are shown in Figure 3.1. Schematic diagram of proposed protection scheme is shown in Figure 3.2. As per proposed scheme the microgrid central protection unit (MCPU) should receive the information such as, status of generating units (mode of operation), adaptive settings, fault location, type of fault and independent load fault location from different parts of microgrid system. The inputs are shown in Figure 3.2. **s**chematically as individual blocks which are processed in MCPU that takes necessary action to clear fault through updating relay settings and tripping circuit breakers at

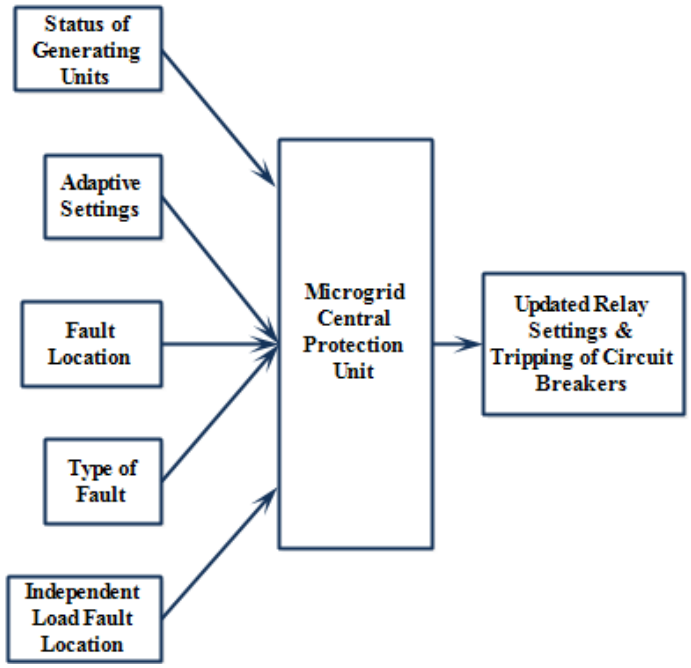

Fig. 3.2. *Block diagram of microgrid central protection unit.*

proper nodes nearest to fault. Proposed algorithms including function of individual blocks are shown in Figures 3.3 – 3.5. If the instantaneous current is more than given r.m.s. value, status is set 1 else 0. Figure 3.1. shows the role of status signals for adaptive protection.

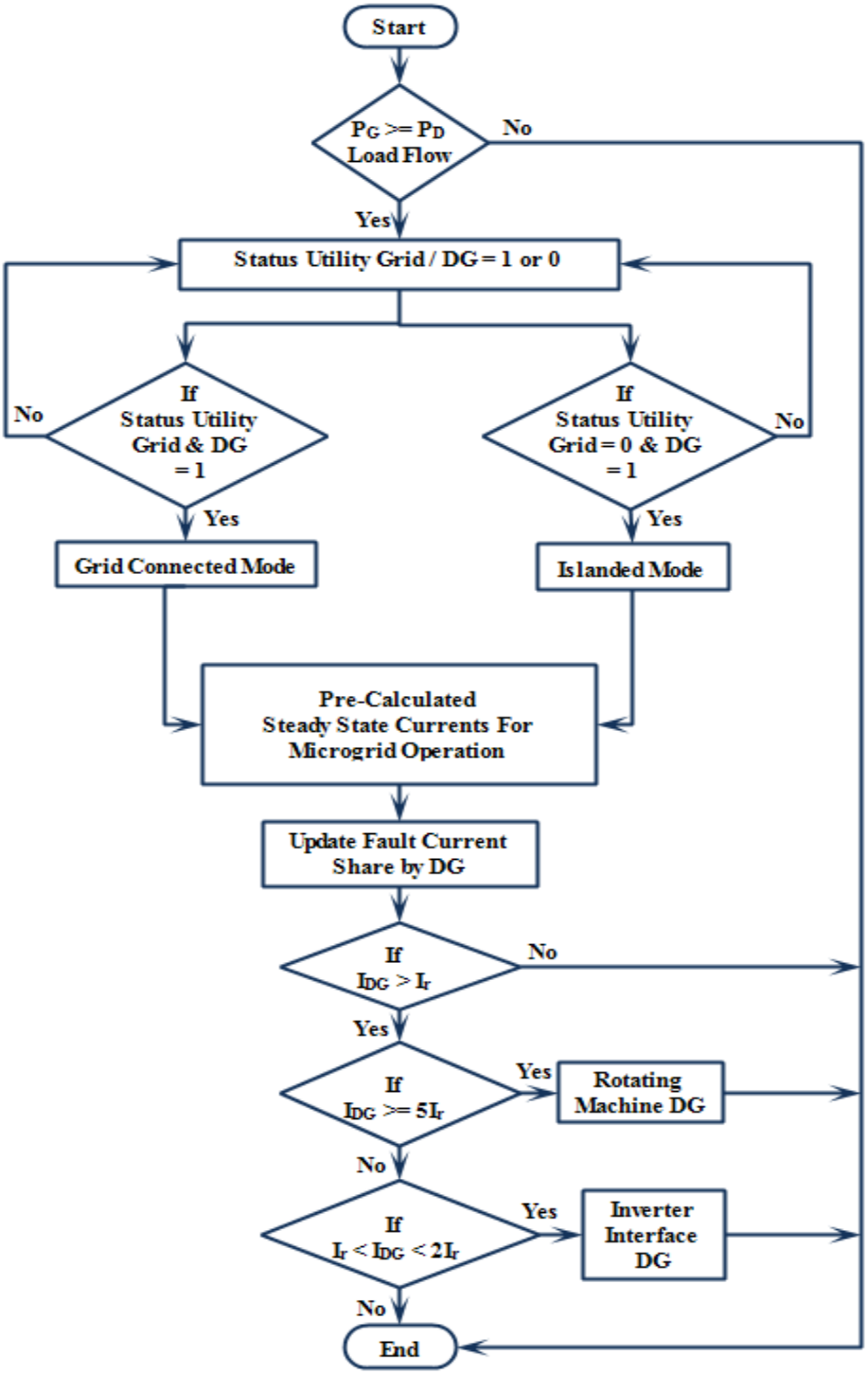

Fig. 3.3. *Algorithm of nature detection of generation in microgrid system*

In Figure 3.3. nature detection algorithm is discussed based on I_{q0} current share of respective DG's during faulty conditions. It starts with first check on whether the load demand is met or not, if generated power is equals to or greater then load demand then next step is activated else no output. Status of DG's and utility are checked as explained for flowchart in Figure 3.1. Once the DG's status is high and during fault I_{DG} is greater than I_r. If I_{DG} share is greater than five times (5 p.u.) the I_r then DG connected is a rotating machine else if I_{DG} lies between 1.2 to 2 p.u. then DG connected is an inverter interfaced DG. In Figure 3.4. fault location detection algorithm is discussed based on I_{q0} fault current available at different nodes during different faulty conditions. First step is same for status check of DG's and utility side.

When *q0* limits are violated and their comparison with steady state values is done. If that difference exceeds predefined limits of 0.15 p.u. for I_q and greater than 0 for I_0. Then comparison

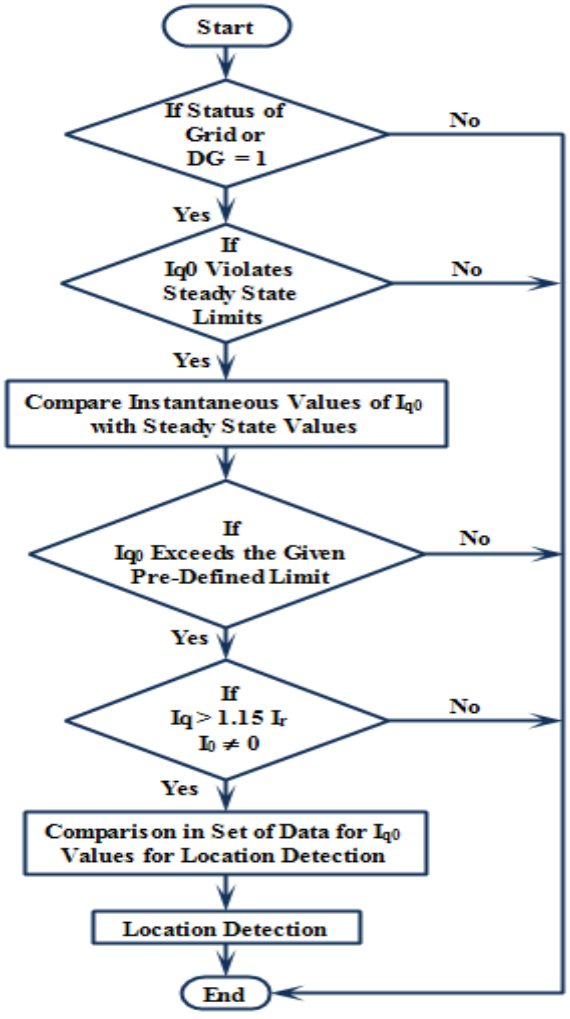

Fig. 3.4. *Algorithm of fault location detection in microgrid system*

of that difference is done for pre-defined values at different nodes and finally fault location is detected. Generation detection feature, as shown in Figure 3.3., differentiates the type of generation according to the share in fault current by respective DG. No detection feature starts based on status signals, whose purpose is to minimize the number of nodes at which fault could be possible, even for same nature of fault at different locations. Change in r.m.s. values of I_0 and V_0 is considered for location detection of fault for simplicity. If utility grid and DG, both are available then fault can occur at any of the nodes from 1-9 in Figure 2.2. In islanded mode, no role of nodes from 1-3 in fault current and if only utility grid is there, no need to consider node 4 and 7 in fault study.

3.4.3.2. Location and nature identification of fault in grid connected mode

In Figure 3.5. fault nature detection algorithm is discussed based on I_{q0} fault current available at different nodes during faulty conditions. The r.m.s. values of *dq0* are considered for

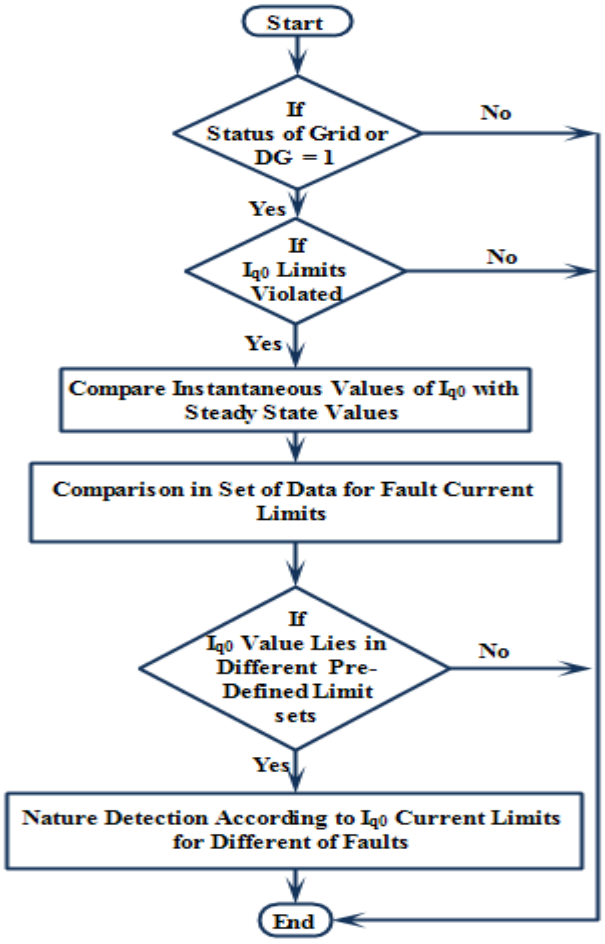

Fig. 3.5. *Algorithm of nature detection of fault in microgrid system.*

further analysis of faults. I_0 and V_0 behave differently at same node for fault at different locations, which solves the purpose for location detection using comparison with steady state values of I_0 and V_0. Three algorithms are proposed to locate fault, identify its nature and know the nature of DG supplying the fault current as shown in Figures 3.1. – 3.5. First step is same for status check of DG's and utility side. When *q0* limits are violated and their comparison with steady state values is done. If that difference exceeds the given set of values for different faults at same location and different locations. Given change in magnitude of I_{q0} decides the nature of fault.

For utility grid, transformer, main feeder at PCC, DG and load end, all kinds of fault as mentioned in principles of fault detection, are considered at all nodes. According to the status of nodes, I_0 and V_0 are compared to detect the location at which abnormal conditions prevail. After location detection, according to this fault location status, fault nature identification detection algorithm is initiated. Fault nature identification algorithm is proposed based on the different nature of faults. It depends on the characteristics of I_{dq0} and V_{dq0} for different faults which are compared to take decision on the nature of fault or type of fault. Figure 3.6 shows the layout of adaptive relay unit.

To minimize the impacts of bidirectional currents at nodes 1-4, all of the six variables are compared to get reliable decision as shown in algorithm for fault nature detection in Figure 3.5. For each and every node, for each and every fault, different sets of conditions and logics are proposed. At load end nodes, fault nature identification can be done for: LL fault based on V_0, I_q

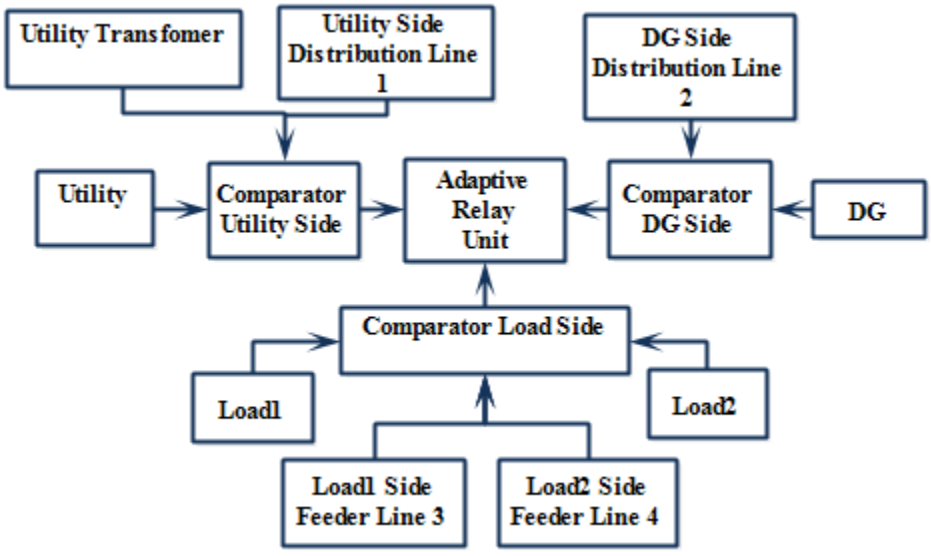

Fig. 3.6. *Layout of adaptive relay unit*

and I_0, For LG fault based on I_0 and I_d, LLG fault based on I_d, I_q and I_0, LLL fault based on I_d, I_q and I_0, LLLG fault based on I_d, I_q and V_0.

3.4.3.3. Rate of change in dq0 components

At the instant fault occurs or at the instant of removal of fault, different behavior in terms of *q0* components are observed and for same fault at different locations behavior is also different. So, rate of change in *q0* components with respect to time is also significant to identify fault location and fault nature detection in microgrid system. The rate of change on *q0* components could easily identify or locate a fault in inverter based DGs as they have low fault currents considering heat-temperature constraints of inverters and low X/R ratio.

3.4.3.4. Protection fractionalization

To make protection system more reliable and to minimize complexity and dependency of central adaptive protection; fractionalization (independently operating relays at all nodes) of microgrid protection is proposed in this research work showing detection of only load side faults independently based on *q0* components of fault current. From Table 3.2, it is clear that amount of zero sequence currents is nearly same in case of LLL and LLLG faults. But the change in zero sequence current is distinguishable during faulty condition as compared to the zero-sequence current during steady state condition. In load side fault detection technique, the Pre-set values change according to the mode of operation. So, three different sets of values are required for reliable operation of fault detection on load side. Table 3.2. shows the one set of values of zero sequence component of fault current in grid connected mode. Q-component of fault current is required only in case of LL and LLL to faults, where zero component of fault current is negligible. In rest of the cases zero components is sufficient for fast detection of fault on microgrid side.

Table 3.2. Zero components of fault current on load side

Fault type on load	I_0 (A) (LL)	I_0 (A) (LG)	I_0 (A) (LLG)	I_0 (A) (LLL)	I_0 (A) (LLLG)
Load1	1 to 3.7×10^{-6}	38 to 48	20 to 34	1 to 7.15×10^{-9}	1.8×10^{-8} to 6.25×10^{-9}
Load2	1 to 3.7×10^{-6}	38 to 48	20 to 34	1 to 7.15×10^{-9}	1.8×10^{-8} to 6.25×10^{-9}

3.5. Results and discussion

To check the feasibility and effectiveness of *q0* component based adaptive protection scheme for different types of faults, a comparison with sequence components is described below.

3.5.1. Sequence and dq0 components

Comparison of *dq0* and sequence-components for the same microgrid system with LLG fault on utility side (0.3-0.5s) and DG side (0.7-0.9s) are shown in Figure 3.7. For DG share in fault current (I_d, I_{+ve} *seq*, I_q and I_{-ve} *seq*) during (0.3-0.5s) when LLG fault is on utility side, the increase in *d*-axis component, positive-sequence component and *q*-axis component for LLG fault on utility side are nearly same. In negative-sequence component, only a spike showing low share for fault on utility side appears because of low X/R of DG.

For DG share in fault current during (0.7-0.9s) when LLG fault is on DG side the increase in *d*-axis component as a negative spike are observed and current increases. For positive-sequence component, negative spike is observed, in case of *q*-axis component negative spike occurs and it

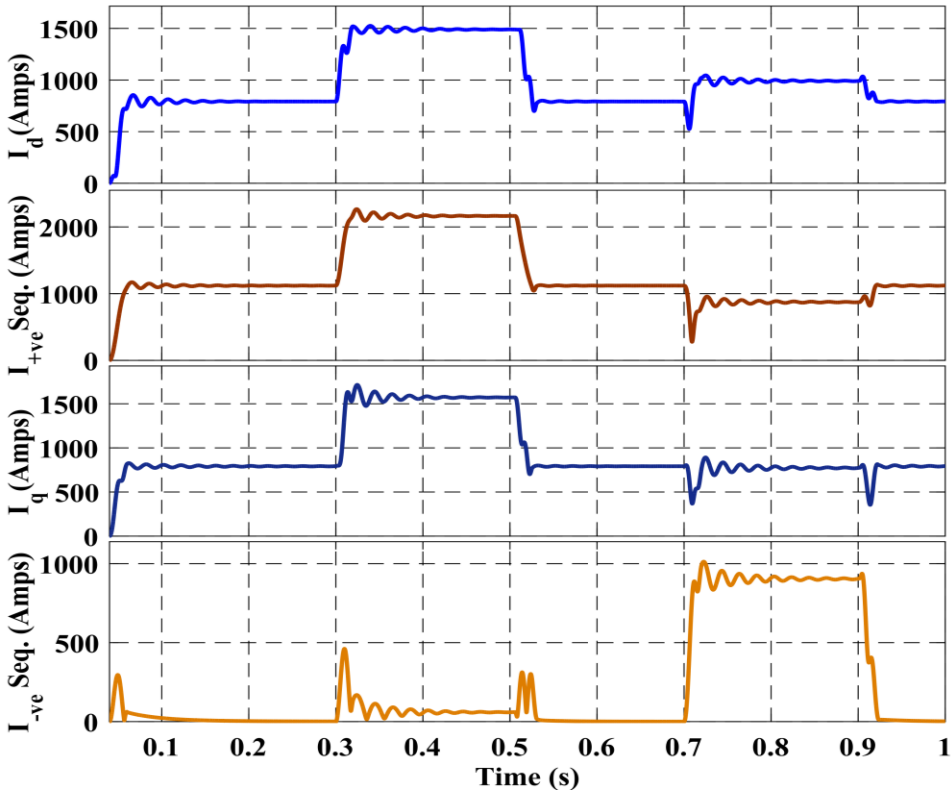

Fig. 3.7. *Comparison of direct axis, positive sequence, quadrature axis, and negative sequence component of current*

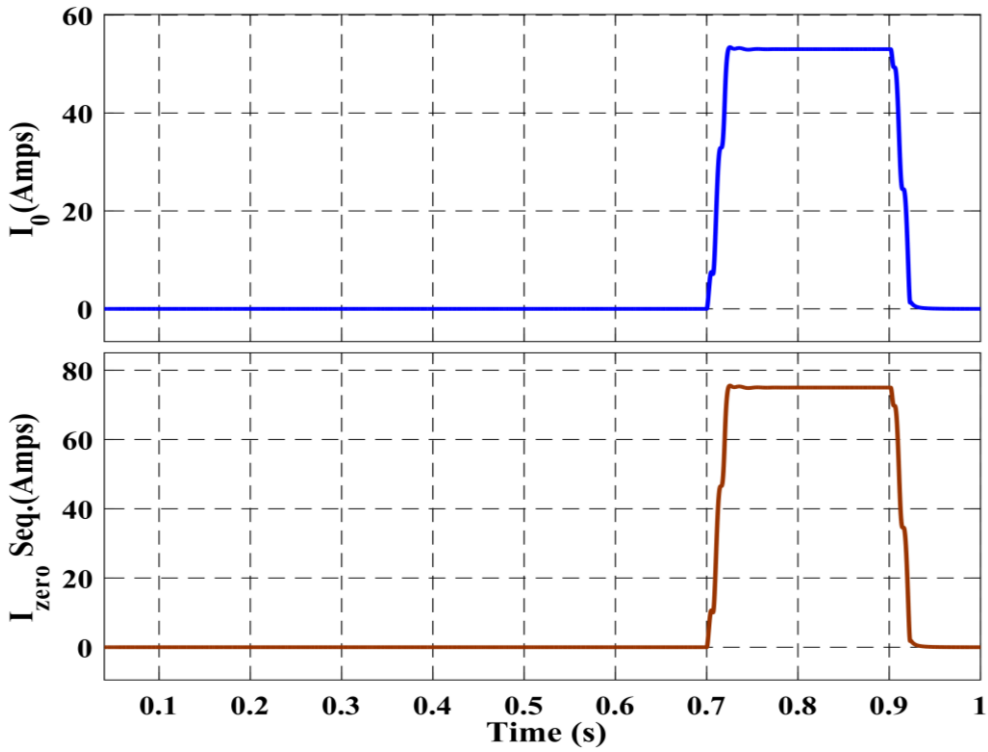

Fig. 3.8. *Comparison of zero axis, and zero sequence component of current*

reaches to steady state while negative-sequence component increases. An increase in I_0 axis component occurs until the fault is present and same change observed in zero sequence current. As shown in Figure 3.8. for LLG fault on utility side no change in I_0 component (0 to 50 A) and I_{zero} sequence component (0 to 50 A) of current shared by DG is observed.

The equation 3.13 represents the location and fault nature matrix *(LN)* which is a sparse matrix. Its order is governed by number of different nodes and type of faults. In (5 × 6) order, Rows 1-5 represent LL, LG, LLG, LLL and LLLG faults. Columns 1-6 represent nodes; utility grid, transformer, feeder, DG, load1 and load2. Elements LN_{11}, in a given matrix is high or 1 showing LL fault at utility grid node and the rest of elements are zero showing no other fault at any other node is no fault condition at other nodes that are transformer (node2), feeder (node3) and load2 (node6). In [15] role of different types of generation during abnormal conditions is discussed only for IIDGs and rotating machines. The *LN* matrix is:

$$LN = \begin{bmatrix} 1 & 0 & 0 & 0 & 0 & 0 \\ 0 & 0 & 0 & 0 & 0 & 0 \\ 0 & 0 & 0 & 0 & 0 & 0 \\ 0 & 0 & 0 & 0 & 0 & 0 \\ 0 & 0 & 0 & 0 & 0 & 0 \end{bmatrix} \quad (3.13)$$

As per equations (3.11) and (3.12) it is revealed that any type of generation shows its own impact on fault current share. Therefore, a nature governing constant is proposed to derive the role of different generation in adaptive protection study of microgrid whereas [22] and [43] have worked about data sharing through wireless as per protocol IEEE 802.16 based WiMAX for adaptive protection.

As per [22] and [43], an adaptive protection system is designed to work according to IEC61850-7-420. The impact of communication delays and relay hierarchy are also discussed. In this present work the role of different faults, location detection and nature identification of faults has been investigated using equations (3.11) - (3.12). The adaptive protection and fractionalization of microgrid protection schemes are considered for improving reliability, decreasing complexity and dependency on one central protection unit.

Problem of uncertain magnitude and direction for upper branch faults [25] is minimized by adaptive protection using change in *q0* components applicable to any mode of operation in radial or ring main network as magnitude of *q0* components are location and nature specific and validated in Matlab/Simulink environment. Instead of one central control strategy, fractionalized protection strategy is used for smooth protection operation on load side. In [25] use of distributed dynamic state estimation is considered for making an adaptive free protection system but that has increased the complexity of protection system and it has made the system more centralized which is going to effect the independency of relays while switching from grid connected to islanded mode of operation and also during only grid connected mode of operation.

A protection for only IIDG scenario and type of faults considered are mainly common for transmission systems like three phase faults and high impedance faults [42] which are very much less in small microgrid structure, no role of zero sequence fault currents and voltages is discussed in fault detection. In this research work role of quadrature and zero sequence components in fault location detection and fault nature detection are verified. As an adaptive protection works in coordination with fault location detection and nature detection it is easily implementable in any type of generation. Only zero sequence components are used in location detection of faults which are common in distribution networks. For three phase faults and their smooth nature detection mainly quadrature and zero sequence components of fault current and voltage are considered.

3.5.2. Adaptive settings

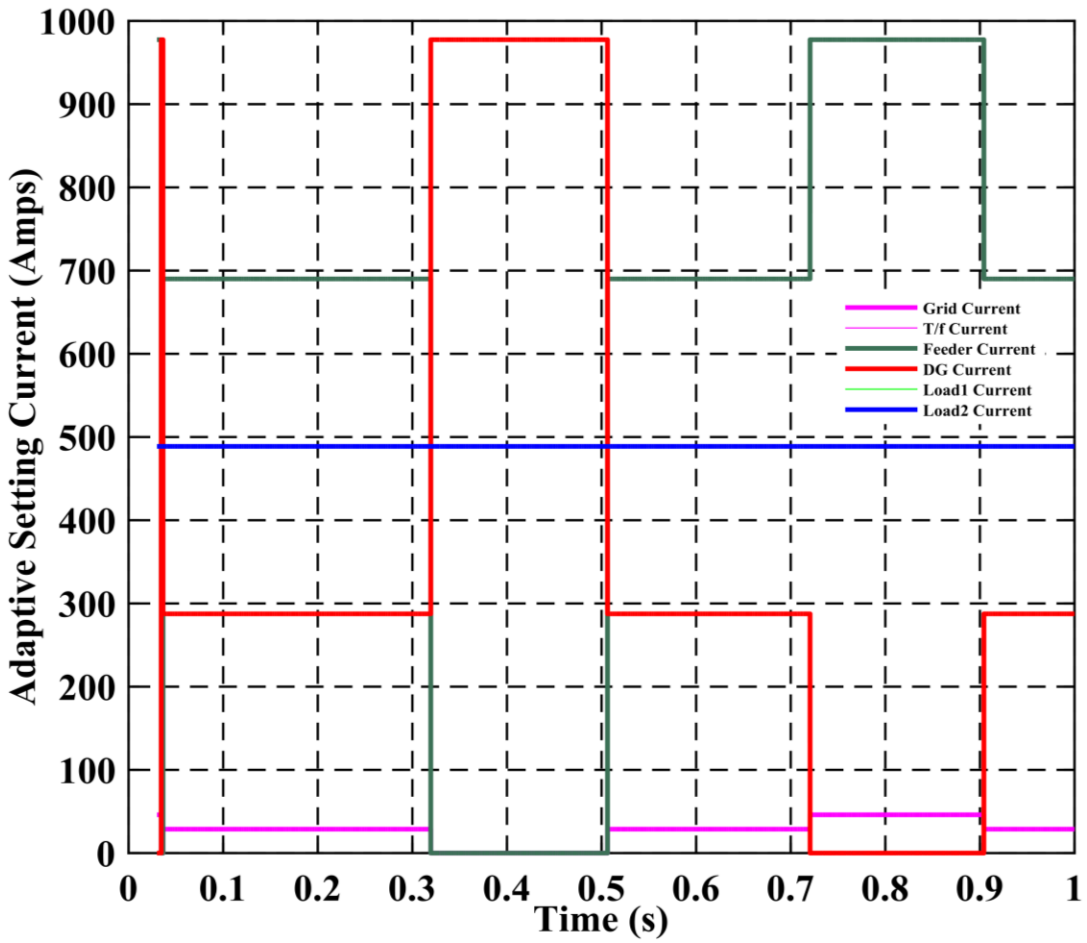

Fig. 3.9. *Output of an adaptive protection algorithm*

Adaptive relay decision is based on change in fault current in terms of dq0 components of current transformer currents. Figure 3.9. shows the trip current settings (Adaptive Settings Current) of adaptive protection scheme for relays which are changed or updated as the microgrid mode of operation changes for any of the modes such as grid connected mode (0 to 0.3 s, 0.5 to 0.7 s and 0.9 to 1 s), islanded mode (0.3 to 0.5 s) and only grid connected mode without DGs (0.7 to 0.9 s). In this research work on adaptive protection scheme; only grid connected mode, while all DGs are available, is taken into account along with other modes. This is normally ignored in most of the cases of microgrid protection. In the extreme case, if none of the DGs are in operation; the trip settings for adaptive protection can be modified promptly with minimum impact due to unavailability of DG in microgrid operation.

3.5.3. Fault location and detection

In this research only dynamics during fault occurrence for every node are considered

independently whose results are shown in Figures 3.10 – 3.15, to make fault detection easier and much simpler. Every node has different dynamic behavior for different faults and for different location of same faults. Also, in [44] prims aided Dijkstra's algorithm is used for fault detection which runs after isolation from utility grid, for which there is delay in fault location detection, but if microgrid is not islanded then prims aided algorithm will not be successful in fault detection, hence reliability of system will be affected. But in this research work, it is done instantaneously at the moment of fault using time derivative. Feed currents retrieved from both ends are processed using MHW to obtain the detail signals, which are used to obtain a primary protection scheme for the feeder and same scheme was investigated for backup protection in islanded and grid connected mode of operation, for radial and looped system for various disturbances, which is a time consuming and complex process [45].

3.5.3.1. LLL fault detection

In this research work, instead of time domain, time derivative is used to get fast relaying action in all applicable modes. As shown in Figure 3.10, it is important to use I_q instead of

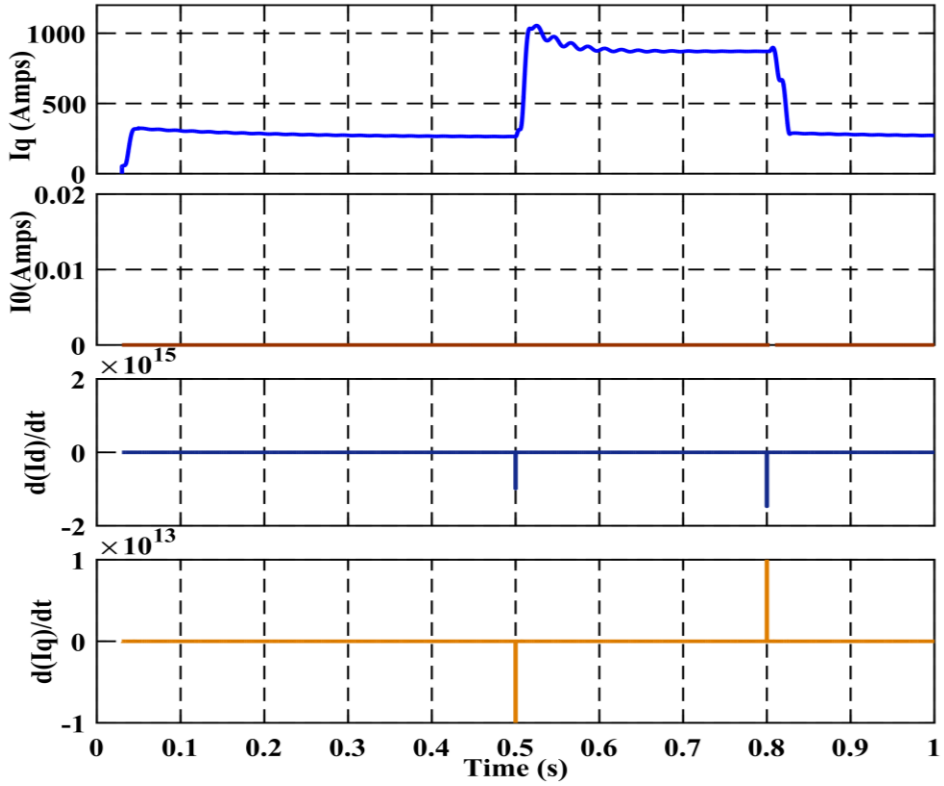

Fig. 3.10. *LLL fault detection on load side with dq0 components*

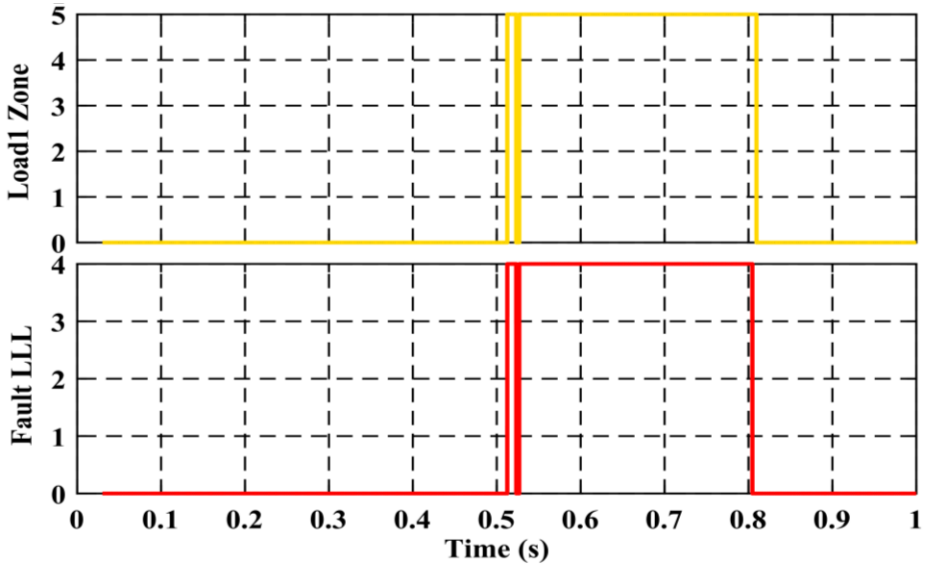

Fig. 3.11. *LLL fault nature detection on load side and zone detection with dq0 components*

I_d for location and fault nature detection. The role of I_0 is to distinguish between locations for same kind of fault at different nodes and between the faults as each and every fault has different I_0. Using time derivative components of fault current components such as $d(I_d)/dt$, $d(I_q)/dt$ and $d(I_0)/dt$ is the proposed strategy to detect faulty or abnormal conditions instantaneously. These new proposed components show easily determinable behavior to identify the location of fault and nature of fault.

Change in each and every component $d(I_d)/dt$, $d(I_q)/dt$ and $d(I_0)/dt$ during faulty conditions is different and is of the order of 10^{15} for I_d component, 10^{13} for I_q component and 10^4 for I_0 component, which helps in easy and instantaneous fault study. As shown in Figure 3.11. load1 Zone shows the location of fault identified during abnormal condition using comparison of instantaneous values of I_q and I_0 based on pre-calculated setting values, whose magnitude represents the node 5 at which fault has occurred.

Fault LLL shows the nature of fault identified, by giving it a different magnitude of 4 as compared to other faults. Current, I_q increases, I_0 also increases. $d(I_d)/dt$, $d(I_q)/dt$ and $d(I_0)/dt$ during faulty conditions is different and is of the order of 10^{15} for I_d component, 10^{14} for I_q component and 10^6 for I_0 component. DG Zone shows the location of fault identified during fault whose magnitude shows node 4 as identified for fault location.

3.5.3.2. LLG and LL fault detection

Figure 3.12. and 3.13. show the fault identified in DG Zone (Flag magnitude 4) and along

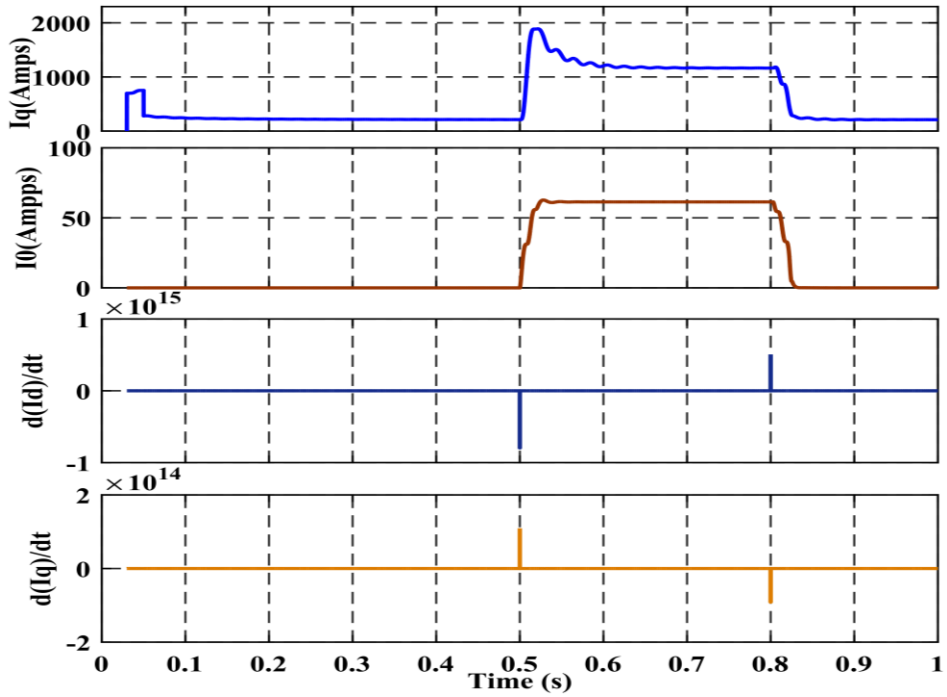

Fig. 3.12. *LLG fault detection on DG side with dq0 components*

with the nature as Fault LLG , by giving it a different magnitude of 3 as compared to other faults. Figure 3.14. and 3.15. shows the behavior of fault current during abnormal condition with increase in quadrature component of fault current, I_q is 125 A, whereas change in zero sequence current, I_0 is very less, of the order of 10^{-3} A. Change in each and every component $d(I_d)/dt$, $d(I_q)/dt$ and

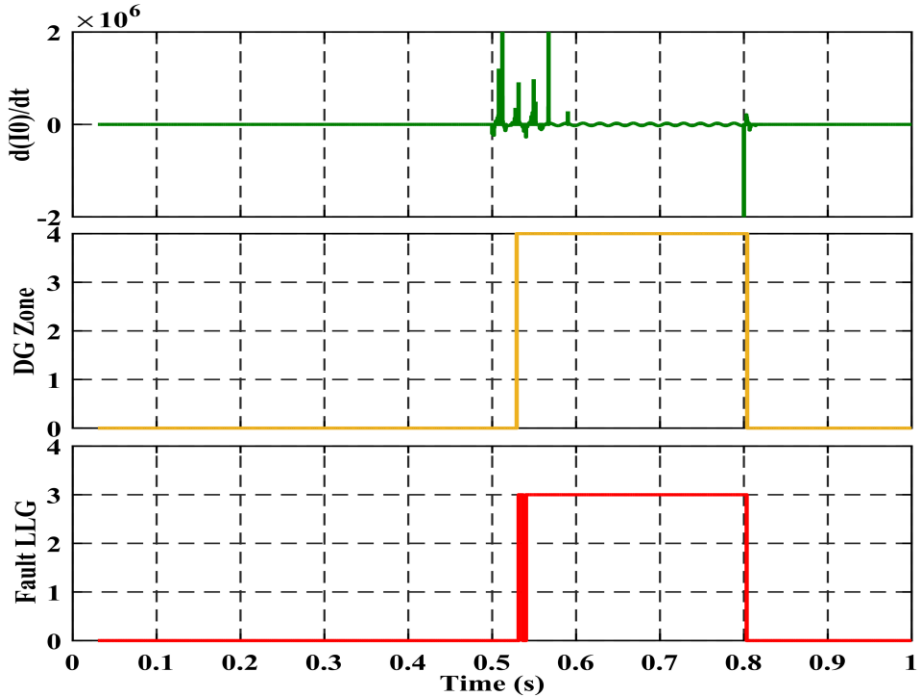

Fig. 3.13. *LLG fault nature detection on DG side and zone detection with dq0 components*

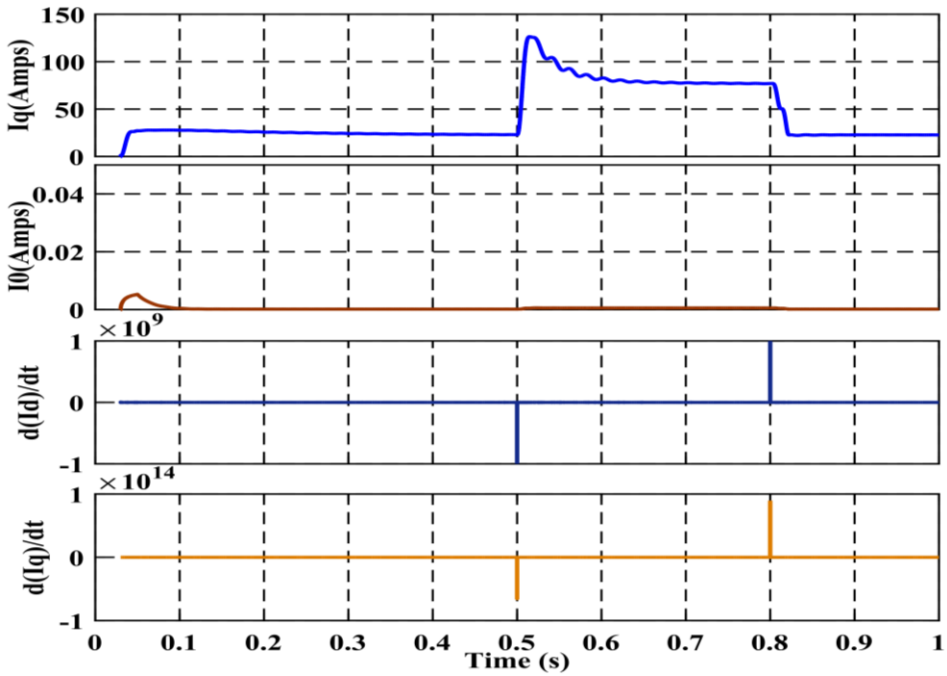

Fig. 3.14. *LL fault on utility grid side with dq0 components*

d(I₀)/dt during faulty conditions is different and is of the order of 10^9 for I_d component, 10^{14} for I_q component and 10^8 for I_0 component. It helps in easy and instantaneous fault study. Grid Zone shows the location of fault identified during abnormal condition whose magnitude shows node 1 as identified for fault location. Fault LL shows the nature of fault identified, by giving it a different magnitude of 1 as compared to other faults I_q and I_0 helps in easy and instantaneous fault study. It concluded that if rate of change of *dq0* components is used the fault location detection and fault nature identification is much faster and more instantaneous.

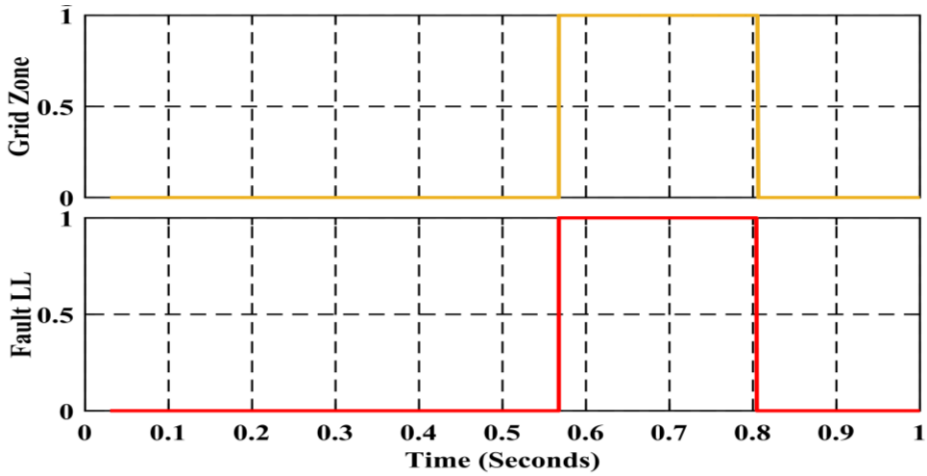

Fig. 3.15. *LL fault nature detection on utility grid side and zone detection with dq0 components*

Rate of change for *dq0* components is different for same fault at different locations also varies according to location of DG's in the microgrid and the rate of change is also different for different faults at same location. The adaptive protection could be easily implemented in another system according to relations presented in equations (3.6) and (3.7) where current share of different DGs having different nature are set according to constant '*G*'.

Chapter Summary

Adaptive protection can be provided for a reliable operation of microgrid. While designing adaptive protection system of a microgrid, the grid connected mode of operation without DGs must also be considered. It is made clear that the DGs with low X/R can feed enough for fault on their side. Whereas, the negative-sequence based detection cannot be used for detection of fault on utility side and DG side. The nature of fault can be identified showing importance for q0 components in microgrid systems. The performance of a protection system dedicated for microgrid highly depends upon nature of DGs connected, fault location detection and fault nature. For satisfactory operation of microgrid, the status of protection system should be available with microgrid central controller in steady state and abnormal situation. To provide good services to the consumers, a dedicated load side protection system can be implemented through fractionalization of the main protection system and it can operate based on q and zero components of fault current. Fault location detection and fault nature identification based on dq0 components is a simple but slow detection method. Instead, consideration of time derivative of dq0 components is the simplest, instantaneous and robust method for location detection and fault nature identification which has been verified in the present work. Based on I_q and I_0 components, the individual adaptive protection schemes can be designed for smart grid components.

Chapter 4

Detection of Faults in Hybrid Microgrid Using a Fuzzy Logic-based Adaptive Protection Scheme

Introduction

At present, the combination of wind turbine and photovoltaic distributed generators are operated together as a hybrid microgrid system which is gaining interest from the clean energy perspective. In this scenario, the study on fault characteristics of wind generator (types I, III and IV) and PV generator-based hybrid microgrid is significant. Based on fault characteristics, the protection system should respond to the abnormal conditions on utility grid or microgrid side, irrespective of its operation in grid connected or islanded mode. During short circuit fault in grid connected mode, the fault currents of higher magnitudes, such as 10–50 times the full load current in p.u., flows from utility grid to the point of fault due to low impedance in microgrid. But, fault current within same range of 5-10 times the full load current can be observed at the same location also in islanded microgrid. So, an adaptive protection is a prime concern to sense the fault current at different states of operation for microgrid [46] - [50]. In this chapter, a fuzzy based adaptive protection scheme is proposed and verified through analysis of the *q0* components of fault current considering the X/R ratio of DGs and frequency change at the instant of fault in the hybrid microgrid system.

4.1. Problem statement

The strategies for sensing the faults in three phase microgrid systems are mainly provided through measurement of three phase voltages and currents as six variables [51] - [56]. So, emphasis is given in this research for minimization of number of variables involved in fault detection and removal. There is an advantage of measurement of *q0* components of fault current since two variables are involved in this process [57] – [60]. A research has been reported in the previous chapter on the detection of fault in microgrid which involves measurement of *q0* components of fault current considering synchronous generators with low X/R ratio as DGs. But actual model PV and wind turbines as DGs were not considered in that work. Hence, the research has been reported in the present chapter on fault characteristics of grid connected and islanded hybrid microgrid using only *q0* components. To sense the fault accurately for proper relaying during different states

of operation, the current characteristic study of different nature of DGs becomes important [61] – [66]. When grid-connected mode is studied with different nature of DGs such as PV generators, types I, III and IV wind generators; it has been observed that the fault currents of higher magnitude are shared by the utility grid.

Type I wind generators have simpler designs with narrow speed range above the synchronous speed, but they have a maximum fault current contribution in interconnected systems which necessitates the study for fault current contribution of wind DGs. Type II wind generators are complex in nature as compared to type I and not considered in this reaserch work since they have high levels of flicker when interconnected to power systems with low short-circuit ratio (SCR). Type III wind generators have the advantage of the very wide range of operation due to back-to-back voltage source converter. Type IV wind generators have the advantage of full converter operation; they can be completely decoupled from the grid side due to losing in the coupling, but expensive in operation.

Types I (with a simpler design and maximum current sharing capacity), III and IV are only considered in this work since in type II, considerable flicker is present. There are a lot of changes to study fault current behaviour of types I–IV wind generators [46]. So, for reliable and efficient protection scheme design, use of types I, III and IV wind DGs are studied in this research work. In islanded microgrid fault current of about five–ten times, the full load current can be observed. This drastic change in fault current may initiate maloperation of protection relays. So, an adaptive protection scheme that can operate with this fuzziness of different modes becomes a prime concern. In some cases, the dq components are also used in protection relaying design but they have not considered zero component of fault current, which corresponds to earth faults. Without sensing the zero component of fault, the current proper reliable relaying is not effective. As discussed in Chapter 1, Section 1.1.1. it has been found that most of the proposed techniques lack study on ground fault component which is zero component. That reduces the capacity of proper identification of fault. The above two methods involve four to six variables for fault detection which needs more circuitry.

Fault current limiters (FCLs) play important role in providing fault ride through capability to a given system. Briefly FCLs are classified as Superconducting and Nonsuperconducting FCLs [160-169]. Nonsuperconducting FCL is the emerging technology in FCLs to minimize the use of switches and resistances for the minimization of power losses. Most of the FCL are meant for

Table 4.1 Existing fault current limiters (FCL) and proposed *q0* protection scheme, [160-169]

FCL	System Type	Protection Coordination	Cost	Circuitry	Switches Used	Open Conductor faults	Lightly Loaded phase faults
Super conducting	High Voltage	Delayed & Mismatch	Very High	Additional Required	More Number	Not Applicable	Not Applicable
Non Super conducting	Med/High Voltage	Delayed and no fuses	Low as FCL	Additional Required	Less Number	Not Applicable	Not Applicable
Proposed q0 Scheme	Low/Med /High Voltage	Fast with Backup Fuses	Very Low	Already Existing	None	Fast Detection	Fast Detection

conventional synchronous generators that are ideal sources but distributed generators are dynamic in nature. So, there is necessity of an adaptive protection scheme that can operate as per dynamicity in hybrid microgrids due to different operation modes and availability of wind and irradiance. Table 4.1 shows comparison among different FCL technologies and proposed *q0* component-based protection scheme.

Further, no research studies have been reported yet on fault characteristics of hybrid microgrid connected with utility grid and islanded modes using only *q0* components. In most of the research, the role of PV DGs, DFIGs and grid feeding fault together is not considered. Further no roles of transient and sub-transient reactance are studied for nature identification of faults and DGs. Nearly half of the schemes are found centralized, but centralized protection schemes are not preferable because of reliability issues.

Fault characteristics of PV, single fed (type I) and doubly fed (type III and IV) induction generators and synchronous DGs (as utility grid) are studied here in terms of *q0* components for proper relaying. Changes in transient and sub-transient reactance are taken into account for nature identification. Power losses are negligible for *q0* components, as they need no extra resistances or contact switches. In this research work location and nature of fault detection including determination of the type of DG feeding the fault are proposed.

In this research work, models of actual PV and wind energy sources have been considered to validate the proposed fuzzy algorithm based on *q0* components for fault detection. Hence the main objective of this research is validation of fuzzy logic algorithm based on *q0* components for

detecting location, type of fault and nature of DGs feeding fault point. This methodology should be effective for any mode of operation of microgrid. In this research, only *q0* components of fault current are compared with sequence components in hybrid mode, islanded mode and grid connected mode to validate acceptability of *q0* components in any mode of hybrid microgrid for fault location, nature of fault detection and for determining the type of DG feeding the fault. All these can be considered as a major contribution of the research reported in the present chapter.

4.2. Modelling of hybrid system

In hybrid system, the PV and wind generators are modelled together so that they can supply maximum fault current for a given fault as discussed in Chapter 2, Section 2.4.2. and 2.4.4.

4.2.1. Photovoltaic DG control

The PV control is provided based on Inverter control - using double synchronous rotating frame (DSRF) for the more flexible fault-ride-through (FRT) control, the inner-loop current control uses the regulators under a DSRF, and the outer-loop voltage control regulates the dc-link voltage to realize maximum power point tracking (MPPT) that is used in [48]. During faulty conditions depending on inverter design operating mode of inverter may change to FRT mode. However, FRT mode is neglected to study maximum current share. Here, the PV controller is designed based on equations (2.5) and (2.6) in Chapter 2. The PV fault current is determined by several factors such as $\beta,\gamma, K, P_0^{'}$ and $Q_0^{'}$ as discussed in Section 2.4.2. in Chapter 2.

4.2.2. Type – I, III and IV wind DG

Wind generators (single (type I) and double fed (type III and IV)) are modelled in this research work that has a variable pitch wind turbine model [46]. This wind turbine model is based on performance coefficient (C_p) of the turbine which is the ratio of mechanical output power of the turbine and wind power. C_p is also a function of wind speed, rotational speed, and pitch angle. C_p reaches its maximum value at zero pitch angle. Torque thus obtained from wind turbine model is fed to the asynchronous doubly fed induction generator (DFIG).

Wind turbine model of type I, III, and IV wind generators is done based on equation (2.7) as discussed in Section 2.4.3, Chapter 2. Type I wind generator is modelled based on squirrel cage induction generator. Converters of DFIGs (type III and IV) are modeled according to [64] as per

equations (2.8), (2.9) and (2.10) as discussed in Section 2.4.4, Chapter 2. The test model is shown in Figure 2.6.

4.3. Fault detection based on q0 components

Transformation of AC three phase current to *dq0* current is done using Park's transformation [42], as mentioned in relations 2.11 and 2.12 of Chapter 2, Section 2.5. As the microgrids comprise of DGs with low X/R and that X/R directly affects the I_q component as mentioned above so considering the variation in I_q component to detect fault justifies that this system works for any X/R ratio system . As given in this reference only *q0* components are sufficient to detect fault and its location. So, the equations are modified accordingly as relations (4.1) and (4.2):

$$I_{relay} = \left(I_{fG} \times Grid_{Status}\right) + \sum_{k=1}^{n}\left(k_i \times I(q,0)_{fDGi} \times DGi_{Status}\right) \quad (4.1)$$

$$Also,\ I(q,0)_{fDGi} = I_{q0rated}^{DGi} \times G \quad (4.2)$$

I_{relay} is relay current, I_{fG} is grid current during fault, $Grid_{Status}$ is 0 or 1, k_i represents the impact factor of i^{th} DG on the fault current of the relay, $I(q,0)_{fDGi}$ is the maximum fault current contribution of i^{th} DG in terms of q and 0 components, DGi_{Status} is 0 or 1, $I_{q0rated}^{DGi}$ is the corresponding maximum q and 0 currents of i^{th} DG and G is current coefficient whose value depends upon the nature of DG. Its impact factor depends on the impedance between the DGs and relays, within radial distribution. So, change in I_{sc} can be used to detect the fault, considering minimum number of parameters, I_d can be neglected and effective protection could be redesigned according to change in relation given as relation (4.3):

$$I_{sc} = f(I_q, I_0) \quad (4.3)$$

Transient currents and reactances of hybrid microgrid are given as in relation (4.4):

$$X' = \omega_s\left(L_m + L_s - \frac{L_m^2}{L_m + L_r}\right) \quad (4.4)$$

where, $T_0 = \frac{L_m + L_r}{R_r}$; $T_s = \frac{\sigma_s L_0}{R_s}$; $X_q = L_q\,\omega$ and $X_0 = \frac{3V}{I}$

$$i_s = \frac{V_s - V_s'}{j\omega_s \sigma_s L_0} e^{j\omega_s t_0} e^{-t/T_s} + \frac{V_s'}{j\omega_s \sigma_s L_0} e^{j\omega_s t} - \frac{L_0 i_r}{\sigma_s L_0} \quad (4.5)$$

$$X_q'' = x_a + \frac{X_{mq} X_{kq}}{X_{mq} + X_{kq}} \quad (4.6)$$

For DFIGs, X' is transient reactance, L_m, L_s and L_r are the mutual, stator and rotor leakage inductance, ω_s is synchronous speed, T_0 is open circuit time constant, T_s stator time constant, V_s and V_s' are stator voltage and stator fault voltage, i_s stator current, R_s stator resistance, L_0 is magnetizing inductance and σ_s stator leakage factor and T_s is stator time constant and for synchronous generator (grid side), X_q'' is sub transient reactance, x_a is armature reactance, X_{mq} is magnetising reactance of q axis and X_{kq} is damper winding reactance of q axis of grid side. X_q is quadrature axis synchronous reactances, L_q is quadrature axis inductance and ω is angular frequency. First component of equation (4.5) is transient component of current. At PCC grid side and DFIG will offer reactance's as mentioned above and PV side will offer minimum reactance that will help in identifying the fault and nature of DG with different and maximum feed.

4.4. Fault current characteristics

In this section, accurate measurement of fault current characteristics in terms of quadrature and zero components of the PV and all type wind generators during LL fault on load1 in system as shown in Figure 2.6. is done. Here, respective PV generator and wind generator (I, III and IV) are individually islanded. Islanded hybrid microgrid mode is also studied without utility grid in operation. A Line-Line fault is applied at the load1 location indicated in Figure 2.6. at t = 1s. In the case studies, focus is on the fault current change in *q0* components for proposed adaptive relaying. Zero component is not shown for LL fault since there is no flow of zero component, but shown in later cases. Different faults are simulated at the different locations (F) but with different DGs considering fault duration same as 0.1 seconds. The faults on node 3 and 9 show the behaviour similar to faults on node 4 and 11 as those have same rating and line parameters.

Case 1: LL fault on load end of islanded PV DG

In this case, the performance characteristics of islanded PV DG are investigated. The change in *q* axis component of fault current for the PV DG feeding individually 400 kW load are

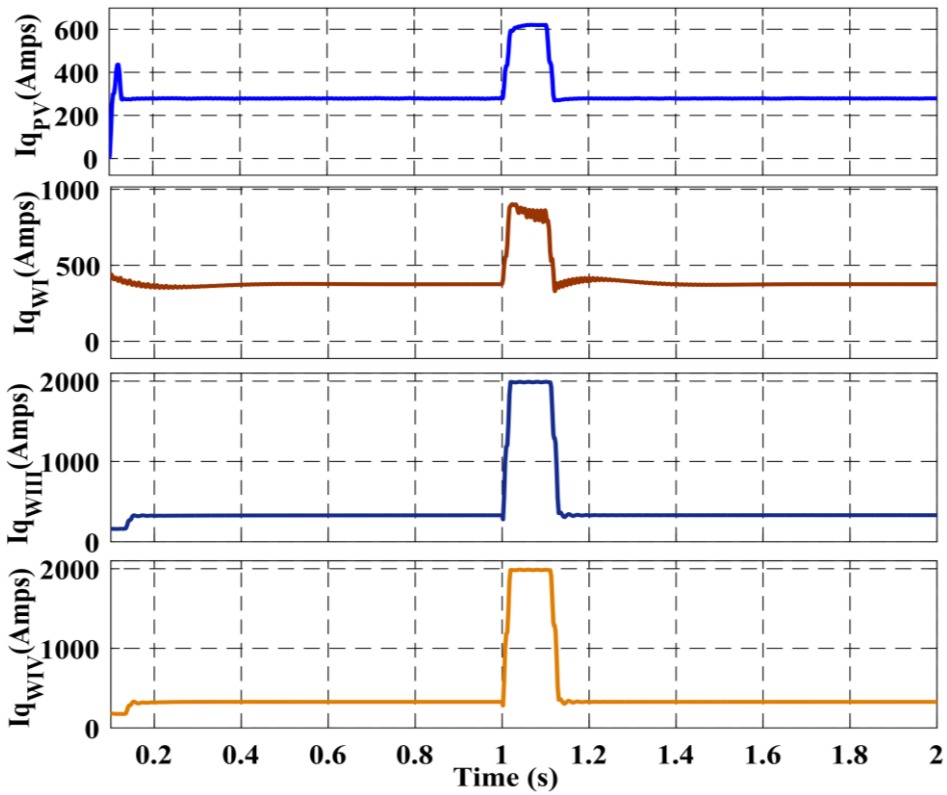

Fig. 4.1. *Quadrature current component of faulted load side feeder with LL fault on islanded PV generator, type I, type III and IV wind generators.*

observed. The variation in *q* component *(I_{qPV})* show the different transients with different magnitude of 280 A to to 610 A in feeder currents for LL fault. It is observed that the current *(I_{qPV})* is increased up to maximum value 2 p.u. approximately as show in Figure 4.1. It is within the the heating limit of power electronic devices used in PV DGs.

Case 2: LL fault on load end of islanded type I, III and IV wind DGs

In this case, the performance of type I generator in islanded mode is investigated. Figure 4.1. depicts the change in q axis component *(I_{qWI})* for islanded type I wind generator connected to individual 400 kW load showing the different transients with different magnitude of 380 A to 980 A. The variation in *q* component of current is found low because of low X/R ratio of type I wind generator system as compared to conventional power generation. But the variation is found higher as compared to PV which has higher resistance as compared to type I wind DGs. *q* components show steep and identifiable rise. Transients in *q* component of feeder fault current depict the role of inertia and inductive component which are unavailable in islanded PV generator-based system discussed earlier. For type III *(I_{qWIII})* and IV *(I_{qWIV})* wind generators, current change in I_{qWIII} and I_{qWIV}

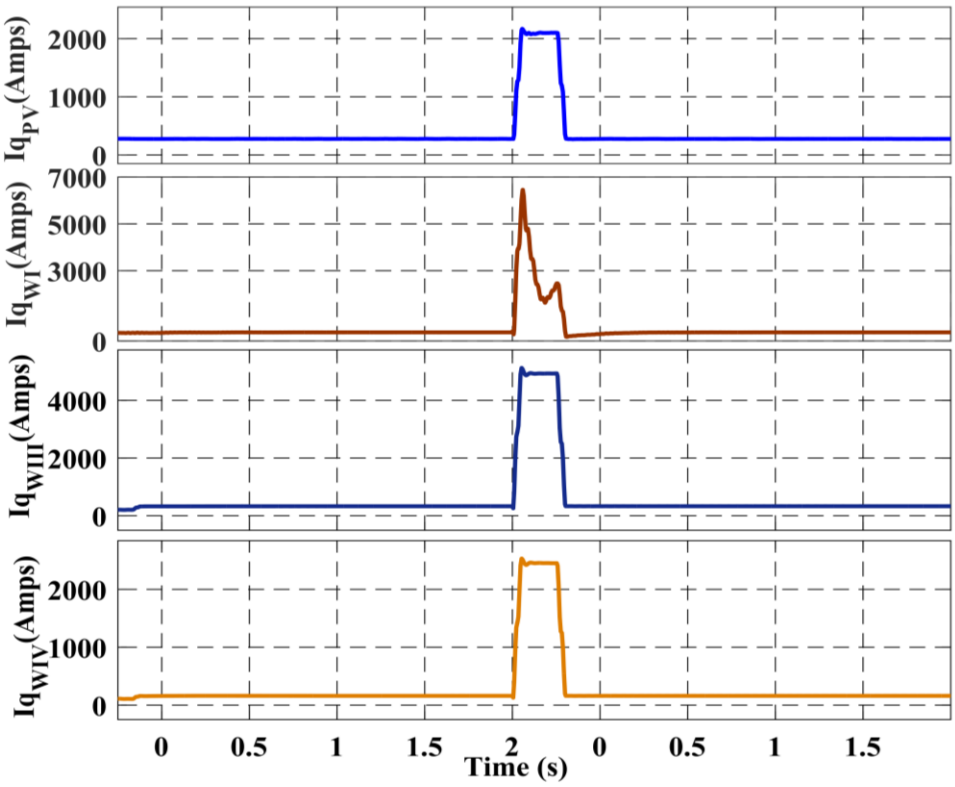

Fig. 4.2. *Quadrature current component of faulted load side feeder with LL fault on grid connected PV, type I, type III and IV wind generators.*

is from 1890 A 1820 A but very much less transients as compared to type I wind generator is observed. This is because of presence of low inertia and convertors in type III and IV generators.

Case 3: LL fault on load end of interconnected PV and grid

In this case, the performance of PV generator in interconnected mode with grid is investigated. Figure 4.2. depicts the change in PV DG current (I_{qPV}) of 2100 A when fault is on PV side load at node 3 as shown in Figure 2.6. In this case, the current is high since the grid is also feeding the fault. Here, sudden increase in *q* component is present. This increase is nearly equal to the sum of *q* currents of PV and grid. This situation shows bi-directional feeding of fault current because of which the need of adaptive relaying is essential. As the fault is on the PV side, so less transients is observed in grid's presence. But the transients are observed more as compared to the first case considered for islanded PV. The grid side synchronous generator governs the characteristics of fault current due to presence of inertia when the fault is occurred on feeder of PV side without inertia. This happens because of its inertia and transient reactance.

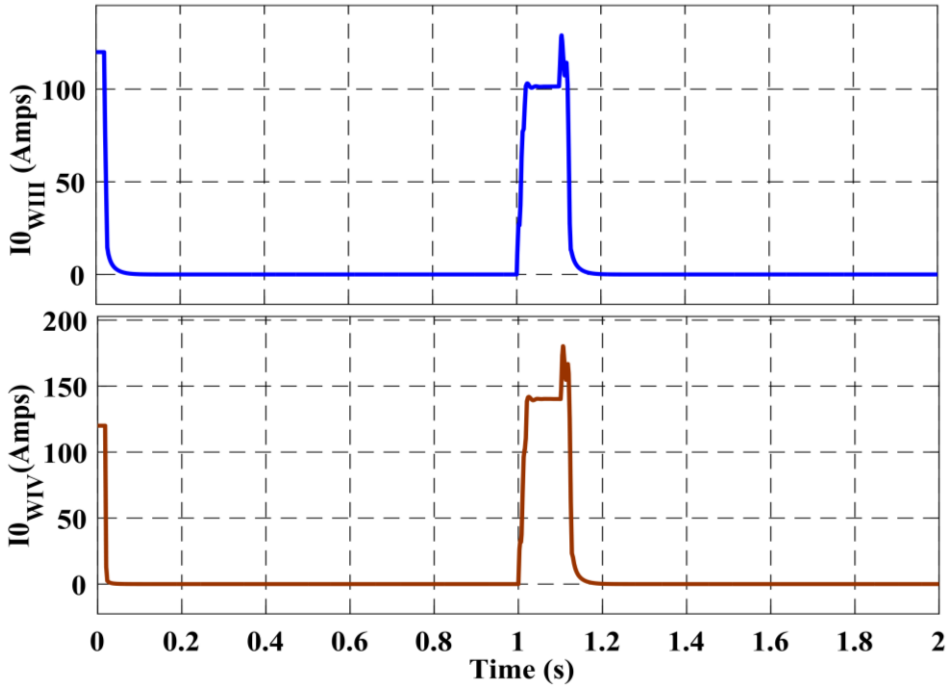

Fig. 4.3. *Zero component of current during LLG fault for type III and IV wind generators*

Case 4: LL fault on load end of interconnected wind (I/III/IV) DG with grid

Figure 4.2. depict the change *q* axis components when fault is on wind generator side load at node point 12 as shown in Figure 2.6. The change in type I wind DG current *(I_{qWI})* up to 6700 A is observed. Increase in *q* component is found like spikes which are very much higher as compared to the previous cases. After occurrence of the spikes in the *q* component, fault current settles at values which are sum of individual fault current shared by islanded type I wind generator and grid. It has been observed that high short circuit capacity, combination of resistive and inductive load and high reactance of type I wind generator and grid also play important role in fault current increment. Also, for type III *(I_{qWIII})* and IV *(I_{qWIV})* more change is in type III fault current as compared to type IV with more transients [46] because of full converter operation in type IV. Again, Figure 4.1. and 4.2., it is concluded that *q* component can replace sequence components [8] for fault identification and location detection. Figure 4.3. shows change in zero component of fault current for Line-Line-Ground (LLG) fault for type III and IV wind generators with different transients and magnitude. This change in transient and magnitude component is used in this research work for fault and nature identification as per equations (4.4), (4.5) and (4.6).

4.5. Frequency variation in hybrid microgrid

Table 4.2. Frequency change during LL fault of hybrid mode

Fault on load side of	Maximum frequency (Hz)	Minimum frequency (Hz)
Only PV DG	50.25	49.8
Only Wind DG	53.3	49.9
PV & Wind DG with fault on PV DG side load	51.5	47.4
PV & Wind DG with fault on Wind DG side load	52.1	48.2
PV & Wind DG connected to Grid with fault on Wind DG side load	50.25(Wind DG side)	48.5 (Wind DG side)
	50.5 (PV DG side)	49.25 (PV DG side)
	50.6 (Grid side)	49.5 (Grid side)

Change in frequency for LL fault during different modes of operation at given location with type I wind DG are shown in Table 4.2. Frequency variation in hybrid microgrid interconnected with the grid is shown in Figure 4.4. Change in frequency is processed to calculate

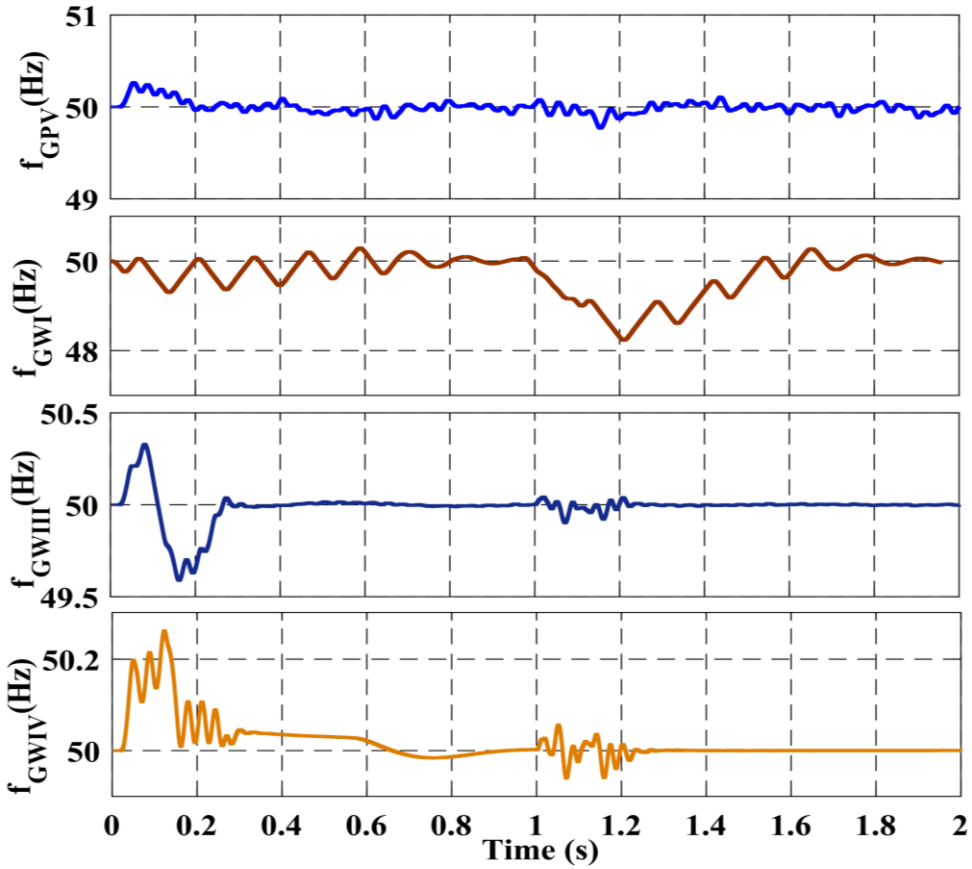

Fig. 4.4. *Frequency change in PV, type I, type III and IV wind generators during LL fault*

change in transient reactance that can easily help in fault detection and its nature and as well as of DGs in microgrid system. Frequency change is felt in all the above cases (case 1-4). These show that there is a considerable impact on the frequency of the system as per change in nature of DGs. This frequency change helps in obtaining change in transient reactance for mode detection and nature identification. The frequency range of different modes of hybrid microgrid during above mentioned case studies is also shown in Table 4.2. Due to presence of different amount of inertia and transient reactance different changes are observed. It is due to inertia and transient reactance of type I wind generator which is highest compared to other cases combined with that of grid which govern the change.

When a fault appears in an interconnected system of type I wind and PV generators, there is change in frequency in the range of 52.1-48.2 Hz which is different from earlier three cases as shown in Table 4.2. Table 4.2 depict frequency variation of the type I wind generator side (48.5-50.25 Hz) which is more as compared to PV (49.5-50.5 Hz) and grid-end (49.5-50.6 Hz) PCC. For standalone condition variation of 3.4 Hz is analysed. In case of PV standalone, the range of frequency variation is as much less as 0.45 Hz. This role of reactance is used in designing proposed technique. For fault duration of grid connected mode of PV *(f_{GPV}),* type I *(f_{GWI}),* III *(f_{GWIII})* and IV *(f_{GWIV})* wind generators connected to load with LL fault on its load end during 1 to 1.1 seconds are shown in Figure 4.4.

4.6. Current sharing in type I, III and IV wind DGs

Table 4.3 and 4.4 shows share of current (I_q and I_0) among PV, type I, III and IV wind

Table 4.3. Change of q and zero current components of Type I, III and IV wind generators during LL fault

	I_q (A)	**I_0 (A)**
Only Type I Wind DG share	980	0
Only Type III Wind DG share	1050	0
Only Type IV Wind DG share	1230	0
Type I Wind DG share with PV	2100	0
Type III Wind DG share with PV	2170	0
Type IV Wind DG share with PV	2310	0

Table 4.4. Change of q and zero current components of Type I, III and IV wind generators during LLG fault

	I_q (A)	I_0 (A)
Only Type I Wind DG share	2000	350
Only Type III Wind DG share	1890	100
Only Type IV Wind DG share	1610	180
Type I Wind DG share with PV	2500	450
Type III Wind DG share with PV	2570	140
Type IV Wind DG share with PV	2710	220

generators during different modes with same LL and LLG fault at same location. From the whole data presented in Table 4.3, the main governing factor for frequency variation is revealed as interconnected system with wind generator and grid. So, wind generator plays an important role during abnormal conditions.

The share of wind generators in terms of *q0* component is shown in Table 4.4. When a fault (LL) occurs across the feeder connected to load in islanded wind generator, bi- directional feeding of fault current is absent; hence the entire current is fed by the wind generator itself. For interconnected wind and PV generator, for fault at same location bi-directional feeding of fault current is present. It makes adaptive protection scheme a necessity in microgrid structures to minimize the impact of bi-directional feeding and false tripping because of a change in impedance. Current share of the different wind generators in terms of *q0* with LG fault for same location is shown in Table 4.4. Wind generator system has greater transient and a sub- transient component of current as compared to the PV generator system which has zero transient component.

4.7. Proposed protection scheme with fuzzy logic-based algorithm

Due to the impact of low fault currents like PV DGs with high R, low X/R ratio of DGs, different transient reactance, a new adaptive protection methodology is proposed based on *q0* components of fault considering equation (4.1) and (4.2). This will also help in detection of fault, its nature and location. In future, most of the DGs are going to be converter interfaced where converters are controlled based on *dq0* components. So, this scheme is going to be very much reliable and cost effective. Adding capacitor during fault instant for charging will need extra

circuitry, first to switch capacitor during fault in the proposed scheme. This is not cost effective for low and medium voltage systems. Also, it will increase the maintenance cost.

4.7.1. Proposed methodology

In case of low/medium voltage (LV/MV) microgrids, the fault current becomes low due to presence of converter interfaced (PV) with low rated DGs having a low X/R ratio. Hence, it becomes very much crucial to determine the fault, its location and nature for proper relaying and coordination among protection devices. The tripping action and detection of mode of operation are implemented based on modified relations as (4.1) and (4.2). It is shown above in Section 4.2 where I_{relay} is the current according to which the relay is to be set for operation. The relay will operate when the relay current becomes more than the set values of *q* and *0* components of fault current during abnormal conditions. *n* is the total number of DGs in the microgrid, in this case it is two (2). But in this research work, the independent *q0* components with transient reactance change are considered for simple and less time-consuming fault detection in less than 30 ms. Also, in [26], transient states of fault current with different DGs are not included. But in this researck work independent *q0* components with transient reactance change are considered which are extended in this research work for further contribution.

4.7.2. Fuzzy logic implementation

The proposed fuzzy rule-based technique for fault and nature detection of feeding DGs is considered, based on *q0* components of current and rate of change in transient reactance which are used to change the settings of adaptive relay for different modes and DGs at their nodes. Table 4.5 also give incitation to input function for fuzzy logic-based relay. Inputs given to quadrature (I_q) and 0 (I_0) axis components and based on fuzzy rules outputs are classified into fault detection, nature detection, fault location detection and nearest DG to fault. Fuzzy system-based nature detection rules are set as follow:

- If (change in i_q is very LOW) and (change in i_0 is very LOW) then (output is PV)
- If (change in i_q is AVERAGE_LOW) and (change in i_0 is very LOW) then (output is PV)
- If (change in i_q is small high) and (change in i_0 is very LOW) then (output is WIND)
- If (i_q is MEDIUM) and (change in i_0 is very LOW) then (output is WIND (IV) + PV+ PV FAULT)

Table 4.5 Input and output membership functions for fault and location detection in hybrid microgrid

	Variable	Membership Function for Adaptive fault detection for PV-Grid-Wind (I, III and IV)							
Input	**Frequency (Hz)**	Low	Medium	High	--	--	--	--	--
	Range	[48.5 49.3 50.25]	[49.75 50.5 51.25]	[50.75 51.625 52.75]	--	--	--	--	--
	Iq (A)	NO FAULT	PV SIDE LL FAULT	W SIDE LL FAULT	WPV LL FAULT W SIDE LOWI	WPV LL FAULT PV SIDE LOWI	WPV LL FAULT W SIDE HIGHI	WPVG LL FAULT W SIDE LOWI	WPVG LL FAULT W SIDE HIGHI
	Range	[300 355 410]	[390 510 630]	[610 815 1020]	[1000 1355 1710]	[1690 1800 1910]	[1890 2450 3010]	[2990 4010 5030]	[5010 6505 8000]
	I_0 (A)	VERY LOW	LOW	MEDIUM	HIGH	VERY HIGH	--	--	--
	Range	0	[30 50 70]	[60 80 100]	[90 110 130]	[120 220 320]	--	--	--
	Output	PV SIDE FAULT	W SIDE FAULT	WPV PV SIDE FAULT	WPV W SIDE FAULT	WPVG W SIDE FAULT	--	--	--
	Range	[0 0.55 1.1]	[0.9 1.5 2.1]	[1.9 2.5 3.1]	[2.9 3.5 4.1]	[3.9 4.95 6]	--	--	--

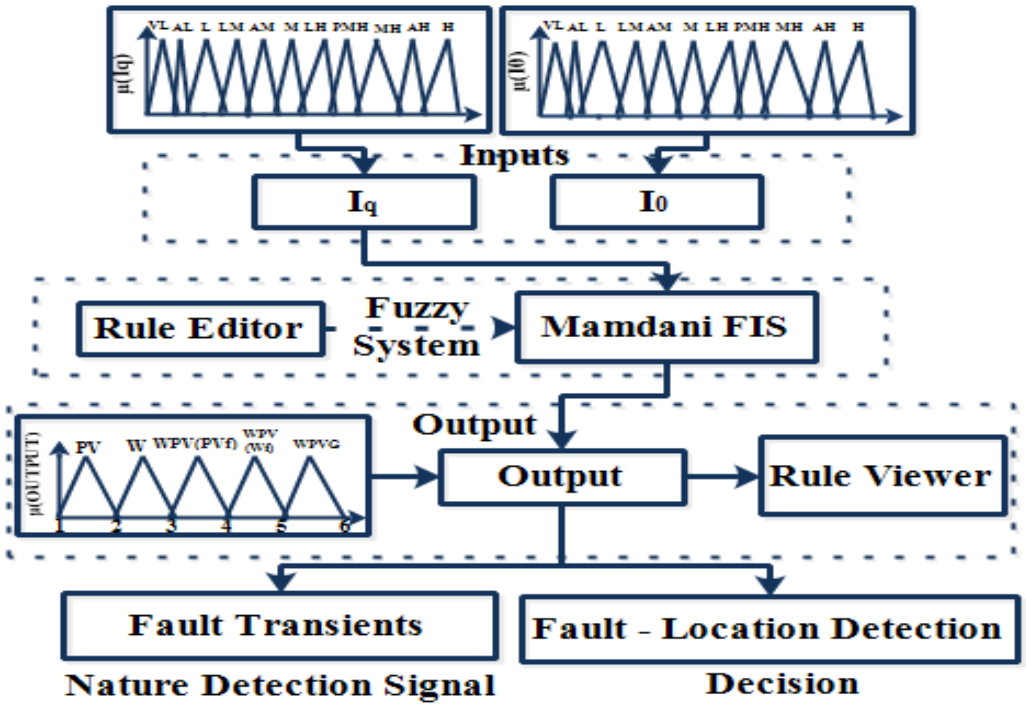

Fig. 4.5. *Fuzzy logic based adaptive nature and fault detection protection scheme*

- If (i_q is MEDIUM high) and (change in i_0 is LOW) then (output is WIND (III)+ PV + W FAULT)
- If (i_q is HIGH) and (change in i_0 is LOW) then (output is WIND (I) + PV + GRID)

Figure 4.5 shows implementation of fuzzy logic for adaptive protection relay. As, Mamdani fuzzy inference system has ability to handle data in both multi input and single output (MISO) as well as multi input and multi output (MIMO) systems it is used in this study [26] and [72]. In fuzzy based nature detection system, the second rule is with medium change in reactance which is calculated corresponding to average low change in I_q [range (590 675 760)] and change for quadrature component I_0 is [-1 0 1] (A) that detects the fault, its nature and nature of connected DG as PV.

The third rule in adaptive relay protection detection fuzzy based system, for transient reactance corresponding to defined for low range change and low range change in I_q [range (1690 1800 1910)] and for low range change for quadrature current components [0 .5 1] (A) then fuzzy system detects fault as LL on the PV side of interconnected wind and PV distributed generators. In similar manner, *q0* components are used to implement fuzzy logic based adaptive protection scheme for Earth faults where I_0 range lies between [1 100] A.

4.7.3. Fault identification

Fault identification algorithm is shown in Figure 4.6. Different network topologies are considered with the optimal relaying action using mixed integer nonlinear programming [65]. But they did not consider the impact of the different nature of DGs, low inertia and transient reactance

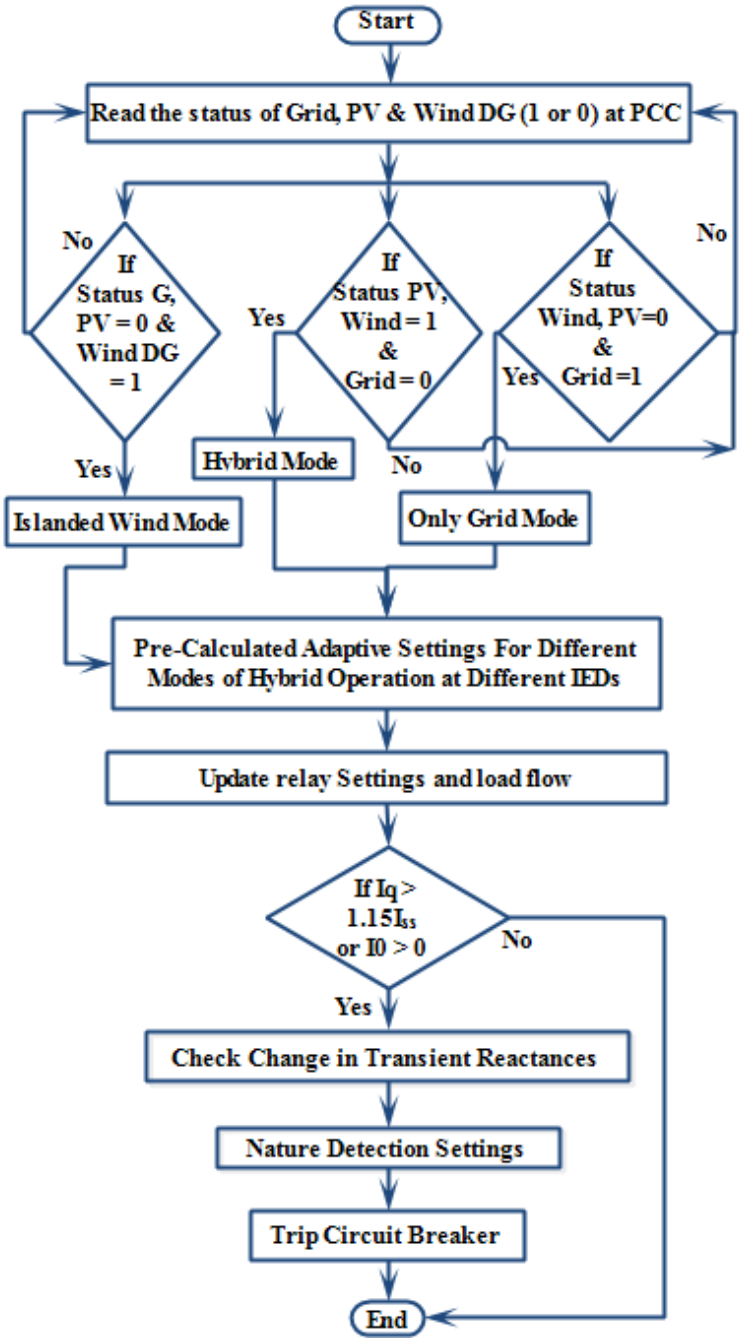

Fig. 4.6. *Algorithm for adaptive protection scheme for fault detection and nature detection for type of generation feeding in hybrid system*

in the protection scheme which are investigated in this research work as a contribution. The results presented in Figure 4.1. - 4.2. shows that the *q* components equally correspond as the change in symmetrical components. So, the protection scheme based on symmetrical components as discussed in [13] and [66] can be replaced by proposed technique. So, protection scheme could be easily modified as given in relation (4.3) of sub section 4.2. This is going to be equally effective for all kind of faults in hybrid microgrid structures with critical clearing time of the range of 230 ms. It has been revealed that change in d component could be neglected as compared to change in *q* component. So, *q0* components are enough for proper detection of fault, type of earth and phase faults, and nature detection in hybrid microgrid. In this research work, an adaptive protection scheme used for different modes of operation is discussed as per the proposed algorithm based on change in *q0* and transient reactance at different nodes shown in Figure 4.6. Status of the utility grid and DG decides the operation of the relay under different modes of operation mentioned above.

Set of values for adaptive relaying action is based on pre-observed steady state values of generator and feeder currents at given IEDs. Decision on selecting a set of values for relaying operation is taken based on mode of operation which changes the initial transient appearance during change of nature of DGs is implemented based on change in transient reactance in different modes of operation, as shown in Figure 4.6. This algorithm differentiates the type of generation according to the respective change in transient component of fault current shared by respective converters connected with PV and wind generators. Behaviour of different faults on different induction generators (DFIG-III and IV) used in wind generators is given main emphasis [46]. Existing literatures show that no study is reported yet for change in transient reactance during different faults in hybrid microgrid.

Also, reactance change during fault on the different load side is used to identify the nature of DGs feeding the load. In Figure 4.6., I_{q0} is the *q0* components of fault current. Islanded mode or change of operational mode could also be easily identified from the change in reactance limits available at different nodes. It is different at different nodes and minimum for PV side node. The proposed adaptive protection scheme is developed based on intelligent protection topology using a systematic fuzzy rule obtained from a decision tree. The scheme can retrieve the instantaneous current signals *(q0)* at all nodes of the corresponding distribution feeder and process *q0* transformation to find out the statistical and transient features of fault as shown in Figure 4.6.

Table 4.6 Relaying for different faults at different generators in hybrid mode of operation

Faulted	LL-DT	LG-DT	LLG-DT	LLL-DT	LLLG-DT	1OC-DT
Utility	80A, 0.0451s	70A, 0.0428s	130A, 0.0329s	200A, 0.0242s	210A, 0.0217s	20A, 0.0334s
WDG I, III & IV	7500A, 0.0443s	1600A, 0.0373s	7510A, 0.0320s	6500A, 0.0313s	6520A, 0.0351s	750A, 0.0321s
PV DG	790A, 0.0321s	800A, 0.0338s	900A, 0.0326s	900A, 0.0325s	890A, 0.0318s	520A, 0.0257s

Similarly, decision trees are built for other hybrid system modes that are with grid PV and wind DGs. Table 4.6 shows the fault currents due to different faults at different locations in hybrid microgrid and fault detection time by the proposed relaying. Fault currents are in terms of q component of fault current, during different faults at different point are shown with detection time (DT) by the proposed relay from the event of fault. It can detect fault in 20-40 ms.

The indicative numerical flags governed by adaptive relay working in different modes for steady state and different shunt and series faults at different locations are shown in Table 4.7. The steady state flag value for different nodes is set to common value flag with magnitude of 0.5 and during fault at any node, flag value changes to assigned flag value depending on location in reference to point of common coupling. In islanded cases of type I, III and IV wind and PV

Table 4.7. Numerical flags in adaptive relay for steady state, fault location, nature of DG feeding the fault and type of fault in hybrid mode

Fault on Wind I, III, IV & PV	Default Steady State	Location of Fault	LL Fault	LLG Fault	LLL Fault	1OC Fault	2OC Fault
Nature of DG Feeding	1.5	PV – 0.5 W – 2.5	1-2	2-3	3-4	1	-1
Node 1-2	0.5	2 – 3	1-2	2-3	3-4	1	-1
Node 4-5	0.5	1.5 – 2	1-2	2-3	3-4	1	-1
Node 3-6	0.5	1 – 1.5	1-2	2-3	3-4	1	-1
Node 7-8	0.5	5 – 6	1-2	2-3	3-4	1	-1
Node 10-11	0.5	3.5 - 4	1-2	2-3	3-4	1	-1
Node 9-12	0.5	3 – 3.5	1-2	2-3	3-4	1	-1
PCC	0.5	4-5	1-2	2-3	3-4	1	-1

generators, the steady state default settings for nature of DG feeding fault point can be derived from Table 4.7. The nature of DGs feeding fault point, steady state default settings for nature of DG feeding fault point is set to a flag with value of magnitude 1.5 that takes value of 0.5 for fault on PV side of hybrid microgrid and 2.5 for fault on wind generator. For, faults between nodes 1 and 2, flag values are assigned 4 and 5, 1 – 1.5 in magnitude for fault between nodes 3 and 6, between 5 - 6 for fault between nodes 7 and 8, between 3.5 - 4 for fault between nodes 10 and 11, between 3 – 3.5 for fault between nodes 9 and 12. For point of common coupling (PCC) in steady state 0.5 magnitude is set and for any transient at PCC in any mode of operation flag carrying value of 4-5 magnitude is set. Operation flags are set with the magnitude range of 1-2, 2-3 and 3-4 during shunt faults.

For series faults like one conductor open (1OC), one phase lightly loaded, two conductors open (2OC) and two phases lightly loaded, with these type of fault values between [-1 1] are set. At any node for wind generator in islanded mode of operation during steady state default settings for nature of DG feeding fault is set to flag with value of magnitude 1.5, which shows value 2.5 during fault on islanded wind generator. PV side microgrid flags are all set to zero. Again, under steady state for islanded wind generator, flag value for different nodes is set to common value flag with magnitude of 0.5 and during fault at any node, the flag value changes to assigned flag value depending on location in reference to point of common coupling. For fault between nodes 7 and 8 it is between 5 - 6, for fault between nodes 10 and 11 it is between 3.5 – 4, for fault between nodes 9 and 12 - it is between 3 – 3.5.

4.8. Effectiveness of proposed methodology

Effectiveness of fuzzy based adaptive protection scheme is verified as a case study, the results of which are represented in Figure 4.7. In different protection schemes different relays are used for phase and earth faults that makes system bulkier and complex [46]. In the proposed scheme, single relay is used at given node. Only one numerical relay or IED is enough for phase and earth faults at given node or location in this scheme.

As compared with technique [63], this scheme is faster. It also needs only two layers of protection- one for islanding and one for grid connected mode. Each IED senses its own change in current and reactance. It sends signal to trip as per settings of different modes. Compared to

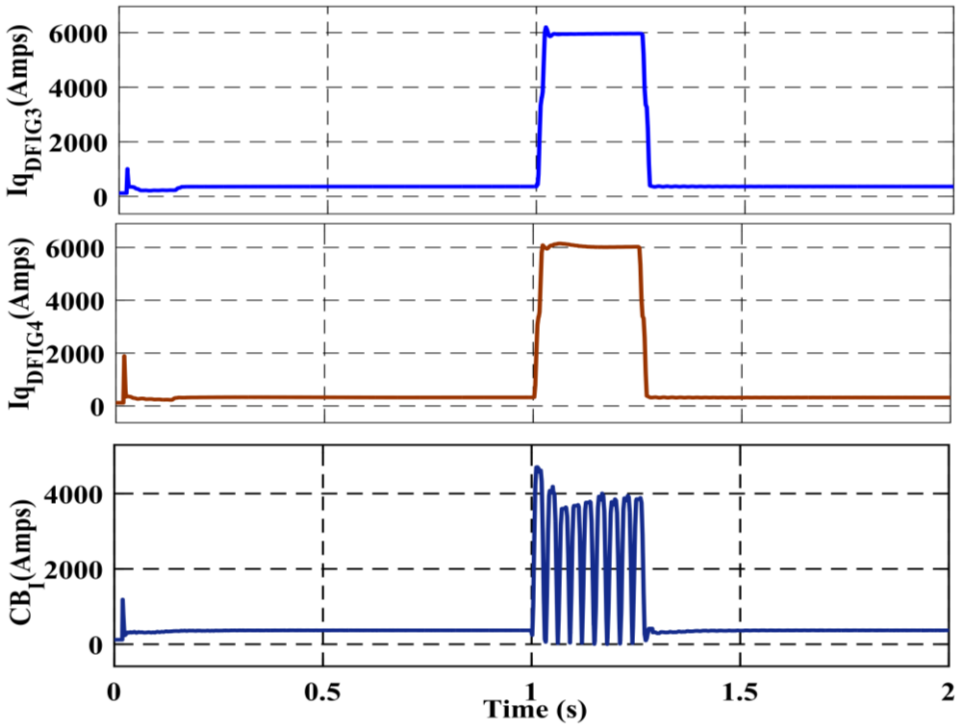

Fig. 4.7. *Quadrature axis current component of faulted load side feeder connected to type III and IV wind generators with PV generator and grid without and with adaptive relaying*

tripping curve for change detection, proposed fuzzy logic technique is faster. It also uses less numbers of relays with better performance for complete hybrid system as compared to [46] that are meant for only DFIG generator protection only.

4.8.1. Shunt fault detection

The changes in *q* axis components (I_{qDFIG3} and I_{qDFIG4}) when fault is on load end of wind generator interconnected with PV generator and grid, are depicted in Figure 4.7. The location of fault depends on DGs of different nature, high short circuit capacity and inertia of grid and wind generator as compared to PV generator. In this research work different types of wind generator are tested with the proposed adaptive protection scheme. For same type of fault on type I, III and IV wind generators it is felt that less drop for type I wind generator during fault as compared to type III and IV. Whereas type III and IV have only 3-4 V drop difference as compared to each other. Adaptive relay sends out signal to circuit breaker (CB8- current change CB_I) and fault is cleared as shown in Figure 4.7. It depicts that the fuzzy logic based adaptive protection can clear the fault within 0.025 seconds of the LL fault occurrence on load side limiting the fault current.

Table 4.8. Change in voltage (AC) at different location during different faults in hybrid microgrid connected to grid and islanded modes

Type of Fault	Grid V_q (kV)	PV V_q (V)	Wind V_q (V)	WindL1 V_q (V)	PVL1 V_q (V)
Steady State	6	480	520	440	440
LL, L1PV, PVI	0	25	0	0	0
LL, L1W, WI	0	0	420	0	0
LL, L1PV, WPV	0	150	275	150	0
LL, L1W, WPV	0	100	150	0	50
LLL, L1W, WPVG	3	0	10	0	0
LLG, L1W, WPV	0	50	100	0	0
OC1/Singlephasing ,L1W, WPV	0	500	580	360	480

Comparison of voltages in quadrature component as q component voltages for different faults at different locations (L1- Load1) is shown in Table 4.8. Figure 4.8 shows nature of generator, location of fault and type of fault which are detected as per change in magnitudes of

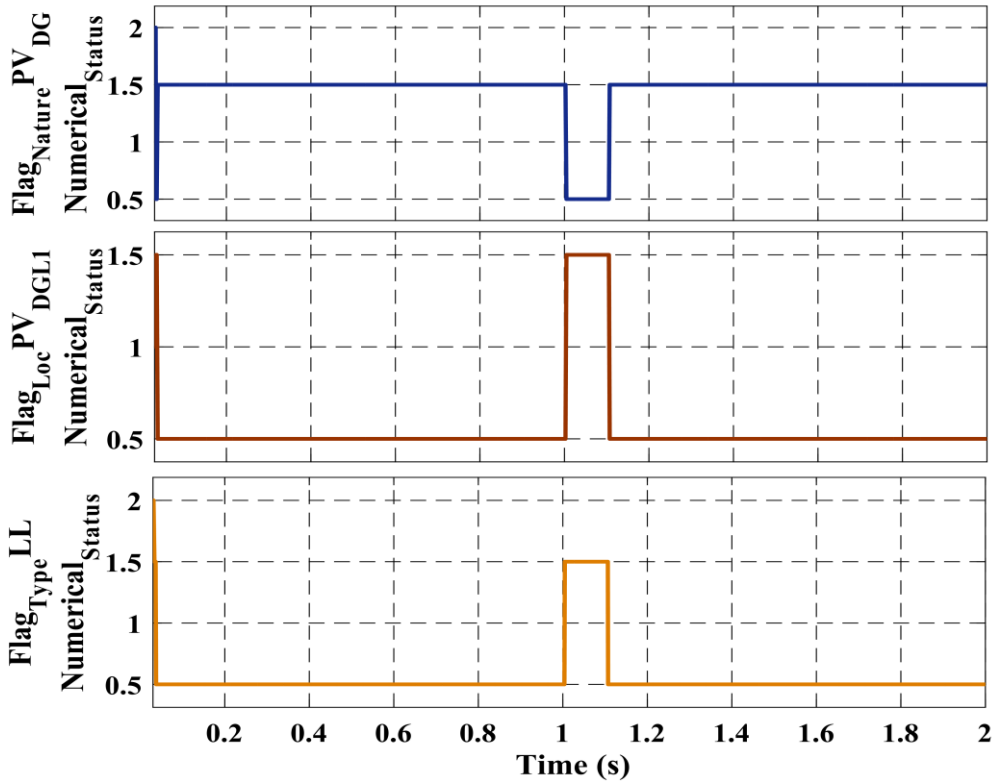

Fig. 4.8. *Numerical flag status for detecting nature of DG, location of fault and type of fault (LL) for LL fault on load1 of islanded PV generator*

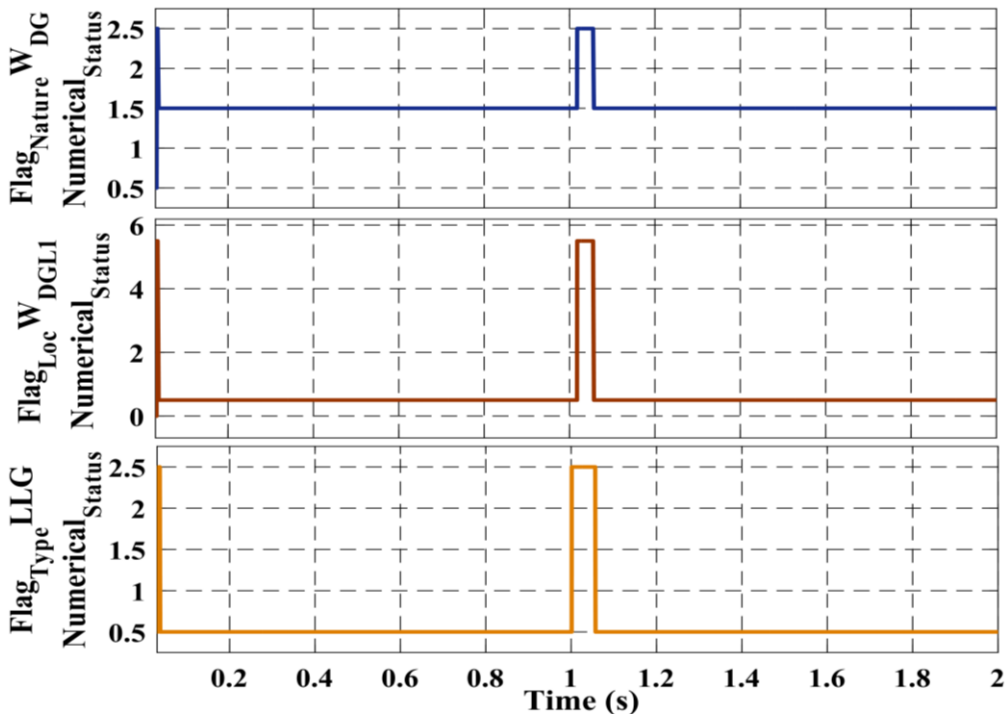

Fig. 4.9. *Numerical flag status for detecting nature of DG, location of fault and type of fault (LLG) for LLG fault on load1 of type I wind generator working in hybrid mode*

flags given in Table 4.7. PV type of generator feeding the fault with change in magnitude of $Flag_{Nature}PV_{DG}$ steady state value 1.5 to 0.5 is identified as type of generation feeding the fault point. Change in $Flag_{Loc}PV_{DGL1}$ magnitude of steady state value from 0.5 to 1.5 identifies location near load1 of PV generator side. Shunt fault is identified as LL fault with change in $Flag_{Type}$LL magnitude 0.5 to 1.5.

Hybrid microgrid operation is considered in Figure 4.9 with same adaptive protection scheme working for interconnected mode of operation. Rate of rise of current is high in hybrid mode of operation. Detection of LLG fault on load1 of wind generator working in hybrid mode is shown in Figure 4.9. Wind type of generator feeding the fault with change in magnitude of $Flag_{Nature}W_{DG}$ steady state value 1.5 to 2.5 is identified as type of generation feeding the fault point. This figure shows location of fault which is identified as fault on load1 of type I wind generator side with change in $Flag_{Loc}W_{DGL1}$ magnitude of steady state value 1.5 to 2.5. Type of shunt fault identified as LLG fault with change in $Flag_{Type}$LLG magnitude of steady state value 0.5 to 2.5.

4.8.2. Series fault detection

For overall effectiveness of proposed adaptive protection scheme, series or open circuit

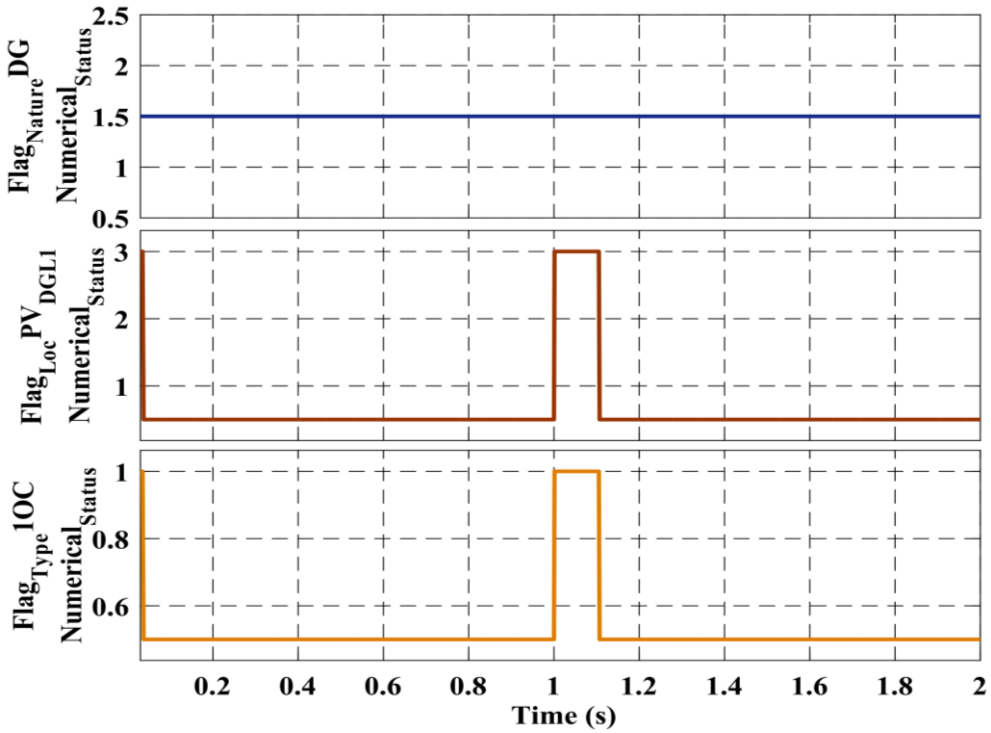

Fig. 4.10. *Numerical flag statuses for one phase lightly loaded (or 1OC) fault on load1 side of PV generator working in hybrid mode.*

faults (lightly loaded phases) are also included and tested on the proposed hybrid microgrid. When fault is simulated from 1.0-1.1 seconds as one phase lightly loaded on load1 side of PV generator working in hybrid mode, both faults are detected as with same flag value as they both act in same manner with only slight change in current and voltage magnitudes. No change in nature of DGs feeding the fault exists as $Flag_{Nature}DG$ shown in Figure 4.10. In open circuit fault or lightly loaded phase there is no feed of current, so magnitude of steady state value 1.5 holds. Location of fault is identified as fault on load1 of PV generator side with change in $Flag_{Loc}PV_{DGL1}$ magnitude of steady state value 0.5 to 1.5. Type of series fault is identified as single phase lightly loaded with fault with change in $Flag_{Type}1OC$ magnitude of steady state value 0.5 to 1.

In the present scheme, single phasing faulty condition has also been simulated by loading only one phase out of three single phases which shows same behaviour as that of two conductors open. Hence, it is considered as fault or detected as fault with two conductors opened or two phases lightly loaded. During simulation, the *q0* currents in two lightly loaded phases are compared with *q0* currents of three phase loads with two conductors open. It is concluded that there is not much change in *q0* components of fault current. During single phasing, change in I_{q0} components of fault current on load side of PV generator for two conductors open is from 450 to 410 A and 0 to 35 A.

Table 4.9. Critical clearing time (CCT) in different modes of hybrid microgrid in coordination with backup fuses

Fault Node	Grid (ms)	W&PV Islanded (ms)	Trip Time (ms)	Fuse Type	Rating (MVA)
12	190	230	160	15T	0.4 load
11	190	230	160	15T	0.4 load
5	190	230	160	12T	0.3 load
6	190	230	160	12T	0.3 load
8	170	210	140	50T	1.0 wind DG
2	180	220	150	25T	0.5 PV DG
13	170	210	140	50T	1.0 Grid

This is like single-phasing on load side. Same change is observed in I_{q0} components of fault current on load side of wind generator for two conductors open and single phasing. From, Figure 4.8., Figure 4.9. and Figure 4.10. the tripping time of different IEDs are shown with numerical flag values as per Table 4.7. Total tolerance value of 40 ms which includes circuit breaker opening time of 30 ms and 10 ms for tolerance. For increasing the feasibility of proposed scheme backup coordination among relay and fuses is proposed as per the relation mentioned as:

$$t_{fuse} - t_{relay} \geq 120ms$$

For the backup of relaying, fuses are used at all nodes and at point of common coupling as shown in Table 4.9. Figure 4.11. shows operation of fuse (Grid Fuse Status (0 to 1) ans Load Fuse

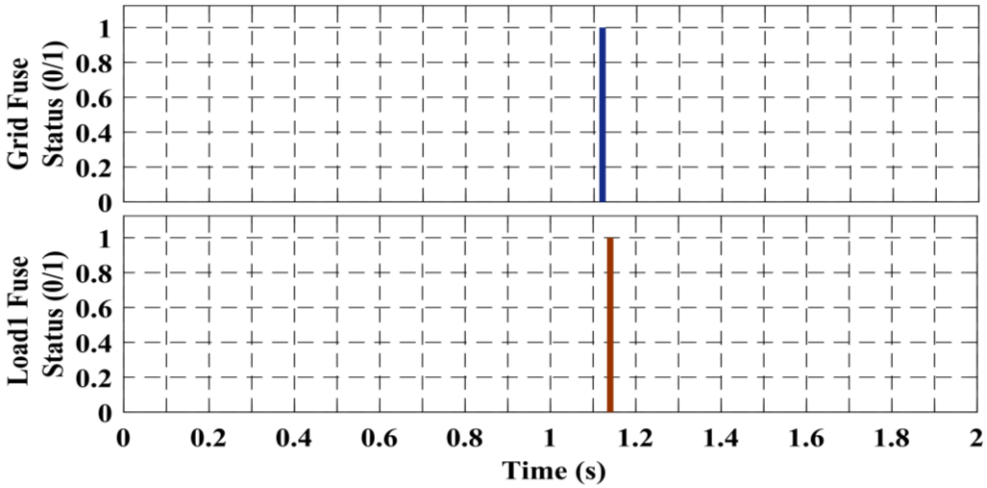

Fig. 4.11. *Blowing of fuse near node 13 grid side feeder and Blowing of fuse near node 12 load side feeder*

Status (0 to 1)) in the event of relay failure which was intentionally introduced to check operation of fuses. Fuses near to DGs operate quickly as compared to fuses at load side as rate of rise of current is higher. Table 4.9 shows the critical time setting, trip time based on operation of proposed relaying with backup fuses and their rating for feeder protection. The above proposed scheme is equally effective for any type of DG connected to the grid.

4.9. Comparison and cost analysis of *q0* component-based protection scheme

Proposed Adaptive protection scheme is feasible and cost effective as it uses small number of components and can be implemented in existing digital relays by taking *q0* components from existing converters. Its superiority and comparison with existing technologies are appended below

4.9.1. Feasibility comparison with existing protection schemes

The existing [46]-[48], [63] and [170]-[174] protection schemes are based on three phase voltage and current components (six variables) of microgrid systems but proposed scheme uses only *q0* components (two variables) of fault current for fault detection. In most of the protection schemes, the data exchange is necessary which needs communication channels but in the proposed scheme there is no exchange of data [52] and [53]. Every IED checks change of magnitude and transient component as *q* and *0* component of fault current based on proposed fuzzy algorithm for fault detection in proposed scheme. Also, existing protection schemes had not considered zero component of fault current for earth fault detection which is of utmost importance for earth fault detection and it is performed in this research work. *q* component of fault current is alone sufficient to detect all kinds of faults. The proposed protection scheme detects and locate faults within 60 to 80 ms which is a fast operation as compared to other technologies [46-48], [63] and [170-174].

It can be easily implemented in existing digital relays available from reputed protection relay manufacturers with and without goose connection circuitry. This scheme is based on static components of fault current it could be easily implemented in DC microgrids without using any dq0 transformation. Existing protection does not work in single phasing or one phase lightly loaded faults, open conductor, and high impedance faults. But proposed protection scheme detects and removes the single phasing or one phase lightly loaded faults, open conductor, and high impedance faults.

4.9.2. Cost analysis

The proposed scheme uses fuses as backup protection which further reduces the cost of operation as referred in [63]. As the proposed scheme uses change in *q0* components of fault current for proper protection operation, it is applicable to all level of voltages and currents. But this will need to replace the existing fuses for higher voltages and currents which will increase the cost. Also, this scheme considers *q0* components from existing converters. So, any extra circuitry for *q0* implementation and phasor measurement units are not needed reducing the cost.

No extra power electronic switches are used in proposed protection scheme that makes it more economical as compared to existing FCLs [167]-[171] and protection strategies [173]-[174]. Implementation of fuses and relays together are very much less expensive as compared to implementation of FCLs for low and medium voltage systems. Since earth, phase, open conductor, and single/two phase lightly loaded faults are also detected and removed, so there is no need of using no-voltage and earth fault relay. It operates as per change in voltage which further reduces the cost and increases the feasibility and applicability of q0 component based adaptive protection relay.

Chapter Summary

The fault characteristics of type I, III and IV wind DGs are studied in islanded mode as well as in PV based hybrid mode of microgrid operation. The simulation results have shown that there are significant variations in q0 components of fault current and the transient reactance for different modes and different types of wind DGs (type I, III and IV). The proposed adaptive protection algorithm is found effective for different types of generation with different X/R ratio during fault condition in microgrid system for series (including lightly loaded phase faults) and shunt faults. The results show that the transient components are different for PV DG and wind DGs (type I, III, IV) that helps in nature detection. The use of fuses reduces the reliability and adaptivity of microgrid structures though their use is good for backup. Proposed protection scheme with backup of fuses is cost effective and reliable. This approach is implemented based on static components; hence it is equally effective in dc microgrids.

Chapter 5

Adaptive Protection Coordination Optimization

Introduction

In conventional power system protection, the overcurrent relay (OCR) has an inverse relationship between the relay operation time and the short-circuit current at a given instant. A relay has time-dial settings *(TDS)* as a tuning parameter, the pickup current (I_p) above which the relay operates. In this chapter, for proper protection coordination optimization (PCO), the objective function is considered for minimization of operation time of relays with constraints as *TDS*, I_p and coordination time interval *(CTI).*

5.1. Background of work & problem statement

In the integration of distributed generators (DGs), this PCO problem has become more complex due to bidirectional feeding, blinding, and maloperation of relays. In addition, this problem becomes more complex while different systems with low inertia and low X/R ratio, such as microgrid, being integrated with conventional power system which has high inertia and X/R ratio. Even the same issue may appear in the microgrid system itself during interconnection of low and high inertia-based DGs. All these can majorly affect the operation of directional OCRs.

Very few literatures have reported emphasizing on the type of DGs connected in microgrid operation. Few literatures have reported considering only PV and Wind DGs which can cater the maximum load connected in a microgrid system. Fault current limiters have significant role in microgrid protection which need either communication channel or central controllers. This research has deliberately taken care of the above-mentioned problems. The fault current magnitudes at a given node depend on the operational mode of microgrid with different DGs. In the perspective of microgrid protection, optimally sizing of fault current limiters (FCL) and subsequent settings for directional overcurrent relays are proposed in [111]. In this reference, the problem has been formulated as a constrained non-linear programming (NLP) problem and is solved using the genetic algorithm (GA) with the static penalty constraint-handling technique. The protection coordination problem has been taken care of based on minimum power loss [112].

Considering dual settings for directional overcurrent relay (DOCR), a scheme is proposed which is capable of properly operating in forward and reverse direction coordinating through

communication channel [113]. Based on the cuckoo optimization algorithm (COA), an optimization tool is developed with linear rogramming (LP) to get optimal coordination protection settings for relays and FCL present at the point of common coupling (PCC) as reported in [108]. For better power quality (PQ) and proper protection coordination (PC), in presence of distributed energy resources (DERs), optimal sizing of solid-state unidirectional fault current limiters (SSUFCLs) are proposed [114].

Harmonic current injection capability of inverter-based distributed generators (IBDGs) is used to implement harmonic DOCR [115]. Considering PV DGs' installation at any location of feeder and level of penetration, the characteristic curve of overcurrent devices is modified with the second strategy limiting the output current of PV sources [28]. Superconducting FCLs are used to provide fault ride-through (FRT) capability with proper protection coordination [116]. Taking care of all possible network topologies the proper protection coordination is designed with the optimal relay settings with N−1 contingency [65]. An optimal protection scheme based on a differential evolution algorithm considering different operating modes of microgrid along with different types of phase fault is proposed in [117].

For proper protection coordination settings considering multi-agent with primary, backup and bus protection layers based on a variable tripping time; a differential protection scheme (VTDPS) is proposed for microgrid protection capable of operating in both grid-connected and islanded modes [63]. The adaptive modified firefly algorithm (AMFA) is used to get the optimum plug setting (PS) and time setting multiplier (TSM) parameters [118]. Using a fuzzy decision-making tool with the help of a multi-objective particle swarm optimization algorithm, an optimal coordination setting is proposed in [119]. Optimal sizing of the supercapacitors is done based on the two-level optimization scheme along with optimizing its controller parameters [120]. Depending upon protective relay blocking, generator rescheduling, and load shedding a new protection coordination scheme is proposed for minimizing power loss for wind DGs in [121].

In [58], a digital over and under frequency relay (DOUFR) is proposed which operates for over and under frequency in coordination with the digital PID controller. The change in impedance of network micro phasor measurement units (µPMUs) sends a signal to update OCRs settings using a communication channel [52]. Virtual inertia is controlled depending on change in frequency during different modes by the optimal PI controller using PSO to minimize the protection coordination time interval [122]. A non-standard tripping characteristic curve with

modified settings for the current multiplier finalized by GA is proposed in [123]. Definite time grading relay using negative sequence resistance for islanded IBDGs is proposed using voltage frequency control [124].

Different protection strategies are proposed based on measurement of three-phase voltages or three-phase currents that involve the use of three or six variables for protection coordination. There are not many protection schemes available for low and medium voltage systems that are backed by fuses which is going to be very much economical in small distribution systems and hybrid microgrids. Also, a protection scheme is needed to be designed that is economical, feasible and reliable for different nature DGs (PV and Wind types I, III and IV), whose efficacy is not hindered by nature of DGs, mode of operation, type of fault and type of system (ac or dc) etc. The main contribution of this research work is that only *q* component (static component) of fault current based strategy is proposed with the usage of fuses. The nature of DGs, mode of operation, type of fault, type of system, and location of fault do not impact the performance of the proposed *q* component-based protection scheme in coordination with backup fuses.

In this work, PV and wind energy (types I, III and IV) sources have been considered to validate the proposed adaptive protection coordination optimization scheme based on *q* component of fault current as main parameter for fault detection. A new concept of fuse constraints for fast fault removal is also validated in the proposed scheme where fuses provide backup to primary and backup relays. Fault characteristics of PV, single fed (type I), doubly fed (type III and IV) induction generators and synchronous DGs (as utility grid) are studied in terms of *q* components for proper protection coordination optimization in adaptive relaying. The proposed adaptive protection coordination optimization scheme changes *PSM* and *TDS* depending on change in mode of operation with minimization of operation time for primary and backup relays with the help of fuses.

5.2. System details & mathematical model

The hybrid microgrid used as a platform for the validation of the proposed adaptive protection scheme. It is modeled as per the specifications given in “Conditions of Supply” by the Punjab State Electricity Regulatory Commission (PSERC) [10]. The load of small Indian coastal village which was earlier fed by the utility is now connected to the hybrid microgrid. The wind speed and solar insolation are available abundantly in coastal India.

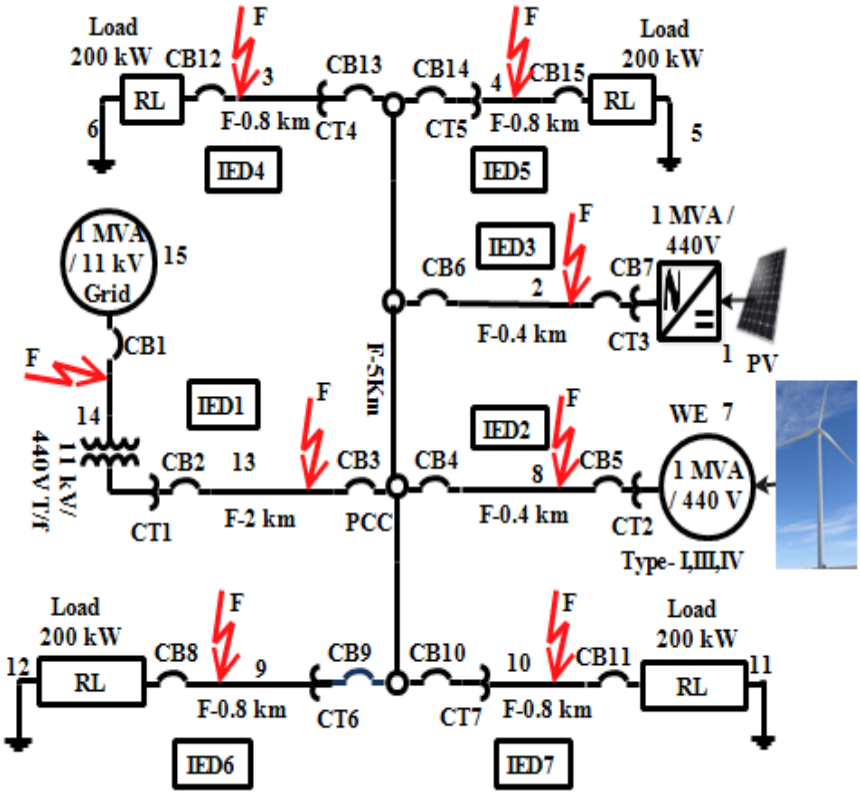

Fig. 5.1. *Block diagram of PV-WE-Grid based hybrid microgrid system*

The loads are mostly resistive and inductive as the domestic and agrarian load (three-phase motive load)) having power consumption level of of 400 kW and the feeders are operated at 415 V. Interconnection of wind turbines (types I/III/IV), PV (hybrid system) based distributed generators (DGs), load and utility resemble a hybrid microgrid.

The proposed hybrid microgrid is self-sufficient to feed the connected loads irrespective of the availability of utility grid. The locations of CBs (Fourteen Circuit Breakers marked as CB1 to CB14), CTs (Seven Current Transformers marked as CT1 to CT7), equal numbers of fuses (F1-F14) placed near circuit breakers and overcurrent relays (R - shown as R1 to R14) as shown in Figure 5.1 and 5.2.

5.2.1. System details of hybrid microgrid model

The schematic diagram of the proposed microgrid model is shown in Figure 5.1. It shows the layout of a three-phase AC microgrid system equipped with 1 MVA / 440 V photovoltaic (PV) system, wind energy (WE-I, III & IV) system of 1 MVA/440 V.

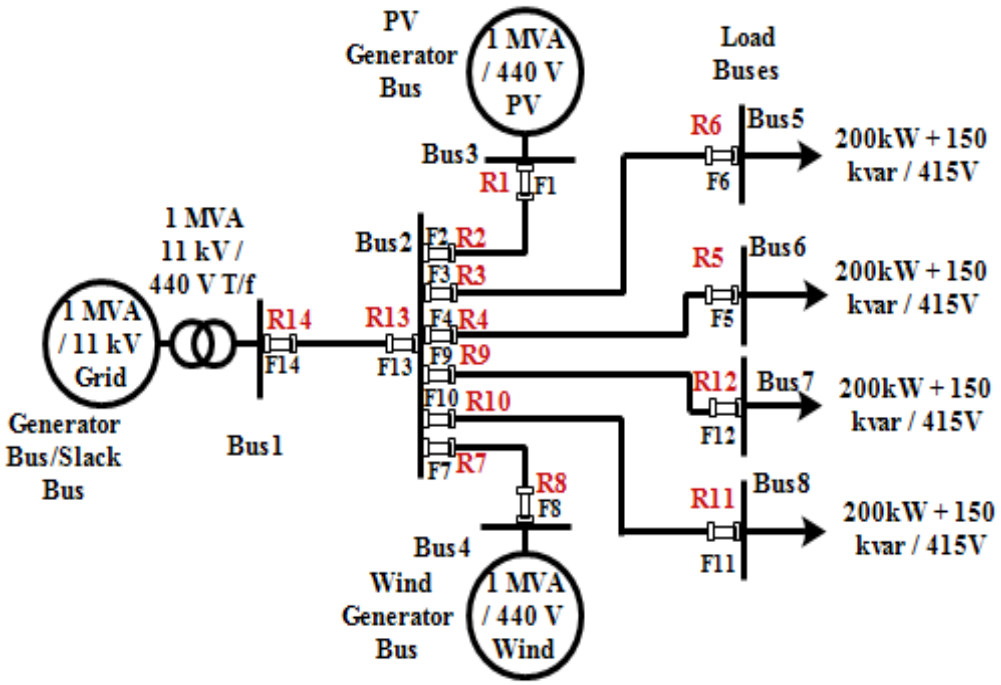

Fig. 5.2. *Single line diagram of hybrid microgrid system, mode1.*

In the design of hybrid microgrid, the PV controller is designed based on equations (2.5) and (2.6) in Chapter 2. Wind DGs for hybrid microgrid are based on wind turbine model of type I, III, and IV wind generators is done based on equation (2.7) as discussed in Section 2.4.3, Chapter 2. Whereas converters of DFIGs (type III and IV) are modeled as per equations (2.8), (2.9) and (2.10) as discussed in Section 2.4.4, Chapter 2. Figure 5.2. shows the single line diagram of hybrid model operating in grid connected mode. All are interconnected with utility grid of 1 MVA and 11 kV capacity through a step-down transformer of 1 MVA, 11 kV/440 V, 50 Hz at point of common coupling (PCC).

The entire system has a resistive load of 800 kW and a reactive load of 600 kvar. The different modes of operation are selected in hybrid microgrid by keeping buses 1, 3, and 4 in hybrid microgrid operation or out of operation as shown in Figure 5.2. (single line diagram) and Table 5.1.

Table 5.1 Mode change during hybrid microgrid operation

	Mode1	**Mode2**	**Mode3**	**Mode4**	**Mode5**	**Mode6**
Utility	1	1	1	0	0	0
Wind DG	1	0	1	1	0	1
PV DG	1	1	0	1	1	0

Different faults are simulated at the same location F but with different DGs for same fault duration of 0.1 second. The PV generator is controlled based on inverter control using double synchronous rotating frame (DSRF) for the more flexible fault-ride-through (FRT) control. The inner-loop current control uses the regulators under a DSRF and the outer-loop voltage control regulates the dc-link voltage to realize maximum power point tracking (MPPT) that is used in [48]. The wind generators (type I) and doubly fed (type III and IV) are modeled with variable pitch in this research work as per [141]. The type I wind generator is modelled as a squirrel cage induction generator. The converters of DFIGs (type III and IV) are modeled according to the reference [64]

5.2.2. Mathematical model & problem formulation

In case of directional overcurrent relays, inverse characteristics of the short circuit current magnitude decides operation time of the relay, it is given as equation (5.1) as per [111].

$$T = \frac{K1 \times TDS}{\left(\frac{If}{CTR \times Ip}\right)^{K2} - 1} \qquad (5.1)$$

where T is trip time, $K1$ and $K2$ are constants dependent on inverse-time characteristics of operation, TDS is time dial setting, CTR is current transformer ratio, I_f is the current through the relay and I_p is pickup current. Normally, the standard inverse is set for relays used in-line protection with $K1$ as 0.014 and $K2$ as 0.02. So, while deciding the optimal solution, the main parameters considered are TDS and I_p. The objective function is to be set aiming minimum operating time of relay. It is represented in equation (5.2), [111]:

$$\min T = \sum_{i=1}^{n} t_i \qquad (5.2)$$

where total number of relays are n and operating time for a relay under consideration is t_i. For utilizing proper optimization tool, three constraints are necessary which are time dial setting, pickup current, and coordination time (CTI). Minimum and maximum constraints for time dial settings and pickup current of relay are bound to lower and upper limits. The lower limit of pickup current tap setting $(I_{pmin\text{-}i})$ is set in such a manner for every relay that threshold of current resultant $(CTR \times I_p)$ is more than rated load current (normally 1.25 p.u.) for the respective part to be protected. Third constraint CTI which is the difference in a minimum operation time gap of a primary and backup relay is to be set as 120 ms. Third constraint is further supported by two newly

defined fuse constraints for primary and backup fuses to back up the primary and backup relays if the relays fail to operate.

The change in the mode of operation of a hybrid microgrid is shown in Table 5.1 where status 1 means utility/DG is in operation and status 0 means utility/DG is not in operation. Load flow studies are performed every time during a change in the hybrid microgrid mode of operation. In most of the literature, only two modes, such as grid-connected and islanded operation of microgrids are considered. In this research work different modes of hybrid microgrid are considered that are grid-connected, islanded and hybrid mode (wind and PV DG working together). The PV and wind DGs together are not considered in most of the literature with proper consideration of low inertia and low reactance. The objective function is the sum of operation time, *T* of all the primary and backup relays in operation during an event of a fault. It is given with modification to equation in [111] as per change in mode of operation as equation (5.3).

$$T_{total} = Min \sum_{m=1}^{nh} \left(\sum_{k=1}^{nf} \left(\sum_{j=1}^{nb} \left(\sum_{i=1}^{np} t_{(i,j,k)} \right) \right) \right) \quad (5.3)$$

Where, T_{total} is the sum of operating times of all relays with nh as the number of modes of operation that depend on the magnitude of *q* component of fault current available at given nf fault locations with *nb* is the number of buses of the system, *nh* is the mode of operation of microgrid system and *np* is the number of primary relays at fault locations. $t_{(i,j,k)}$ is the time of operation of relay $R_{(i,j)}$ for fault occurrence at the bus number *k*, $R_{(i,j)}$ is the relay in-branch *i-j* near bus *i*. Similarly, $R_{(i,i)}$ is the relay at the generator bus *i*. $t_{(i,j,k)}$ is the time of operation of relay $R_{(i,j)}$ for fault occurrence at the bus number *k*. $I_{f(i,j,k)}$ is fault current between bus number *i* and bus number *j* for fault at bus *k*. $I_{p(i,j,k)}$ is the pickup value of relay $R_{(i,j)}$, value of $I_{p(i,j,k)min}$ with I_{p_min} is chosen in such a manner that overload current margin range is 15-25 percent. $t_{(i,j,k)}$ is calculated as inverse-time characteristic function with *K1* as 0.014 and *K2* as 0.02 and given by equation (5.4).

$$t_{(i,j,k)} = \frac{K1 \times TDS}{\left(\frac{I_{f(i,j,k)}}{CTR \times I_{p(i,j,k)}} \right)^{K2} - 1} \quad (5.4)$$

The constraints of objective function are assigned for *TDS* and I_p where $TDS_{min\text{-}i}$, and $TDS_{max\text{-}i}$ are minimum and maximum limits on time dial settings, $PSM_{pmin\text{-}i}$ and $PSM_{pmax\text{-}i}$ are minimum and maximum limits on plug setting multiplier, $I_{pmin\text{-}i}$ and $I_{pmax\text{-}i}$ are minimum and maximum limits for pickup current for i^{th} relay. There are some relays ready for backup relay

operation for each fault. So, for proper coordination of backup relays, coordination constraint per fault is needed to be satisfied which is given as coordination time interval *(CTI)* which is taken to be 0.120 s. The constraints in limits that are set to minimizing objective function are as follows [111]:

$$TDS_{min\text{-}i} \leq TDS_i \leq TDS_{max\text{-}i}$$

$$PSM_{pmin\text{-}i} \leq PSM_{pi} \leq PSM_{pmax\text{-}i}$$

$$t_{hij}^{bkr} - t_{hij}^{pr} \geq CTI$$

In, t_{hij}^{bkr} and t_{hij}^{pr}, *h* represents the operation mode, it is either grid-connected or islanded or hybrid mode, l is the location of the fault, *bkr* means *(k)* number of backup relays, and *pr* means primary relay in operation. New, *CTI* constraints are proposed for backup to primary relay and backup relay. *CTI* for primary backup fuses (t_{pfuse}) to back up the primary relay is taken to be 0.05s in addition to *CTI* of backup relay (t_{brelay}). CTI for backup fuses (t_{bfuse}) to back up the backup relay is taken to be 0.100s in addition to *CTI* of primary fuse .

$$t_{pfuse} - t_{prelay} \geq 170ms$$

$$t_{bfuse} - t_{prelay} \geq 220ms$$

Based on *q0* components of fault current the relations are modified and proposed as equation (5.5):

$$I_p = I_{relay}(q,0) \qquad (5.5)$$

Equation (5.1) is modified and proposed for accordingly for I_i and I_p as follows:

$$T = \frac{K1 \times TDS}{\left(\frac{Ii(q,0)}{CTR \times Ip(q,0)}\right)^{K2} - 1} \qquad (5.6)$$

The proposed modification is validated using a differential evolutionary algorithm (DEA) in the next Section below. *CTR* for grid side and wind DGs is 400, 300 for PV DGs, and 200 for all the load side nodes. For the minimization of many variables involved in the adaptive protection schemes, transformation of AC three-phase current to *dq0* current is done using Park's transformation as per [42] which is mentioned by equations in Section 2.5 of Chapter 2 as 2.11 and 2.12.

The microgrids comprise of DGs with low X/R which directly affects the I_q component as mentioned above. So, the variation in the I_q component is considered to detect fault which justifies that this system works for any X/R ratio. As given in this reference, only *q0* components are sufficient to detect a fault and its location. To minimize the impact of dynamicity in hybrid microgrid, an adaptive feature in the protection scheme is implemented based on the equations 3.11 and 3.12 of Section 3.4.1 of Chapter 3. Furthermore, out of two components *q* and *0*, only *q* component of fault current is used fault detection from equations (4.1) and (4.2) as discussed in Section 4.3 of Chapter 4. So, change in I_{sc} can be used to detect the fault, considering a minimum number of parameters discussed as relation 4.3 in Section 4.3 of Chapter 4. The I_d and I_0 can be neglected and effective protection could be redesigned according to change in relation given as equation 5.7:

$$I_{sc} = f(\mathrm{I}_q) \tag{5.7}$$

An adaptive protection coordination optimization scheme based on equation (5.7) can easily detect any fault at any location with any number and any type of DG. But, for differentiating among phase and earth faults; zero component of fault current is equally important as q component. The new constraints are defined for proper protection coordination among relays and fuses which helps in understanding of slow relay operation of PV DG side system in comparison to wind DG side. Selection of *PSM* and *TDS* for different modes of hybrid microgrid is based on relations (4.1) and (4.2) as discussed in Section 4.3. of Chapter 4.

5.3. Algorithm

In this research work, protection coordination problem is optimized based only on *q* component and *0* component is for identification among phase and earth fault component of fault current in a hybrid microgrid. The hybrid microgrid has different types of wind generators as types I, III, IV, and PV DG connected with the utility grid. These proposed adaptive optimization settings resolve all the issues arising due to the integration of different Wind DGs (type I, III, and IV) with utility and PV DGs. For the optimization of linear as well as a nonlinear problem as shown in equations 1 and 2, the best technique is meta-heuristic hybrid differential evolutionary algorithm (DEA). It is also validated that *q* components of fault current are sufficient with the help of zero components. Zero component of fault current helps in identifying earth faults which was not

considered earlier in resolving protection coordination problems. DEA considering only *q* component (one variable) of fault current is proposed for getting optimal settings of *PSM*, *TDS*, and optimum protection coordination time for primary and backup relays. Figure 5.3, shows flowchart of proposed q component based adaptive protection coordination optimization scheme.

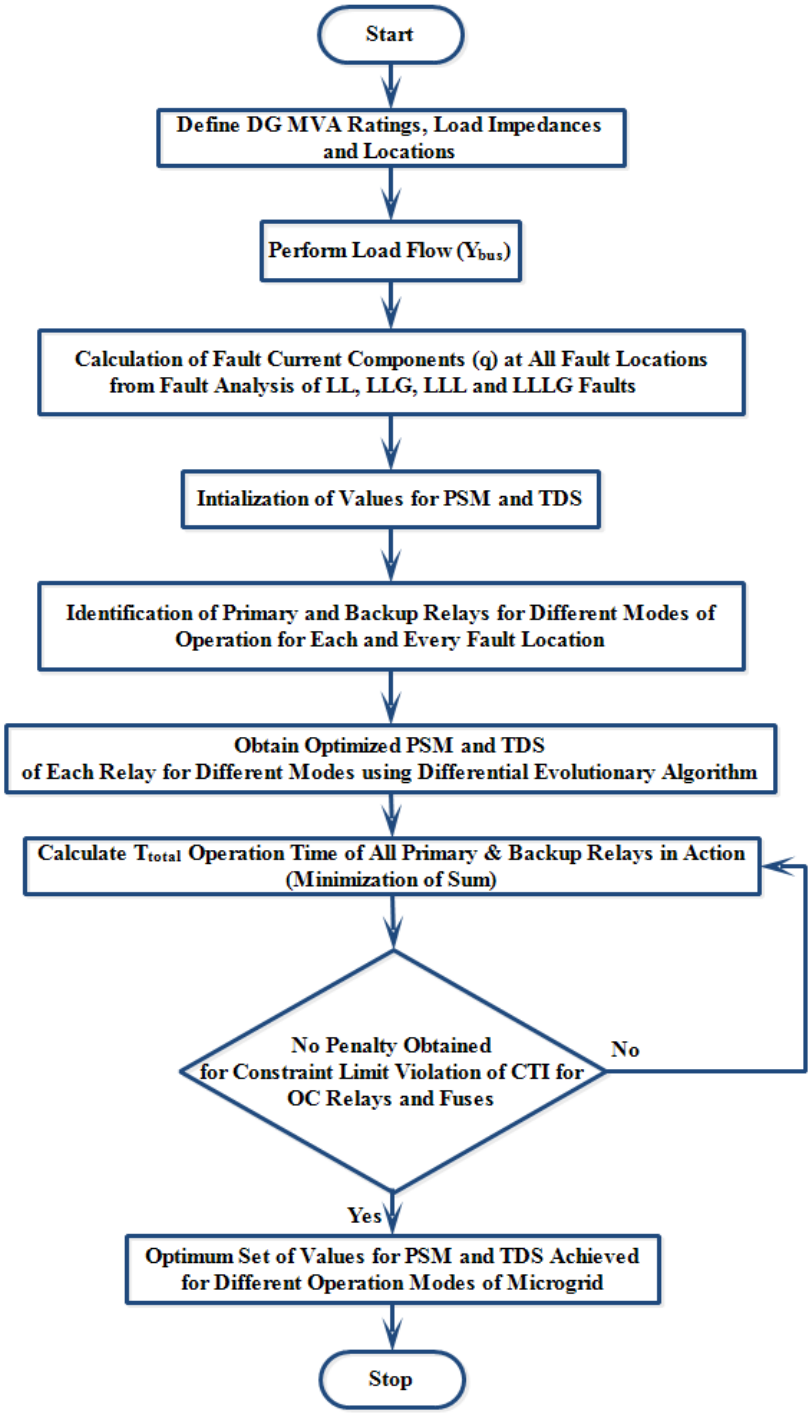

Fig. 5.3. *Flowchart of proposed adaptive protection coordination for hybrid microgrid.*

Storn and Price introduced the population-based stochastic algorithm in 1995 [174]. It is simple and fast in implementation with the ability of finding out global best available values [175]. DEA has four steps that are with first being initialization of parameters, mutation, crossover, and selection with good convergence properties. The above-mentioned steps are repeated until the optimal global setting values are obtained. Iteration number and objective function stop updating only when best fit global settings are obtained. In this research work with the approach of obtaining optimal solution meta-heuristic, DEA considering q components of fault current is found to be the best meta-heuristic algorithm.

The main emphasis of this research work is on obtaining the best adaptive optimum protection coordination settings with only *q* component of fault current in a hybrid microgrid with any number and any type of DGs which was not done earlier. A brief explanation of DEA can be found in [174]-[175]. The flowchart in Figure 5.3 shows the *q* component-based DEA flow for obtaining the adaptive optimal set of *PSM* and *TDS* of relay settings for the hybrid microgrid. The flowchart shows setting up hybrid microgrid parameters such as DG and grid ratings, load impedances, and load locations. After that load flow studies are performed to check the feasibility of proposed hybrid microgrid followed by different fault current calculations at every location for different modes of operation for a hybrid microgrid. The procedure of DEA based optimization process for the hybrid microgrid is as follow:

a. Set utility grid and DG MVA ratings and system impedances depending on location and load.

b. Check load flow for all the possible modes of operation for hybrid microgrid.

c. Calculate fault current *q* component at all fault locations for different fault during all possible modes of hybrid microgrid.

d. Input: Maximum (2.5) and minimum (0.5) limits of *PSM* with step size 0.05 and Maximum (2.5) and minimum (0.5) of *TDS* with step size 0.01 with a discrimination time of 120 ms along with the different *CTR* at different buses is given as input. Also, the input parameters for the DEA are considered as generation number and population size. A maximum generation number of 1000 with a population size of 45 is set.

e. Initialization: *PSM* and *TDS* are initialized from lower bounds as shown in constraint equalities and are initialized for all the 14 relays in the proposed hybrid microgrid.

f. Data Recreation: Recreation of data is possible by mode of operation of hybrid microgrid as shown in Table I. Dynamic nature of hybrid microgrid modes of operation not only changes the fault current levels but also alters the primary and backup relay pairs to be activated for given fault locations. Phase and earth faults have different levels of fault current. So, it is very much important to get primary-backup relay pairs for different short circuit currents for each kth phase and earth faults for every mode of operation in a hybrid microgrid.

g. Fitness function calculation: The minimum values of objective function given in relation is calculated. For any constraint's violation, the penalty is added from error values obtained. Obtained setting values must satisfy all the constraints.

h. Update vector: As per the mutation strategy of DEA, the update vector is generated for *PSM* and *TDS* settings of every relay of each i^{th} fault location.

i. Stopping criteria: Termination of DEA happens for the minimum threshold value of penalty function (0 or 10^{-5}).

5.4. Results & discussion

The hybrid microgrid single line diagram is shown in Figure 5.2. in which 14 relays are installed as R_1 - R_{14} and fuses F_1 - F_{14} for proper protection and back- up by an equal number of fuses. Table 5.1 shows all possible modes of operation for hybrid microgrid where status 1 shows utility, wind, and PV DGs which are active in that mode of operation whereas, the 0 means inactive. The phase and earth faults are simulated for proper hybrid microgrid protection coordination. Proposed relay settings for *PSM* and *TDS* for different modes of operation are shown in Tables 5.2 to 5.7 to achieve adaptive optimum protection coordination. Table 5.8 shows different types of fuses used to assist primary and backup relay for fast adaptive protection coordination. Table 5.9 to 5.20 show operation time (OT) and coordination time (CT) of primary (P) and backup (B) relay with assistance from fuses in different modes of operation for three phase and earth faults at different locations. Table 5.21 shows steady state, minimum pickup current and

fault current values of *q* component of fault current for different modes of hybrid microgrid operation for different faults at different locations. Out of the given set of relays, primary relays installed must operate first and if primary fails, the backup relay must operate within a specified coordination time interval *(CTI)* as discussed in [111]. In the proposed scheme if in any case, primary and backup relaying fails, the fuses will coordinate with the given backup relay and blows after coordination time interval of backup relay as per fuse constraints discussed in Section 5.2. Minimum *CTI* constraint for backup relay is set as 120 ms, for primary fuse is 0.05s in addition to backup relay *CTI* and for backup fuse it is 0.1s in addition to backup relay *CTI*.

For the validation of the proposed adaptive protection coordination optimization scheme, hybrid microgrid operation modes are discussed as optimal adaptive settings of *PSM* and *TDS* for different modes of operations with phase and earth faults. *PSM* decides severity of fault by giving the magnitude of fault current over reference current value and *TDS* decides delay given to relay operation. For only PV feeding the load buses while buses 1 and 4 are not in operation, mode 5 is set as shown in Figure 5.4.

In the proposed hybrid microgrid when only PV DG is feeding the connected load irrespective of the availability of utility grid and wind DG relay settings change as per the availability of current. The locations of CBs (Ten Circuit Breakers), CTs (Five Current Transformers), ten numbers of fuses placed near circuit breakers and overcurrent relays (Ten in number) as shown in Figure 5.1 and Figure 5.4.

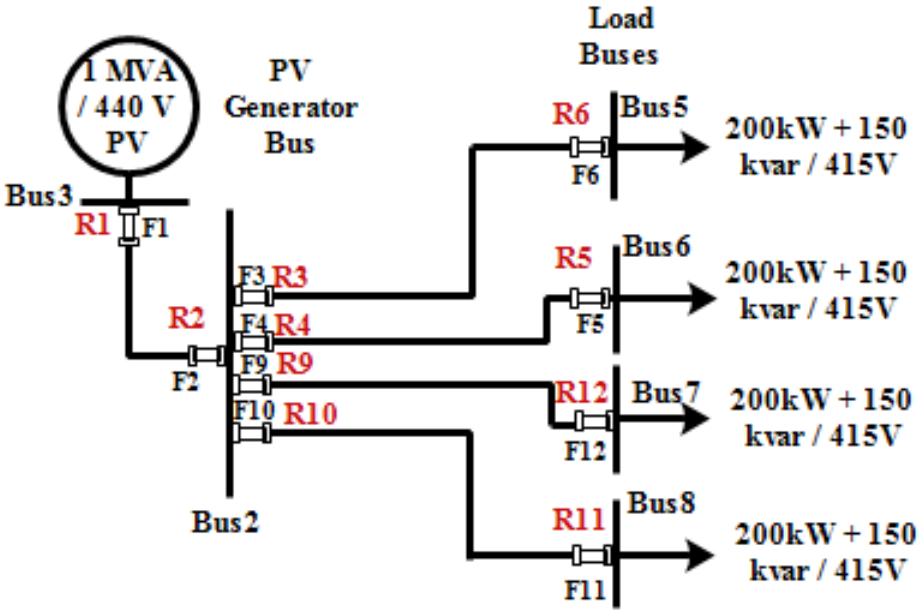

Fig. 5.4. *Single line diagram of islanded PV microgrid, mode5.*

Table 5.2 *TDS* and *PSM* for Mode5

Relays	*PSM*	*TDS*
1	2.25	0.25
2	2.25	0.25
3	1.75	0.20
4	1.75	0.20
5	1.75	0.20
6	1.75	0.20

Table 5.3 *TDS* and *PSM* for Mode6

Relays	*PSM*	*TDS*
7	2.5	0.15
8	2.5	0.15
9	1.85	0.12
10	1.85	0.12
11	1.85	0.12
12	1.85	0.12

Table 5.2 and Table 5.3 show the proposed adaptive *PSM* and *TDS* settings for phase and earth faults detected using q components of fault current for hybrid microgrid for mode 5 (PV DG feeding load in islanded mode) and mode 6 (wind DG feeding load in islanded mode). As islanded wind DG has more current share as compared to islanded PV DG so severity of fault will be more for wind DG in comparison to PV DG.

Table 5.2 and Table 5.3 show this fault severity by setting *PSM* higher for wind DG as compared to PV DG by proposed adaptive protection coordination optimization scheme. As, *TDS* is the delay depending on the severity of fault corresponding to which relay takes *action*. Severity of fault is high for wind DG connection in comparison to PV DG connection so *TDS* is low for islanded wind DG connection as compared to islanded PV DG connection.

For same type of phase fault at same location that is load end, *TDS* is 0.25 for PV DG and 0.15 for wind DG. If only wind DGs feed the load-buses, then the buses 1 and 3 are not in operation, hence the microgrid is operated in mode 6 as shown in Figure 5.5.

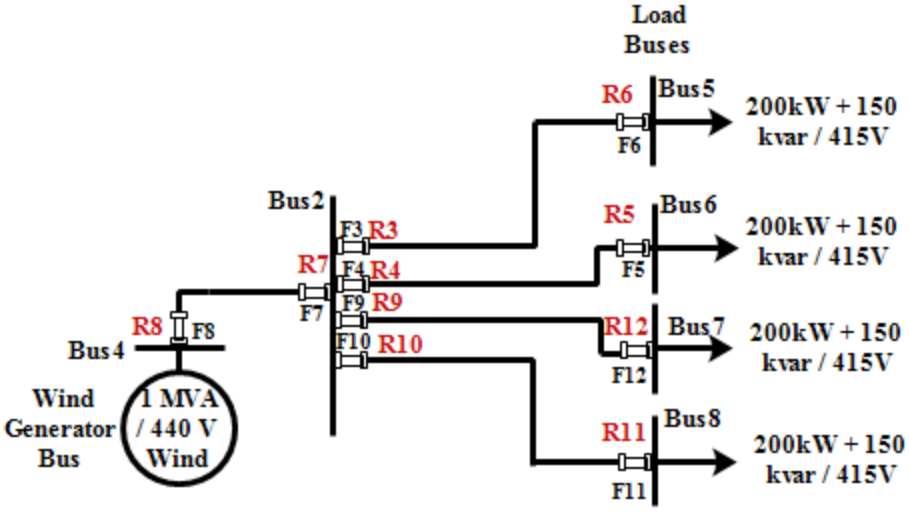

Fig. 5.5. *Single line diagram of islanded wind microgrid, mode6.*

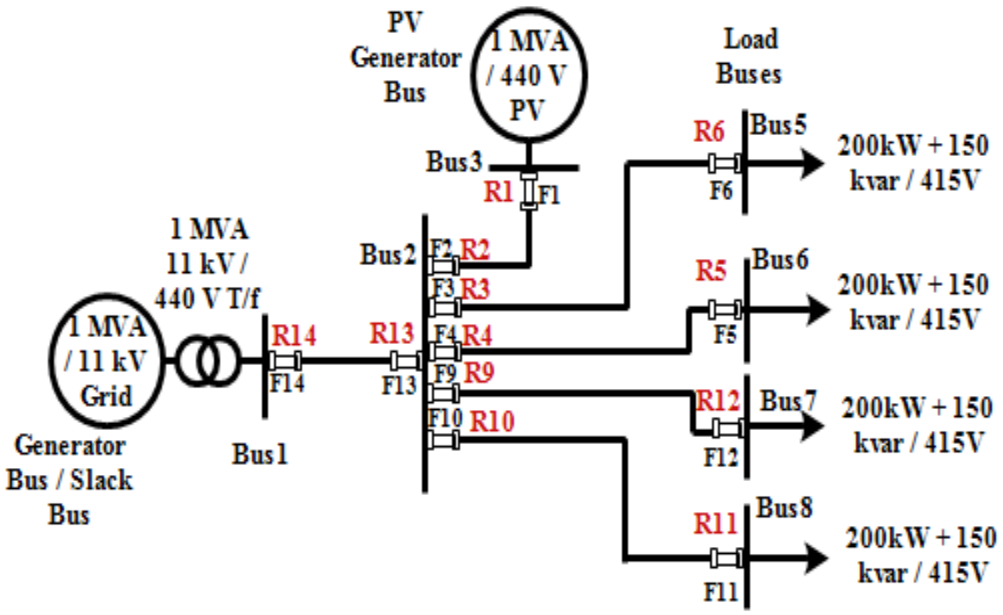

Fig. 5.6. *Single line diagram of grid connected PV microgrid, mode2.*

For a hybrid microgrid in mode 2 where PV DG and utility grid are in operation and feeding the load as shown in Figure 5.6. With every change in mode of operation number of available CTs, relays, fuses and circuit breakers changes. Table 5.4 and Table 5.5 show the proposed adaptive *PSM* and *TDS* settings for phase and earth faults detected using q components of fault current. As wind DG and utility grid (mode 3) have more current share as compared to PV DG and utility grid (mode 2) so severity of fault will be more for mode 3 in comparison to mode 2.

Table 5.4 and Table 5.5 show this fault severity by setting *PSM* higher for wind DG and utility grid as compared to PV DG and utility grid. In similar manner depending on severity of fault *TDS* is low for wind DG and grid connection in comparison to PV DG and grid connection. For same type of phase fault at same location that is DG end, *TDS* is 0.20 for PV DG and 0.12 for wind DG.

Table 5.4 *TDS* and *PSM* for Mode3

Relays	***PSM***	***TDS***
7	2.45	0.12
8	2.45	0.12
9	1.95	0.18
10	1.95	0.18
11	1.95	0.18
12	1.95	0.18
13	2.5	0.10
14	2.5	0.10

Table 5.5 *TDS* and *PSM* for Mode2

Relays	***PSM***	***TDS***
1	2.15	0.2
2	2.15	0.2
3	1.9	0.18
4	1.9	0.18
5	1.9	0.18
6	1.9	0.18
13	2.5	0.14
14	2.5	0.14

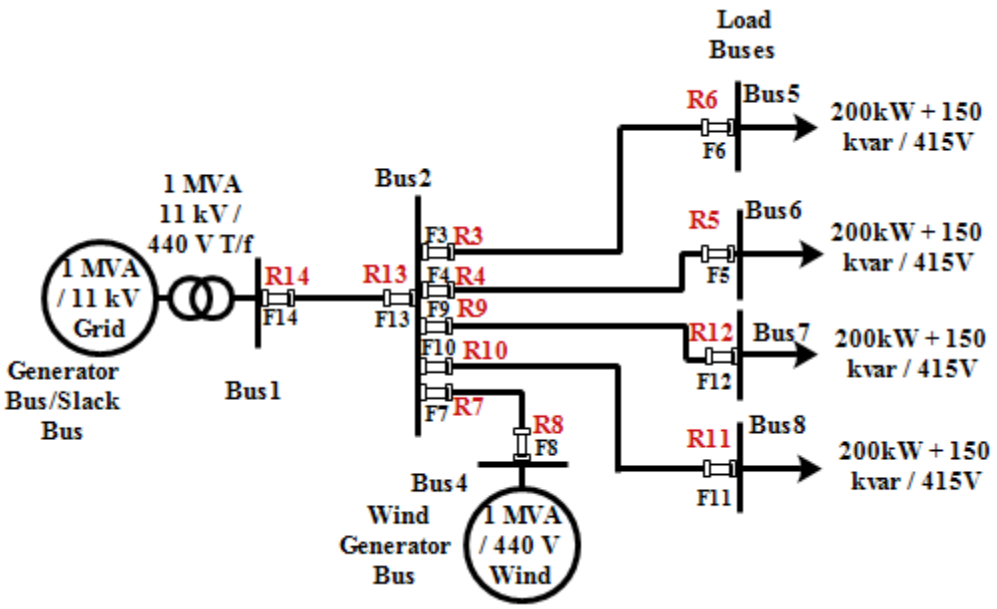

Fig. 5.7. *Single line diagram of grid connected wind microgrid, mode3.*

When wind DG and grid feed the loads, only bus 3 is not in operation, hence the microgrid can be set in mode 3 operation as shown in Figure 5.7. When PV and wind DGs feed the loads, only bus 1 is not in operation, hence the system operates in mode 4 as shown in Figure 5.8. When the PV DG and grid feed the loads; only bus 4 is not in operation, hence the microgrid is set in mode 2 as shown in Figure 5.8. When PV DG, wind DG and grid are feed the loads and all buses are in operation, then the system is set in mode 1 as shown in Figure 5.2.

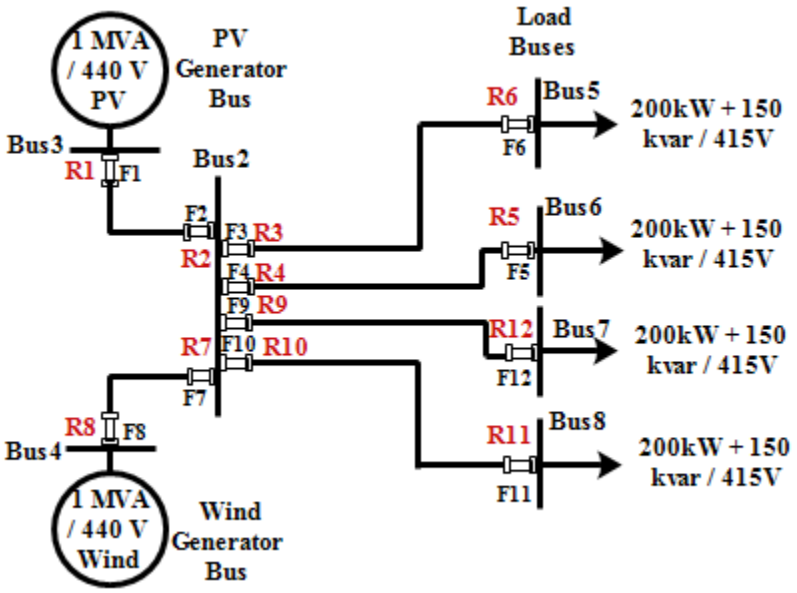

Fig. 5.8. *Single line diagram of islanded wind-PV hybrid microgrid, mode4.*

Table 5.6 *TDS* and *PSM* for Mode4

Relays	*PSM*	*TDS*
1	2.25	0.2
2	2.25	0.2
3	1.75	0.15
4	1.75	0.15
5	1.75	0.15
6	1.75	0.15
7	2.35	0.1
8	2.35	0.1
9	1.8	0.15
10	1.8	0.15
11	1.8	0.15
12	1.8	0.15

Table 5.7 *TDS* and *PSM* for Mode1

Relays	*PSM*	*TDS*
1	2.3	0.15
2	2.3	0.15
3	1.7	0.2
4	1.7	0.2
5	1.7	0.2
6	1.7	0.2
7	2.45	0.10
8	2.45	0.10
9	1.85	0.15
10	1.85	0.15
11	1.85	0.15
12	1.85	0.15
13	2.5	0.05
14	2.5	0.05

Table 5.6 and Table 5.7 show the proposed adaptive *PSM* and *TDS* settings for phase and earth faults found using *q* components of fault current for a hybrid microgrid in mode 4 as shown in Figure 5.8., PV and wind DGs feeding load in PV-wind hybrid mode and mode 1 PV, wind DGs and utility grid feeding load in hybrid-grid mode. As wind DG, PV DG and utility grid (mode 1) have more current share as compared to PV DG and wind DG (mode 4) so severity of fault will be more for mode 1 in comparison to mode 4. Table 5.6 and Table 5.7 show this fault severity by

Table 5.8 Fuses used as backup for backup relay in hybrid microgrid

Node	**Fuse Type**	**Rating (MVA)**
1	50T	1 PV DG
2	50T	1 PV DG
3	15T	0.3 load
4	15T	0.3 load
5	15T	0.3 load
6	15T	0.3 load
7	50T	0.3 load
8	50T	0.3 load
9	25T	0.4 load
10	25T	0.4 load
11	25T	0.4 load
12	25T	0.4 load
13	50T	1.0 Grid
14	50T	1.0 Grid

setting *PSM* higher for wind DG, PV DG and grid as compared to wind DG and PV DG together. In similar manner depending on severity of fault *TDS* is low for wind DG, PV DG and grid connection in comparison to wind DG and PV DG connection. Fuses are used in proposed hybrid microgrid that are present near relays and acting as backup protection for backup relays. Table 5.8 shows the fuses that are used in the proposed hybrid microgrid.

Table 5.9 shows the operation time (OT) and coordination time (CT) of primary relay 6 (R6P) and backup relay 3 (R3B) with backup fuses for three-phase faults (LLL) at node 3 during microgrid operation in mode 5 as shown in Figure 5.4. R6P has OT of 0.157 seconds with zero coordination time as it is a primary relay. R3B has OT of 0.336 seconds with 0.179 seconds delay for coordination time as it is a backup relay. The backup fuses do not operate until backup relays fail to operate. Primary backup fuse which is present near R6P operates only if R3B fails. Primary backup fuse does not operate till 0.336 seconds and operates with minimum delay of 50 ms (as per primary fuse constraint) added to OT of R3B. Secondary backup fuse which is present near R3B operates only if primary backup fuse fails to operate. Secondary backup fuse does not operate till 0.392 seconds and operates with minimum delay of 100 ms (as per secondary fuse constraint) added to OT of primary fuse. CT for backup fuse is 0.501 seconds. The Table 5.9 shows three-phase faults at node 1 in mode 5 as shown in Figure 1. In similar manner the OT and CT of primary relay 1 (R1P) and backup relay 2 (R2B) are obtained with backup fuses using proposed only q component based adaptive protection coordination optimization scheme.

Table 5.9 Operation and coordination time of primary (P) and backup (B) relay with fuses in mode 5 for three phase fault (LLL)

Relays	OT(s)	CT of Relays(s)	Fuse Type	CT of Fuses(s)
R6P	0.157	0	15T	0.392
R3B	0.336	0.179	15T	0.501
R1P	0.197	0	50T	0.413
R2B	0.356	0.159	50T	0.533

Table 5.10 Operation and coordination time of primary (P) and backup (B) relay with fuses in mode 5 for earth fault s (LG-LLG)

Relays	OT(s)	CT of Relays(s)	Fuse Type	CT of Fuses(s)
R6P	0.197	0	15T	0.448
R3B	0.393	0.196	15T	0.556
R1P	0.208	0	50T	0.430
R2B	0.367	0.159	50T	0.543

Table 5.10 shows the OT and CT time of primary relay 6 (R6P) and backup relay 3 (R3B) with backup fuses for earth faults (LG and LLG) during mode 5 at node 3 shown in Figure 5.4. Also, in Table 5.10, it is shown that during earth faults at node 1, in mode 5, the OT and CT of primary relay 1 (R1P) and backup relay 2 (R2B) are available with backup fuses as shown in Figure 5.4. R6P has OT of 0.197 seconds with zero coordination time as it is a primary relay. R3B has OT of 0.393 seconds with 0.196 seconds delay for coordination time as it is a backup relay. The backup fuses do not operate until backup relays fail to operate. Primary backup fuse which is present near R6P operates only if R3B fails. Primary backup fuse does not operate till 0.393 seconds and operates with minimum delay of 50 ms (as per primary fuse constraint) added to OT of R3B. Secondary backup fuse which is present near R3B operates only if primary backup fuse fails to operate. Secondary backup fuse does not operate till 0.448 seconds and operates with minimum delay of 100 ms (as per secondary fuse constraint) added to OT of primary fuse. CT for backup fuse is 0.556 seconds. Three-phase and earth faults are not considered on node 4 in mode 5 as this will also obtain nearly the same values of OTs and CTs for same faults on node 3 (since the load and line parameters are same). Furthermore, there is no role of relays from R7 to R14, as in mode 5 these relays remain out of operation due to the PV DG islanded mode.

Table 5.11 shows the OT and CT of primary relay 12 (R12P) and backup relay 9 (R9B) at node 9 with three-phase fault and OT and CT of primary relay 8 in mode 6, OT and CT of primary relay 8 (R8P) and backup relay 7 (R7B) with backup fuses for LLL faults at node 8 during mode

Table 5.11 Operation and coordination time of primary (P) and backup (B) relay with fuses in mode 6 for three phase fault (LLL)

Relays	OT(s)	CT of Relays(s)	Fuse Type	CT of Fuses(s)
R12P	0.174	0	25T	0.441
R9B	0.379	0.205	25T	0.553
R8P	0.153	0	50T	0.382
R7B	0.321	0.168	50T	0.494

Table 5.12 Operation and coordination time of primary (P) and backup (B) relay with fuses in mode 6 for earth faults (LG-LLG)

Relays	OT(s)	CT of Relays(s)	Fuse Type	CT of Fuses(s)
R12P	0.205	0	25T	0.463
R9B	0.407	0.202	25T	0.525
R8P	0.160	0	50T	0.378
R7B	0.321	0.160	50T	0.438

6 as shown in Figure 5.5. R12P has OT of 0.174 seconds with zero coordination time as it is a primary relay. R9B has OT of 0.379 seconds with 0.205 seconds delay for coordination time as it is a backup relay. The backup fuses do not operate until backup relays fail to operate. Primary backup fuse which is present near R12P operates only if R9B fails. Primary backup fuse does not operate till 0.379 seconds and operates with minimum delay of 50 ms (as per primary fuse constraint) added to OT of R9B. Secondary backup fuse which is present near R9B operates only if primary backup fuse fails to operate. Secondary backup fuse does not operate till 0.441 seconds and operates with minimum delay of 100 ms (as per secondary fuse constraint) added to OT of primary fuse. CT for backup fuse is 0.553 seconds. In similar manner the OT and CT of primary relay 8 (R8P) and backup relay 7 (R7B) are obtained with backup fuses using proposed only *q* component based adaptive protection coordination optimization scheme.

Table 5.12 shows the OT and CT of primary relay 12 (R12P) and backup relay 9 (R9B) at node 9 with Earth fault and OT and CT of primary relay 8 in mode 6, OT and CT of primary relay 8 (R8P) and backup relay 7 (R7B) with backup fuses for earth faults at node 8 during mode 6 as shown in Figure 5.5. R12P has OT of 0.205 seconds with zero coordination time as it is a primary relay. R9B has OT of 0.407 seconds with 0.202 seconds delay for coordination time as it is a backup relay. The backup fuses do not operate until backup relays fail to operate. Primary backup fuse which is present near R12P operates only if R9B fails. Primary backup fuse does not operate till 0.407 seconds and operates with minimum delay of 50 ms (as per primary fuse constraint) added to OT of R9B. Secondary backup fuse which is present near R9B operates only if primary backup fuse fails to operate. Secondary backup fuse does not operate till 0.463 seconds and operates with minimum delay of 100 ms (as per secondary fuse constraint) added to OT of primary fuse. CT for backup fuse is 0.525 seconds. Three-phase fault and earth fault are not considered on node 10 in mode 5, as this will also obtain nearly the same values of OTs and CTs as for the same faults on node 9 (load and line parameters are the same).

Furthermore, there is no role of relays from R1 to R6, R13 and R14, as in mode 6 these relays remain out of operation due to the Wind DG islanded mode. From Tables 5.9 to Table 5.12, CT for primary relays in operation is zero. The Tables 5.9 to Table 5.12 show that OT and CT of primary and backup relays are different during three-phase fault and earth fault. As q component of fault current differs with a change in nature of DGs feeding the fault, mode of operation of hybrid microgrid and with the type of fault.

Adaptive settings for different relays must be varying in accordance with the obtained optimum relay settings during the islanded mode of operation for hybrid microgrid. As shown in Table 5.9 to Table 5.12, primary and backup relays with backup fuses are working in minimum time with no constraint violation.

Tables 5.13 and 5.14 show the OTs and CTs of primary and backup relays for LLL and LLG faults at nodes 3, 1, and 14 during mode 2 as shown in Figure 5.6. of hybrid microgrid operation. R6P has OT of 0.171 seconds with zero coordination time as it is a primary relay. R3B has OT of 0.299 seconds with 0.128 seconds delay for coordination time as it is a backup relay. The backup fuses do not operate until backup relays fail to operate. Primary backup fuse which is present near R6P operates only if R3B fails. Primary backup fuse does not operate till 0.299 seconds and operates with minimum delay of 50 ms (as per primary fuse constraint) added to OT of R3B. Secondary backup fuse which is present near R3B operates only if primary backup fuse fails to operate. Secondary backup fuse does not operate till 0.356 seconds and operates with minimum delay of 100 ms (as per secondary fuse constraint) added to OT of primary fuse. CT for backup fuse is 0.418 seconds. In similar manner the OT and CT of primary relay 1 (R1P), backup relay 2 (R2B), primary relay 14 (R14P) and backup relay 13 (R13B) are obtained for earth faults

Table 5.13 Operation and coordination time of primary (P) and backup (B) relay with fuses in mode 2 for three phase fault (LLL)

Relays	OT(s)	CT of Relays(s)	Fuse Type	CT of Fuses(s)
R6P	0.171	0	15T	0.356
R3B	0.299	0.128	15T	0.418
R1P	0.164	0	50T	0.441
R2B	0.383	0.159	50T	0.512
R14P	0.157	0	50T	0.372
R13B	0.314	0.157	50T	0.435

Table 5.14 Operation and coordination time of primary (P) and backup (B) relay with fuses in mode 2 for earth faults (LG-LLG)

Relays	OT(s)	CT of Relays(s)	Fuse Type	CT of Fuses(s)
R6P	0.143	0	15T	0.356
R3B	0.295	0.152	15T	0.420
R1P	0.167	0	50T	0.443
R2B	0.386	0.159	50T	0.507
R14P	0.145	0	50T	0.347
R13B	0.290	0.145	50T	0.415

with backup fuses using proposed only q component based adaptive protection coordination optimization scheme. During mode 2, wind DG and Loads of nodes 12 and 11 are disconnected, so no role of relays R7 to R12 exist.

Tables 5.15 and 5.16 show the OTs and CTs of primary and backup relays for LLL and LLG faults at nodes 9, 8, and 14 during mode 3 as shown in Figure 5.7. of hybrid microgrid operation. R12P has OT of 0.165 seconds with zero coordination time as it is a primary relay. R9B has OT of 0.295 seconds with 0.130 seconds delay for coordination time as it is a backup relay. The backup fuses do not operate until backup relays fail to operate. Primary backup fuse which is present near R12P operates only if R9B fails. Primary backup fuse does not operate till 0.295 seconds and operates with minimum delay of 50 ms (as per primary fuse constraint) added to OT of R9B. Secondary backup fuse which is present near R9B operates only if primary backup fuse fails to operate. Secondary backup fuse does not operate till 0.352 seconds and operates with minimum delay of 100 ms (as per secondary fuse constraint) added to OT of primary fuse. CT for backup fuse is 0.421 seconds. In similar manner the OT and CT of primary relay 8 (R8P), backup relay 7 (R7B), primary relay 14 (R14P) and backup relay 13 (R13B) are obtained for earth faults with backup fuses using proposed only *q* component based adaptive protection coordination

Table 5.15 Operation and coordination time of primary (P) and backup (B) relay with fuses in mode 3 for three phase fault (LLL)

Relays	OT(s)	CT of Relays(s)	Fuse Type	CT of Fuses(s)
R12P	0.165	0	25T	0.352
R9B	0.295	0.130	25T	0.421
R8P	0.179	0	50T	0.359
R7B	0.300	0.121	50T	0.421
R14P	0.146	0	50T	0.348
R13B	0.292	0.146	50T	0.411

Table 5.16 Operation and coordination time of primary (P) and backup (B) relay with fuses in mode 3 for earth faults (LG-LLG)

Relays	OT(s)	CT of Relays(s)	Fuse Type	CT of Fuses(s)
R12P	0.157	0	25T	0.338
R9B	0.281	0.124	25T	0.402
R8P	0.167	0	50T	0.344
R7B	0.288	0.122	50T	0.417
R14P	0.150	0	50T	0.359
R13B	0.300	0.150	50T	0.421

optimization scheme. During mode 3, PV DG and Loads of node 6 and 5 are disconnected so no role of relays R1 to R6 exist.optimization scheme. It is clear from Tables 5.13 – 5.16 that the OT and CT of primary and backup relays are different during three phase and Earth faults in different operation modes of the hybrid microgrid. Also, the *q* component of fault current is considered in the minimization of the main objective function with Tables 5.13 - 5.16 clearly showing different adaptive settings for different modes and faults without any constraint violation. All the primary and backup relays are operating with optimum protection coordination with proper backup given by fuses to backup relays.

Tables 5.17 and 5.18 show the OTs and CTs of primary and backup relays for LLL and LLG faults at nodes 3, 1, 8, and 9 during mode 4 as shown in Figure 5.8. of hybrid microgrid operation. R6P has OT of 0.140 seconds with zero coordination time as it is a primary relay. R3B has OT of 0.284 seconds with 0.144 seconds delay for coordination time as it is a backup relay. The backup fuses do not operate until backup relays fail to operate. Primary backup fuse which is present near R6P operates only if R3B fails. Primary backup fuse does not operate till 0.284

Table 5.17 Operation and coordination time of primary (P) and backup (B) relay with fuses in mode 4 for three phase fault (LLL)

Relays	OT(s)	CT of Relays(s)	Fuse Type	CT of Fuses(s)
R6P	0.140	0	15T	0.341
R3B	0.284	0.144	15T	0.406
R1P	0.194	0	50T	0.401
R2B	0.353	0.159	50T	0.433
R12P	0.167	0	25T	0.350
R9B	0.291	0.124	25T	0.421
R8P	0.162	0	50T	0.339
R7B	0.282	0.121	50T	0.403

Table 5.18 Operation and coordination time of primary (P) and backup (B) relay with fuses in mode 4 for earth faults (LG-LLG)

Relays	OT(s)	CT of Relays(s)	Fuse Type	CT of Fuses(s)
R6P	0.142	0	15T	0.353
R3B	0.293	0.151	15T	0.417
R1P	0.197	0	50T	0.417
R2B	0.356	0.159	50T	0.483
R12P	0.173	0	25T	0.359
R9B	0.300	0.128	25T	0.423
R8P	0.142	0	50T	0.319
R7B	0.263	0.121	50T	0.385

Table 5.19 Operation and coordination time of primary (P) and backup (B) relay with fuses in mode 1 for three phase fault (LLL)

Relays	OT(s)	CT of Relays(s)	Fuse Type	CT of Fuses(s)
R6P	0.147	0	15T	0.321
R3B	0.267	0.121	15T	0.382
R1P	0.159	0	50T	0.373
R2B	0.318	0.159	50T	0.434
R12P	0.142	0	25T	0.315
R9B	0.262	0.121	25T	0.371
R8P	0.141	0	50T	0.344
R7B	0.288	0.147	50T	0.395
R14P	0.154	0	50T	0.341
R13B	0.283	0.129	50T	0.393

seconds and operates with minimum delay of 50 ms (as per primary fuse constraint) added to OT of R3B. Secondary backup fuse which is present near R3B operates only if primary backup fuse fails to operate. Secondary backup fuse does not operate till 0.341 seconds and operates with minimum delay of 100 ms (as per secondary fuse constraint) added to OT of primary fuse. CT for backup fuse is 0.406 seconds. In similar manner the OT and CT of primary relay 1 (R1P), backup relay 2 (R2B), primary relay 12 (R12P), backup relay 9 (R9B), primary relay 8 (R8P) and backup relay 7 (R7B) are obtained for earth faults with backup fuses using proposed only q component based adaptive protection coordination optimization scheme. During mode 4, the utility grid with nodes 13 and 14 is disconnected, so no role of relays R13 to R14 exists.

Tables 5.19 and 5.20 show the OTs and CTs of primary and backup relays for LLL and

Table 5.20 Operation and coordination time of primary (P) and backup (B) relay with fuses in mode 1 for earth faults (LG-LLG)

Relays	OT(s)	CT of Relays(s)	Fuse Type	CT of Fuses(s)
R6P	0.162	0	15T	0.340
R3B	0.283	0.122	15T	0.393
R1P	0.162	0	50T	0.374
R2B	0.321	0.159	50T	0.433
R12P	0.142	0	25T	0.322
R9B	0.262	0.120	25T	0.379
R8P	0.167	0	50T	0.353
R7B	0.291	0.124	50T	0.411
R14P	0.150	0	50T	0.324
R13B	0.270	0.120	50T	0.376

LLG faults at nodes 3, 1, 8, 9, and 14 during mode 1 of hybrid microgrid operation. During mode 1 as shown in Figure 5.1., all the nodes are in action, so consecutively all the relays are in operation. In Table 5.19, R6P has OT of 0.147 seconds with zero coordination time as it is a primary relay. R3B has OT of 0.267 seconds with 0.121 seconds delay for coordination time as it is a backup relay. The backup fuses do not operate until backup relays fail to operate. Primary backup fuse which is present near R6P operates only if R3B fails.

Primary backup fuse does not operate till 0.321 seconds and operates with minimum delay of 50 ms (as per primary fuse constraint) added to OT of R3B. Secondary backup fuse which is present near R3B operates only if primary backup fuse fails to operate. Secondary backup fuse does not operate till 0.382 seconds and operates with minimum delay of 100 ms (as per secondary fuse constraint) added to OT of primary fuse. CT for backup fuse is 0.382 seconds. In similar manner the OT and CT of primary relay 1 (R1P), backup relay 2 (R2B), primary relay 12 (R12P), backup relay 9 (R9B), primary relay 8 (R8P), backup relay 7 (R7B), primary relay 14 (R14P) and backup relay 13 (R13B) are obtained for earth faults with backup fuses faults at nodes 4 and 10

Table 5.21 Steady state, minimum pickup current and fault current values in quadrature (q) axis component of fault current for different modes of hybrid microgrid operation for faults at different locations

Mode, Faulted side	**Steady state, I_q (A)**	**Iminpickup, I_q (A)**	**I_q for LL Fault (A)**	**I_q & I_0 for LLG Fault (A)**	**I_q for LLL Fault (A)**
PVI, PV	600	750	770	820, 40	840
WI, W	780	975	3500	3550, 130	3700
PVG, PV	600	750	790	860, 100	900
PVG, G	30	37.5	130	170, 50	200
WG, W	780	975	5000	2500, 150	4500
WG, G	30	37.5	160	220, 80	235
WPV, PV	600	750	780	800, 160	820
WPV, W	780	975	4300	6000, 200	8000
WPVG, PV	600	750	880	900, 300	915
WPVG, W	780	975	7500	7800, 350	8300
WPVG, G	30	37.5	230	280, 90	340
Load1PVside	300	375	620-6000	710- 6300, 50-200	800-7700
Load2PVside	300	375	620-6000	710- 6300, 50-200	800-7700
Load1Wside	390	487.5	900- 6500	930-7000, 50-300	950-8000
Load2Wside	390	487.5	900- 6500	930-7000, 50-300	950-8000

are not considered as they have the same load and line parameters as that of nodes 3 and 9. If faults are simulated at nodes 4 and 10 the optimum values obtained for OTs and CTs for relays R4-R5 and relays R10-R11 are going to be nearly the same to relays R6-R3 and relays R12-R9.

Table 5.21 shows steady state and minimum pickup current values in terms of quadrature axis component of fault current for different modes of hybrid microgrid operation. Quadrature axis component share of fault current for PV DG, wind DG, grid and all loads during different modes of operation is also shown in Table 5.21. For different loads, range of quadrature axis component of fault current during phase and earth faults for different modes of hybrid microgrid operation is also presented in Table 5.21. Also, Table 5.21 helps in understanding which side of microgrid will see the fast operation as compared to other parts of hybrid microgrid. Also, relay and fuse operation on grid side is faster in comparison to wind DG and PV DG sides. Relays on PV DG side are slower as the rate of rise of quadrature axis current on PV DG side system is small as compared to wind DG and utility grid (G).

Furthermore, it is also been concluded that the relay and fuse operation on wind DG side is faster in comparison to PV DG side. Direct axis current components are not considered to reduce the protection coordination dependency on the greater number of variables. *q* component of fault current alone provides satisfactory protection coordination settings as concluded from above results. The proposed methodology considers a smaller number of iterations and generation number as compared to [111] and [117]. Also, the q component based PCO is fast in comparison with [117] In comparison to [63], the proposed scheme is equally effective with reduced number of variables. The efficiency and accuracy of the relay settings can be examined by observing the primary relay operational time and coordination time interval during faulty conditions. It can be observed that all the primary relays are operating within 1.5 sec under phase and earth fault.

Moreover, it reflects the range of *CTI* for all operational modes of the microgrid. In this research work, the CTI range has been considered as 0.120 and 0.150 (primary fuse *CTI* 50 ms and backup fuse *CTI* 100 ms) sec for relays and fuses, and it can observe that none of the relay operations is violating the *CTI* constraint. From the operation of primary and backup relays with backup fuses for respective faults in different modes with different DGs at different nodes, it can be observed that all the primary and backup are in coordination with the fuses. All relays and fuses can operate in a coordinated manner within minimum time subjected to all constraints. There is no need for earth fault relays or any of the additional circuitry to measure *q0* components as they are

already available in interfaced converters. The proposed scheme easily removes the significantly changing fault currents with any fault, any type of DG and location with a single variable for the dynamicity observed due to operating modes of the hybrid microgrid. So, the presented adaptive protection scheme provides an efficient and cost-effective solution for protection schemes in ac-dc hybrid microgrids.

Chapter Summary

Designing the feasible, reliable, and economical adaptive protection scheme for hybrid microgrids makes the relay coordination problem more complicated. In this research work, a new approach of adaptive protection coordination optimization based on q component of fault current for hybrid microgrid is proposed which is equally effective for three-phase and earth faults. It works efficiently with minimum operation time using backup fuses for different nature of DGs, operating modes of hybrid microgrid with the minimum number of fault detection variables. The newly defined fuse constraints make the proposed adaptive protection coordination cheaper as it reduces number of backup relays which also reduces coordination time delay. The proposed scheme reduces the dependability on earth fault relay as q component of fault current can detect the changes corresponding to earth faults. DEA is used for optimal relay coordination among primary relays, backup relays, and fuses. The proposed adaptive relay settings for all the relays during different modes of operation with different DGs can coordinate in the proper sequence within defined fuse constraints for respective faults and locations. The newly defined fuse constraints for optimum protection coordination among relays helps in easy and quick removal of fault or isolation of fault. The proposed adaptive protection coordination is economical, feasible, and reliable under different conditions. This approach is tested on hybrid microgrid feeding agrarian and domestic loads of rural India. In future work, this scheme will be tested on hybrid microgrid with fuel cells, micro-turbines and diesel generators with low X/R ratio.

Chapter 6

Conclusions and future scope of research

India needs adequate and quality power for the rural and agriculture loads which remain one of the major concerns before planning and design of new distributed power plants. Reduction in the emission of harmful gases due to fossil fuel consumption are to be given due consideration. Currently; PV, biomass and small hydro resources are mostly employed to cater the rural and motive loads. India has vast plain lands with high irradiance level and coastal areas have plenty of solar and wind potential, so microgrid can be designed as per load requirements of an area depending on availability of DERs. But this needs financial as well as technical support. Microgrid design and implementation is the first step towards clean, cheap and reliable energy for rural and agricultural sectors. Keeping in mind the target set by NITI Aayog in 2015 that India must achieve 175 GW of renewable energy as source by 2022, new location based microgrids are designed. Since most of the rural villages throughout India have average load of 400 kW and 415 V supplied by distribution transformer, so microgrid structure has been designed accordingly in this research following the guidelines issued by Central Electricity Regulatory Commission of India. However, proper operation, control and protection systems should be provided to extract the maximum benefit of microgrid system. This research has been focused on the design of novel adaptive protection system involving various challenges in microgrids related to selection of structure, modeling of adaptive relaying-based protection schemes and design of optimum adaptive microgrid protection schemes for relay coordination.

6.1. Conclusions

In the first microgrid structure designed, the X/R ratio of synchronous generator acting as DG is considered low with magnitude of 5. Here, biomass energy can be used to run synchronous generator which is abundantly available in rural India. The second microgrid structure is designed with PV DG replacing the above synchronous generator since solar irradiance is abundantly available throughout India. The third microgrid structure is designed based on the concept of hybrid microgrid. In this hybrid microgrid system, the PV DG and Wind DG both have replaced the synchronous generators with same load. This kind of hybrid microgrid structure is suitable for

the countries where solar irradiance and wind speed both are abundantly available like central and Coastal India. PV DG and Wind DG both can individually feed the loads. The fourth microgrid system designed is based on same hybrid microgrid concept where PV DG and Wind DG both are replacing the above-mentioned synchronous generators with increased individual capacity to feed nearby loads. Based on voltage, current and frequency behaviour studied in above designed microgrid systems, it is revealed that during changes in modes of operation of microgrid, the protection scheme must adapt depending upon change in mode of operation. It is also found in this research that the provision of adaptive protection scheme is a necessity in microgrid system.

Adaptive protection can be provided for reliable operation of a microgrid. The grid connected mode of operation without DGs must also be considered along with grid connected mode of operation with DGs and islanded mode of microgrid operation. It is found that the low X/R DGs can feed enough for fault on their side. But negative sequence-based detection cannot be used for detection of fault on utility side and DG side. Its nature identification is possible showing importance for q0 components in microgrid systems. The performance of a protection system dedicated for microgrid highly depends upon nature of DGs connected, fault location detection and fault nature. For satisfactory operation of microgrid, the status of protection system should be available with microgrid central controller in steady state and abnormal situation. To provide good services to the consumers, a dedicated load side protection system can be implemented through fractionalization of the main protection system and it can operate based on zero sequence components of fault current. Fault location detection and fault nature identification based on dq0 components is a simple but slow detection method. Instead, consideration of time derivative of dq0 components is the simplest, instantaneous and robust method for location detection and fault nature identification which has been verified in the present work. Based on I_q and I_0 components, individual adaptive protection schemes can be designed for smart grid components. A single trip circuit as well as individual trip circuits can be set to trip protection relays during faulty conditions in smart grid or microgrid. Microgrid current coefficients can be further studied for stability analysis based on linear equations using state variable approach. A significant future scope of the present work may be considered as the optimization of proper coordination among relays in microgrid protection should coordinate in hierarchy in the vicinity of fault without interrupting the static switch at the PCC.

The fault characteristics of hybrid microgrid have been studied in this research work. A hybrid microgrid with PV and wind generator has the capability to supply different loads. The simulation results have shown that there are significant variations in q0 components of fault current and frequency for different modes, different types of DGs and different loads. The proposed adaptive protection algorithm is found effective for different types of generation with different X/R ratio during fault condition in microgrid system for series and shunt faults. Accordingly, adaptive protection scheme for hybrid microgrid should be proposed for robust and reliable protection system. The q0 component will play important role in protection of converter based microgrid as converter control is solely based on dq0 components.

The fault characteristics of type I, III and IV wind DGs are studied in islanded mode as well as in hybrid (with PV) mode of microgrid. The simulation results have shown that there are significant variations in q0 components of fault current and transient reactance for different modes and different types of DGs (Wind types I, III and IV). The proposed adaptive protection algorithm is found effective for different types of generation with different X/R ratio during fault condition in microgrid system for series (including lightly loaded phase faults) and shunt faults. Results show transient component is different for DGs (Wind types I, III, IV and PV) that helps in nature detection. The use of fuses reduces the reliability and adaptivity of microgrid structures, but it is shown that their use is good for backup. Proposed protection scheme with backup of fuses is cost effective and reliable. The proposed approach is implemented based on static components; hence it is equally effective in dc microgrids.

Designing the feasible, reliable, and economical adaptive protection scheme for hybrid microgrids makes the relay coordination problem more complicated. In this research work, a new approach of adaptive protection coordination optimization based on q component of fault current for hybrid microgrid is proposed which is equally effective for three-phase and earth faults. It works efficiently with minimum operation time using backup fuses for different nature of DGs, operating modes of hybrid microgrid with the minimum number of fault detection variables. Newly defined fuse constraints make the proposed adaptive protection coordination cheaper as it reduces the number of backup relays which also reduces coordination time delay. Proposed scheme reduces the dependability on earth fault relay as q component of fault current is detecting the changes corresponding to earth faults. DEA is used for optimal relay coordination among primary relays, backup relays, and fuses. Proposed adaptive relay settings for all the relays in operation

during different modes of operation with different DGs are coordinating in the proper sequence within defined fuse constraints for respective faults and locations. Newly defined fuse constraints for optimum protection coordination among relays helps in easy and quick removal of fault or isolation of fault. The proposed adaptive protection coordination is economical, feasible, and reliable under different conditions. The proposed approach is tested on hybrid microgrid feeding agrarian and domestic loads of rural India.

6.2. Future scope of research

Renewable energy is the best and simplest solution for the reduction in carbon emission. Efficient technologies for proper utilization of DERs have good future scope as they help in maintaining power quality irrespective of environmental constraints. Simulation studies on microgrid structures will help in drawing out future plan for different nature of DGs' installation as per load demand, environmental and capital cost constraints. Simulation work on microgrid will help in reducing the planning cost. Different combinations of existing technologies in microgrid and conventional power system can help in reducing the capital cost of microgrid structures. From simulation case studies, brief outlines for different DERs can be drawn to get maximum benefits from the available DERs. Further with the real time implementation of DERs, for scattered load distribution, the losses will be minimized. Scattered load demand can further open a vast area of research on switching from microgrid to nano grid consists of small DGs feeding individual domestic loads of the range of 5 – 50 kW. Adaptive relay in coordination with fuses is reliable and less expensive solution to protection coordination problems. A significant future scope of the present work may be considered as the optimization of proper coordination among relays in microgrid protection for those particular relays which should coordinate in hierarchy in the vicinity of fault without interrupting the static switch at the PCC. In future work, this scheme will be tested on hybrid microgrid with fuel cells, microturbines and diesel generators with low X/R ratio in real time simulators with improved and fast adaptive relaying. Different optimization techniques can be studied and implemented for reliable adaptive protection scheme to minimize protection coordination problem with and without fuses in future microgrids.

References

[1] National Institution for Transforming India, Government of India.: 'Report of the Expert Group on 175 GW RE by 2022', 2015

[2] Lasseter, R. H.: 'Microgrid', Proc. IEEE Power Emg. Soc. Winter Meeting, vol. 1, New York, 2002, pp. 305–308

[3] Nikkhajoei, H. and Lasseter, R. H.: 'Microgrid Protection', Proc. IEEE Power Eng. Soc. General Meeting, 2007, pp. 1–6

[4] Oudalov, Alexander et al.: 'Microgrids: Architectures and Control', (John Wiley & Sons, Ltd., 2014)

[5] Fusheng, L., et al.: 'Microgrid Technology and Engineering Application', (Academic Press, 2016, pp. 47-67)

[6] Beheshtaein, S., Cuzner, R., Savaghebi, M., et al.: 'Review on microgrids protection', IET Generation, Transmission & Distribution, 2019, 13, (6), pp. 743–759

[7] Memon, A.A. and Kauhaniemi, K.: 'A Critical Review of AC Microgrid Protection Issues and Available Solutions', Elsevier, Electric Power Systems Research, 2015, 129, pp. 23-31

[8] Basak, Prasenjit et al.: 'A Literature Review on Integration of Distributed Energy Resources in the Perspective of Control, Protection and Stability of Microgrid', Elsevier Renewable and Sustainable Energy Reviews, 2012, 16, pp. 5545–5556

[9] Mohanty, P., Bhuvaneswari, G. and Balasubramanian, R.: 'Optimal Planning and Design of Distributed Generation Based Micro-grids', IEEE 7th International Conference on Industrial and Information Systems (ICIIS), 2012, pp. 1-6

[10] Punjab State Electricity Regulatory Commission.: 'Conditions of Supply', Punjab State Power Corporation Limited (PSPCL), Patiala, India, 2013, pp. 5-8.

[11] Brahma, Sukumar M. and Girgis, A. A.: 'Development of Adaptive Protection Scheme for Distribution Systems with High Penetration of Distributed Generation', IEEE Transactions on Power Delivery, 2004, 19, (1), pp. 56-63

[12] Sallam, A.A., Malik, O.P.: 'Electric Distribution Systems', (John Wiley & Sons, New York, NY, USA, 2011, pp. 163–235)

[13] Mirsaeidi, S., Dong, X., Shi, S., et al.: 'Challenges, Advances and Future Directions in Protection of Hybrid AC/DC Microgrids', IET Renewable Power Generation, 2017, 11, (12), pp. 1495–1502

[14] Hatziargyriou, N. (Ed.): ‘Microgrids: Architectures and Control’, (John Wiley & Sons, Hoboken, NJ, USA, 2014)

[15] Ustun, T.S., Ozansoy, C., Ustun, A.: ‘Fault Current Coefficient and Time Delay Assignment for Microgrid Protection System with Central Protection Unit’, IEEE Trans. Power Syst., 2013, 28, (2), pp. 598–606

[16] Nthontho, M.P., Chowdhury, S.P., Winberg, S., et al.: ‘Protection of Domestic Solar Photovoltaic Based Microgrid’. Proc. Int. Conf. Developments in Power Systems Protection, Birmingham, UK, April 2012, pp. 1–6

[17] Buque, C., Ipinnimo, O., Chowdhury, S., et al.: ‘Modeling and Simulation of an Adaptive Relaying Scheme for a Microgrid’, Power and Energy Society General Meeting, San Diego, CA, USA, July 2012, pp. 1–8

[18] IEEE 802.16: ‘IEEE Standard for Local and Metropolitan Area Networks’, 2004, pp. 16–20

[19] Lin, H., Guerrero, J.M., Vásquez, J.C., et al.: ‘Adaptive Distance Protection for Microgrids’. IECON 2015 – 41st Annual Conference of the IEEE Industrial Electronics Society, Yokohama, Japan, November 2015, pp. 725– 730

[20] Ozansoy, C.: ‘A Methodology for Determining Fault Current Impact Coefficients of Distributed Energy Resources in an Adaptive Protection Scheme’. Proc. Int. Conf. ELECO, Bursa, Turkey, November 2015, pp. 479–483

[21] Ustun, T.S., Ozansoy, C., Zayegh, A.: ‘Modeling of A Centralized Microgrid Protection System and Distributed Energy Resources According to IEC 61850-7-420’, IEEE Trans. Power Syst., 2012, 27, (3), pp. 1560–1567

[22] Ustun, T.S., Khan, R.H.: ‘Multiterminal Hybrid Protection of Microgrids Over Wireless Communications Network’, IEEE Trans. Smart Grid, 2015, 6, (5), pp. 2493–2500

[23] Jin, L., Jiang, M., Yang, G.: ‘Fault Analysis of Microgrid and Adaptive Distance Protection Based on Complex Wavelet Transform’. Proc. Int. Conf. Power Electronics and Application Conf. and Exposition (PEAC), Shanghai, China, November 2014, pp. 360–364

[24] Orji, U., Schantz, C., Leeb, S.B., et al.: ‘Adaptive Zonal Protection for Ring Microgrids’, IEEE Trans. Smart Grid, 2017, 8, (4), pp. 1843–1851

[25] Barker, P.P., De Mello, R.W.: ‘Determining the Impact of Distributed Generation on Power Systems. I. Radial Distribution Systems’, IEEE Power Engineering Society Summer Meeting, Seattle, WA, USA, July 2000, vol. 3, pp. 1645–1656

[26] Kar, S., Ranjan Samantaray, S.: ‘A Fuzzy Rule Base Approach for Intelligent Protection of Microgrids’, Electr. Power Compon. Syst., 2015, 43, (18), pp. 2082–2093

[27] Cintuglu, M.H., Ma, T., Mohammed, O.A.: ‘Protection of Autonomous Microgrids Using Agent-Based Distributed Communication’, IEEE Trans. Power Deliv., 2017, 32, (1), pp. 351–360

[28] Fani, B., Bisheh, H., Sadeghkhani, I.: ‘Protection Coordination Scheme for Distribution Networks with High Penetration of Photovoltaic Generators’, IET Generation, Transmission & Distribution, 2017, 12, (8), pp. 1802–1814

[29] Farhan, M.A., Swarup, K.S.: ‘Mathematical Morphology-Based Islanding Detection for Distributed Generation’, IET Generation, Transmission & Distribution, 2016, 10, (2), pp. 518–525

[30] Gururani, A., Mohanty, S.R., Mohanta, J.C.: ‘Microgrid Protection Using Hilbert–Huang Transform Based-Differential Scheme’, IET Generation, Transmission & Distribution, 2016, 10, (15), pp. 3707–3716

[31] Kar, S., Samantaray, S.R., Zadeh, M.D.: ‘Data-Mining Model Based Intelligent Differential Microgrid Protection Scheme’, IEEE Syst. J., 2017, 11, (2), pp. 1161–1169

[32] Liu, X., Shahidehpour, M., Li, Z., et al.: ‘Protection Scheme for Loop-Based Microgrids’, IEEE Trans. Smart Grid, 2017, 8, (3), pp. 1340–1349

[33] Mishra, M., Rout, P.K.: ‘Detection and Classification of Micro-Grid Faults Based on HHT and Machine Learning Techniques’, IET Generation, Transmission & Distribution 2017, 12, (2), pp. 388–397

[34] Muda, H., Jena, P.: ‘Superimposed Adaptive Sequence Current Based Microgrid Protection: A New Technique’’, IEEE Trans. Power Deliv., 2017, 32, (2), pp. 757–767

[35] Habib, H.F., Lashway, C.R., Mohammed, O.A.: ‘A Review of Communication Failure Impacts on Adaptive Microgrid Protection Schemes and the Use of Energy Storage as A Contingency’, IEEE Trans. Ind. Appl., 2018, 54, (2), pp. 1194–1207

[36] Piesciorovsky, E.C., Schulz, N.N.: ‘Fuse Relay Adaptive Overcurrent Protection Scheme for Microgrid with Distributed Generators’, IET Generation, Transmission & Distribution, 2017, 11, (2), pp. 540–549

[37] Choi, S., Meliopoulos, A.S.: 'Effective Real-Time Operation and Protection Scheme of Microgrids Using Distributed Dynamic State Estimation', IEEE Trans. Power Deliv., 2017, 32, (1), pp. 504–514

[38] Dutta, R., Samantaray, S.R.: 'Assessment of Impedance Based Fault Locator for AC Micro-grid', Renewable. Energy Focus, 2018, 26, pp. 1–10

[39] Som, S., Samantaray, S.R.: 'Efficient Protection Scheme for low-voltage DC Micro-grid', IET Generation, Transmission & Distribution, 2018, 12, (13), pp. 3322–3329

[40] Kundur, P., Balu, N.J., Lauby, M.G.: 'Power System Stability and Control' (McGraw-hill, New York, NY, USA, 1994)

[41] Bimbhra, P.S.: 'Electrical Machines' (Khanna Publisher, New Delhi, India, 2014)

[42] Krause, P., Wasynczuk, O., Sudhoff, S.D., et al.: 'Analysis of Electric Machinery and Drive Systems' (John Wiley & Sons., New York, NY, USA, 2013)

[43] Oureilidis, K.O., Demoulias, C.S.: 'A Fault Clearing Method in Converter dominated Microgrids with Conventional Protection means', IEEE Trans. Power Electron., 2016, 31, (6), pp. 4628–4640

[44] Swathika, O.G., Hemamalini, S.: 'Prims-aided Dijkstra Algorithm for Adaptive Protection in Microgrids', IEEE J. Emerging Sel. Topics Power Electron., 2016, 4, (4), pp. 1279–1286

[45] Farhan, M.A.: 'Mathematical Morphology-based Islanding Detection for Distributed Generation', IET Generation, Transmission & Distribution, 2017, 11, (14), pp. 3449–3457

[46] Haj-ahmed, M.A., Feilat, E.A., Khasawneh, H.J., Abdelhadi, A.F. and Awwad, A.A.: 'Comprehensive Protection Schemes for Different Types of Wind Generators', IEEE Transactions on Industry Applications, 2018, 54, (3), pp. 2051-2058

[47] Dhar, Snehamoy, and Pradipta Kishore Dash.: 'Differential Current-based Fault Protection with Adaptive threshold for multiple PV-based DC Microgrid', IET Renewable Power Generation, 2017, 11, (6), pp. 778-790

[48] Jia, K., Gu, C., Xuan, Z. and Lin, Y.: 'Fault Characteristics Analysis and Line Protection Design within a large-scale Photovoltaic power plant', IEEE Transactions on Smart Grid, 2018, pp. 4099 - 4108.

[49] Teimourzadeh, Saeed, Farrokh Aminifar, Mahdi Davarpanah, and Mohammad Shahidehpour.: 'Adaptive Protection for preserving Microgrid Security', IEEE Transactions on Smart Grid, 2017, 10, (1), pp. 592-600

[50] Jain, Rishabh, David L. Lubkeman, and Srdjan M. Lukic.: 'Dynamic Adaptive Protection for Distribution Systems in Grid-Connected and Islanded Modes', IEEE Transactions on Power Delivery, 2018, 34, (1), pp. 281-289

[51] Lin, Hengwei, Kai Sun, Zheng-Hua Tan, Chengxi Liu, Josep M. Guerrero, and Juan C. Vasquez.: 'Adaptive Protection Combined with Machine Learning for Microgrids', IET Generation, Transmission & Distribution, 2019, 13, (6), pp. 770-779

[52] Zanjani, Mohsen Ghalei Monfared, Kazem Mazlumi, and Innocent Kamwa.: 'Application of μPMUs for Adaptive Protection of Overcurrent Relays in Microgrids', IET Generation, Transmission & Distribution, 2018, 12, (18), pp. 4061-4068

[53] Zheng, T., Zhao, Y. and Zhu, Y.: 'Overcurrent Protection Scheme for Collector lines in Wind farm based on Fault Component Current Correlation Analysis and Multi-agent System', IET Renewable Power Generation, 2019, 14, (2), pp. 313-320

[54] Rezaei, N., Uddin, M.N., Amin, I.K., Othman, M.L. and Marsadek, M.: 'Genetic Algorithm-Based Optimization of Overcurrent Relay Coordination for Improved Protection of DFIG Operated Wind Farms', IEEE Transactions on Industry Applications, 2019, 55, (6), pp. 5727-5736

[55] Eissa, M.M.: 'Developing Three-Dimensional-phase surface-based Wide Area Protection Centre in a Smart grid with Renewable Resources', IET Energy Systems Integration, 2019, 1, (2), pp. 65-73

[56] Ravikumar, K.G. and Srivastava, A.K.: 'Designing Centralised and Distributed System Integrity Protection Schemes for Enhanced Electric Grid Resiliency', IET Generation, Transmission & Distribution, 2019, 13, (8), pp. 1194-1203

[57] Zarei, M.E., Platero, C.A., Nicolás, C.V. and Arribas, J.R.: 'Novel Differential Protection Technique for Doubly Fed Induction Machines', IEEE Transactions on Industry Applications, 2019, 55, (4), pp. 3697-3706

[58] Mohamed, E.A., Magdy, G., Shabib, G., Elbaset, A.A. and Mitani, Y.: 'Digital Coordination Strategy of Protection and Frequency Stability for An Islanded Microgrid', IET Generation, Transmission & Distribution, 2018, 12, (15), pp. 3637-3646

[59] Chang, Y., Hu, J., Tang, W. and Song, G.: 'Fault Current Analysis of Type-3 WTS Considering Sequential Switching of Internal Control and Protection Circuits in Multi Time scales during LVRT', IEEE Transactions on Power Systems, 2018, 33, (6), pp. 6894-6903.

[60] Xie, X., Liu, W., Liu, H., Du, Y. and Li, Y.: 'A System-Wide Protection Against Unstable SSCI in Series-Compensated Wind Power Systems', IEEE Transactions on Power Delivery, 2018, 33, (6), pp. 3095-3104

[61] Chen, S., Tai, N., Fan, C., Liu, J. and Hong, S.: 'Adaptive Distance Protection for Grounded Fault of Lines Connected with Doubly-Fed Induction Generators', IET Generation, Transmission & Distribution, 2017, 11, (6), pp. 1513-1520

[62] El-Arroudi, K. and Joós, G.: 'Performance of Interconnection Protection Based on Distance Relaying for Wind Power Distributed Generation', IEEE Transactions on Power Delivery, 2017, 33, (2), pp. 620-629

[63] Aghdam, T.S., Karegar, H.K. and Zeineldin, H.H., 'Variable Tripping Time Differential Protection for Microgrids Considering DG Stability', IEEE Transactions on Smart Grid, 2019, 10, (3), pp. 2407-2415

[64] Petersson, A.: 'Analysis, Modeling and Control of Doubly-Fed Induction Generators for Wind Turbines', PhD thesis, Chalmers University of Technology, Goteborg, Sweden, 2005

[65] Saleh, K.A., Zeineldin, H.H. and El-Saadany, E.F.: 'Optimal Protection Coordination for Microgrids Considering N-1 Contingency', IEEE Transactions on Industrial Informatics, 2017, 13, (5), pp. 2270-2278

[66] Saleh, S.A., Ozkop, E. and Aljankawey, A.S.: 'Developing and Testing Phaselet frames-based Digital Protection for Distributed Generation units', IEEE In Industry Applications Society Annual Meeting, 2015, pp. 1-13

[67] Guo, W.M., Mu, L.H. and Zhang, X.: 'Fault Models of Inverter-Interfaced Distributed Generators within a Low-Voltage Microgrid', IEEE Transactions on Power Delivery, 2017, 32, (1), pp. 453-461

[68] Xu, X., Mitra, J., Wang, T. and Mu, L.: 'An Evaluation Strategy for Microgrid Reliability Considering the Effects of Protection System', IEEE Transactions on Power Delivery, 2016, 31, (5), pp. 1989-1997

[69] Saleh, S.A., Aljankawey, A.S., Abu-Khaizaran, M.S. and Alsayid, B.: 'Influences of Power Electronic Converters on Voltage–Current Behaviors During Faults in DGUs—Part I: Wind Energy Conversion systems', IEEE Transactions on Industry Applications, 2015, 51, (4), pp. 2819-2831

[70] Oudalov, Alexandre, and Antonio Fidigatti.: 'Adaptive Network Protection in Microgrids', International Journal of Distributed Energy Resources, 2009, 5, (3), pp. 201-226

[71] Kumar, Dhivya Sampath, Dipti Srinivasan, Anurag Sharma, and Thomas Reindl.: 'Adaptive Directional Overcurrent Relaying Scheme for Meshed Distribution Networks', IET Generation, Transmission & Distribution, 2018, 12, (13), pp. 3212-3220

[72] Swathika, OV Gnana, S. Angalaeswari, V. Anantha Krishnan, K. Jamuna, and JL Febin Daya.: 'Fuzzy Decision and Graph Algorithms Aided Adaptive Protection of Microgrid', Energy Procedia, 2017,117, pp. 1078-1084

[73] Kumar, J., Memon, A.A., Kumpulainen, L., Kauhaniemi, K. and Palizban, O.: 'Design and Analysis of New Harbour Grid Models to Facilitate Multiple Scenarios of Battery Charging and Onshore Supply for Modern Vessels', Energies, 2019, 12, (12), pp. 1-18

[74] Patsidis, A., Tzelepis, D., Dyśko, A. and Booth, C.: 'Investigation of the Performance of ROCOF-Based LOM Protection in Distribution Networks with Virtual Synchronous Generators', IET 15th International Conference on Developments in Power System Protection, 2020

[75] Bountouris, P., Guo, H., Tzelepis, D., Abdulhadi, I., Coffele, F. and Booth, C.: 'MV Faulted Section Location in Distribution Systems Based on Unsynchronized LV Measurements', International Journal of Electrical Power & Energy Systems, 2020, 119, pp. 1-14

[76] Coffele, F., Booth, C. and Dyśko, A.: 'An Adaptive Overcurrent Protection Scheme for Distribution Networks', IEEE Transactions on Power Delivery, 2014, 30, (2), pp. 561-568

[77] Pradhan, A.K., Jóos, G.: 'Adaptive Distance Relay Setting for Lines Connecting Wind farms', IEEE Trans. Energy Convers., 2007, 22, (1), pp. 206–213

[78] Le Blond, S. P., & Aggarwal, R. K.: 'Design of Adaptive Autoreclosure Schemes for 132 kV Network with high Penetration of Wind—Part I: real-time modeling', IEEE Transactions on Power Delivery, 2012, 27, (3), pp. 1055-1062.

[79] Le Blond, S.P. and Aggarwal, R.: 'Design of Adaptive Autoreclosure Schemes for 132 kV With High Penetration of Wind—Part II: Real-Time Development and Testing', IEEE Transactions on Power Delivery, 2011, 27, (3), pp. 1063-1070

[80] Dubey, R., Samantaray, S.R. and Panigrahi, B.K.: 'Adaptive Distance Protection Scheme for Shunt FACTS Compensated Line Connecting Wind Farm', IET Generation, Transmission & Distribution, 2016, 10, (1), pp. 247-256

[81] Hsieh, S.C., Chen, C.S., Tsai, C.T., Hsu, C.T. and Lin, C.H.: 'Adaptive Relay Setting for Distribution Systems Considering Operation Scenarios of Wind Generators', IEEE Transactions on Industry Applications, 2013, 50, (2), pp. 1356-1363

[82] Chen, L., Chen, H., Yang, J., He, H., Liu, X., Yu, Y., Xu, Y., Wang, Z. and Ren, L.: 'Conceptual Design and Performance Evaluation of a 35-kV/500-A flux coupling-type SFCL for Protection of a DFIG-based Wind farm', IEEE Transactions on Applied Superconductivity, 2017, 28, (3), pp. 1-7

[83] Zhao, Y., Shi, L., Yao, L., Xu, Z. and Ni, Y.: 'Zone Partitioning Protection Strategy for DC systems incorporating Offshore Wind farm', IET Renewable Power Generation, 2017, 11, (12), pp. 1509-1516

[84] Zolfaghari, M., Chabanlo, R.M., Abedi, M. and Shahidehpour, M.: 'A Robust Distance Protection Approach for Bulk AC Power System Considering the effects of HVDC interfaced Offshore Wind units', IEEE Systems Journal, 2017, 12, (4), pp. 3786-3795

[85] Kauffmann, T., Karaagac, U., Kocar, I., Jensen, S., Mahseredjian, J. and Farantatos, E.: 'An Accurate type III Wind Turbine Generator short circuit model for Protection applications', IEEE Transactions on Power Delivery, 2016, 32, (6), pp. 2370-2379

[86] Saleh, S.A., Meng, R. and McSheffery, R.: 'Evaluating the Performance of Digital Modular Protection for Grid-Connected Permanent-Magnet Generator-based Wind Energy Conversion Systems with Battery Storage Systems', IEEE Transactions on Industry Applications, 2017, 53, (5), pp. 4186-4200

[87] Tang, Y. and Ayyanar, R.: 'Methodology of Automated Protection Analysis for Large Distribution Feeders with High Penetration of Photovoltaic Systems', IEEE Power and Energy Technology Systems Journal, 2017, 4, (1), pp. 1-9

[88] Chen, L and Mei, S.: 'An Integrated Control and Protection System for Photovoltaic Microgrids', CSEE J. Power Energy Syst., 2015, 1, (1), pp. 36–42

[89] Zhao, Y. et al.: 'Line–Line Fault Analysis and Protection Challenges in Solar Photovoltaic Arrays', IEEE Trans. Ind. Electron., 2013, 60, (9), pp. 3784– 3795

[90] Fani, B., Dadkhah, M., and Horestani, A.: 'Adaptive Protection Coordination Scheme Against the Staircase Fault Current Waveforms in PV-dominated Distribution systems', IET Generation, Transmission & Distribution, 2018, 12, (9), pp. 2065-2071

[91] Manohar, Murli., Koley, Ebha. and Ghosh, Subhojit.: 'Reliable Protection Scheme for PV Integrated Microgrid using an Ensemble Classifier Approach with Real-time validation', IET Science, Measurement & Technology, 2017, 12, (2), pp. 200-208

[92] Kavi, Moses., Mishra, Yateendra. and Vilathgamuwa, Mahinda.: 'Morphological Fault Detector for Adaptive Overcurrent Protection in Distribution Networks with Increasing Photovoltaic Penetration', IEEE Transactions on Sustainable Energy, 2018, 9, (3), pp. 1021-1029

[93] Saleh, S. A., Aljankawey, A. S., Alsayid, B. and Abu Khaizaran, M. S.: 'Influences of Power Electronic Converters on Voltage-Current Behaviors during Faults in DGUs—Part II: Photovoltaic systems', IEEE Trans. Ind. Appl., 2015, 51, (4), pp. 2832–2845

[94] Chen, Guangwei. et al.: 'Variable Frequency based Relay Protection for Isolated Micro Grid constructed with VSCs', IEEE PES Asia-Pacific Power and Energy Conference (APPEEC), 2016. pp. 23-1-2304

[95] Yang, Yongheng., Blaabjerg, Frede. and Wang, Huai.: 'Low-Voltage Ride-Through of Single-Phase Transformerless Photovoltaic Inverters', IEEE Transactions on Industry Applications, 2014, 50, (3), pp. 1942-1952

[96] Charalambous, Charalambos A., Kokkinos, Nikolaos D. and Christofides, Nikolas.: 'External Lightning Protection and Grounding in Large-Scale Photovoltaic Applications', IEEE Transactions on Electromagnetic Compatibility, 2014, 56, (2), pp. 427-434

[97] Muda, Harikrishna. and Jena, Premalata.: 'Real Time Simulation of New Adaptive Overcurrent Technique for Microgrid Protection', IEEE, National Power Systems Conference (NPSC), 2016, pp. 1 - 6

[98] Chen, Zhi., Pei, Xuejun. and Peng, Li.: 'Harmonic Components Based Protection Strategy for Inverter Interfaced AC Microgrid', IEEE Energy Conversion Congress and Exposition (ECCE), 2016, pp. 1 - 6

[99] Dhar, Snehamoy. and Dash, Pradipta Kishore.: 'Adaptive Threshold Based New Active Islanding Protection Scheme for Multiple PV based Microgrid application', IET, Generation, Transmission & Distribution, 2017, 11, (1), pp. 118-219

[100] Sharma, A., Kiran, D. and Panigrahi, B.K.: 'Planning the Coordination of Overcurrent Relays for Distribution Systems Considering Network Reconfiguration and Load Restoration', IET Generation, Transmission & Distribution, 2017, 12, (7), pp. 1672-1679

[101] Hooshyar, Ali. et al.: 'Fault Type Classification in Microgrids Including Photovoltaic DGs', IEEE Transactions on Smart Grid, 2016, 7, (5), pp. 2218- 2229

[102] Guo, Wen-Ming., Mu, Long-Hua. and Zhang, Xin.: 'Fault Models of Inverter-Interfaced Distributed Generators Within a Low-Voltage Microgrid', IEEE Transactions on Power Delivery, 2017, 32, (1), pp. 453- 461

[103] Zarei, Seyed Fariborz. and Parniani, M.: 'A Comprehensive Digital Protection Scheme for Low-Voltage Microgrids with Inverter-Based and Conventional Distributed Generations', IEEE Transactions on Power Delivery, 2017, 32, (1), pp. 441-452

[104] Shen, Z. John.: 'Ultrafast Solid-State Circuit Breakers', IEEE Electrification Magazine, 2016, pp. 66-70

[105] Lin, Hengwei., et al.: 'Adaptive Overcurrent Protection for Microgrids in Extensive Distribution Systems', 42nd Annual Conference of the IEEE Industrial Electronics Society, IECON, 2016, pp. 4042 – 4047

[106] Rezaei, Nima. et al.: 'Coordination of Overcurrent Relays Protection Systems for Wind Power Plants', IEEE International Conference on Power and Energy (PECon), 2014, pp. 394 - 399

[107] Singh, Dinesh Kumar. et al.: 'Wind Power Generation by PMSG and Fault protection Using OverCurrent and Differential Frequency Relay', IEEE, Region 10 Humanitarian Technology Conference (R10-HTC), 2016, pp. 1 – 6

[108] Dehghanpour, Ehsan. et al.: 'Optimal Coordination of Directional Overcurrent Relays in Microgrids by Using Cuckoo-Linear Optimization Algorithm and Fault Current Limiter', IEEE Transactions on Smart Grid, DOI 10.1109/TSG.2016.2587725

[109] Collier, David E. and Key, Thomas S.: 'Electrical Fault Protection for a Large Photovoltaic Power Plant Inverter', IEEE Photovoltaic Specialists Conference, 1988, 2, pp. 1035-1042

[110] Padullaparti, Harsha V. et al.: 'Analytical Approach to Estimate Feeder Accommodation Limits Based on Protection Criteria', IEEE Access, 2016, 4, pp. 4066-4081

[111] Najy, W.K., Zeineldin, H.H. and Woon, W.L.: 'Optimal Protection Coordination for Microgrids with Grid-Connected and Islanded Capability', IEEE Transactions on industrial electronics, 2012, 60, (4), pp. 1668-1677

[112] Khorshid-Ghazani, B., Seyedi, H., Mohammadi-ivatloo, B., Zare, K. and Shargh, S.: 'Reconfiguration of Distribution Networks Considering Coordination of the Protective devices', IET Generation, Transmission & Distribution, 2017, 11, (1), pp. 82-92

[113] Sharaf, H.M., Zeineldin, H.H. and El-Saadany, E.: 'Protection Coordination for Microgrids with Grid-Connected and Islanded Capabilities Using Communication Assisted Dual Setting Directional Overcurrent Relays', IEEE Transactions on Smart Grid, 2016, 9, (1), pp. 143-151

[114] Dahej, A.E., Esmaeili, S. and Hojabri, H.: 'Co-optimization of Protection Coordination and Power Quality in Microgrids using Unidirectional Fault Current limiters', IEEE Transactions on Smart Grid, 2017, 9, (5), pp. 5080-5091

[115] Saleh, K.A. and Mehrizi-Sani, A.: 'Harmonic Directional Overcurrent Relay for Islanded Microgrids With Inverter-Based DGs', IEEE Systems Journal, 2020, pp. 1-12

[116] He, H., Chen, L., Yin, T., Cao, Z., Yang, J., Tu, X. and Ren, L.: 'Application of a SFCL for Fault Ride-Through Capability Enhancement of DG in a Microgrid System and Relay Protection Coordination', IEEE Transactions on Applied Superconductivity, 2016, 26, (7), pp. 1-8

[117] Sharma, A. and Panigrahi, B.K.: 'Phase Fault Protection Scheme for Reliable Operation of Microgrids', IEEE Transactions on Industry Applications, 2017, 54, (3), pp. 2646-2655

[118] Tjahjono, A., Anggriawan, D.O., Faizin, A.K., Priyadi, A., Pujiantara, M., Taufik, T. and Purnomo, M.H.: 'Adaptive Modified Firefly Algorithm for Optimal Coordination of Overcurrent Relays', IET Generation, Transmission & Distribution, 2017, 11, (10), pp. 2575-2585

[119] Baghaee, H.R., Mirsalim, M., Gharehpetian, G.B. and Talebi, H.A.: 'MOPSO/FDMT-based Pareto-optimal solution for Coordination of Overcurrent Relays in Interconnected Networks and multi-DER Microgrids', IET Generation, Transmission & Distribution, 2018, 12, (12), pp. 2871-2886

[120] Habib, H.F., El Hariri, M., Elsayed, A. and Mohammed, O.A.: 'Utilization of Supercapacitors in Protection Schemes for Resiliency Against Communication Outages: A Case Study on Size and Cost Optimization', IEEE Transactions on Industry Applications, 2018, 54, (4), pp. 3153-3164

[121] Liu, Z., Høidalen, H.K., Saha, M.M. and Popov, M.: 'Coordinated Protection and Control Strategy with Wind Power Integration for Distribution Network', The Journal of Engineering, 2018, (15), pp. 1204-1208

[122] Magdy, G., Shabib, G., Elbaset, A.A. and Mitani, Y.: 'A Novel Coordination Scheme of Virtual Inertia Control and Digital Protection for Microgrid Dynamic Security Considering High Renewable Energy Penetration', IET Renewable Power Generation, 2018, 13, (3), pp. 462-474.

[123] El-Naily, N., Saad, S.M., Hussein, T. and Mohamed, F.A.: 'A Novel Constraint and Non-Standard Characteristics for Optimal Over-Current Relays Coordination to Enhance Microgrid Protection Scheme', IET Generation, Transmission & Distribution, 2019, 13, (6), pp. 780-793

[124] Zarei, S.F., Mokhtari, H. and Blaabjerg, F.: 'Fault Detection and Protection Strategy for Islanded Inverter-Based Microgrids', IEEE Journal of Emerging and Selected Topics in Power Electronics, 2019, pp. 1-12

[125] Salam, A. A. et al.: 'Technical Challenges on Microgrids', ARPN Journal of Engineering and Applied Sciences, 2008, 3, (6), pp. 64-69

[126] Zamani, M. Amin. et al.: 'A Communication-Assisted Protection Strategy for Inverter-Based Medium-Voltage Microgrids', IEEE Transactions on Smart Grid, 2012, 3, (4), pp. 2088-2099

[127] Ma, Jing. et al.: 'An Adaptive Protection Scheme for Distributed Systems with Distributed Generation', IEEE Power and Energy Society General Meeting, 2011, pp. 1 – 6

[128] Khederzadeh, M.: 'Adaptive Setting of Protective Relays in Microgrids in Grid-Connected and Autonomous Operation', IET 11th International Conference on Developments in Power Systems Protection, 2012, pp. 1 – 4

[129] Laaksonen, Hannu. et al.: 'Adaptive Protection and Microgrid Control Design for Hailuoto Island', IEEE Transactions on Smart Grid, 2014, 5, (3), pp. 1486-1493

[130] Basic Communication Structure for Substation and Feeder Equipment –Compatible Logical Node Classes and Data Classes. International Electro technical Commission, Geneva, Switzerland, Draft Standard 61850-7-4, IEC 2001."

[131] Transmission Protocols, General Structure of Application Data, IEC Std. 60870, 1992.

[132] Li, Z. C. et al.: 'A Protection Method for Microgrids based on Information Sharing', IET 12th International Conference on Developments in Power System Protection, 2014, pp. 1-5

[133] Voima, Sampo and Kauhaniemi, Kimmo.: 'Using Distance Protection in Smart Grid Environment', IEEE PES Innovative Smart Grid Technologies, 2014, pp. 1 – 6

[134] Voima, S. et al.: 'Adaptive Protection Scheme for Smart Grids', IET Conference Publications Developments in Power System Protection, 2014, pp. 1 – 6

[135] Lijuan, Jin. et al.: 'Fault Analysis of Microgrid and Adaptive Distance Protection based on Complex Wavelet Transform', IEEE International Power Electronics and Application Conference and Exposition, 2014, pp. 360 – 364

[136] Zamani, Amin. et al.: 'A Protection Strategy and Microprocessor-Based Relay for Low Voltage Microgrids', IEEE Transactions on Power Delivery, 2011, 26, (3), pp. 1873-1883

[137] Dang, Ke et al.: 'An Adaptive Protection Method for The Inverter Dominated Microgrid', IEEE Conference Publications Electrical Machines and Systems (ICEMS), 2011, pp. 1 – 5

[138] Jafari, Rahim. et al.: 'Compensation of DGs Impact on Overcurrent Protection System of Smart Micro-Grids', IET 22nd International Conference and Exhibition on Electricity Distribution, CIRED, 2013, pp. 1 – 4

[139] Islam, Md Razibul. and A. Gabbar, Hossam.: 'Analysis of Microgrid Protection Strategies', IEEE International Conference on Smart Grid Engineering (SGE), 2012, pp. 1 – 6

[140] Venkata, S. S. (Mani). et al.: 'Advanced and Adaptive Protection for Active Distribution Grid', IET 22nd International Conference and Exhibition on Electricity Distribution, 2013, pp. 1 – 4

[141] Haj-ahmed, Mohammed A. et al.: 'Investigation of Protection Schemes for Flexible Distribution of Energy and Storage Resources in an Industrial Microgrid', IEEE 50th Industrial & Commercial Power Systems Technical Conference, 2014, pp. 1 – 10

[142] Tummasit, N. et al.: 'Adaptive Overcurrent Protection Considering Critical Clearing Time for a Microgrid System', IEEE Conference Publications Smart Grid Technologies - Asia (ISGT ASIA), 2015, pp. 1 – 6

[143] Fan, Wenchao. et al.: 'Preliminary Study on Adaptive Fast-Tripping Current Protection for Microgrid', IEEE Conference Publications Smart Grid Technologies (ISGT ASIA), 2015, pp. 1 – 6

[144] Papaspiliotopoulos, Vasileios A.: 'Protection Coordination in Modern Distribution Grids Integrating Optimization Techniques with Adaptive Relay Setting', IEEE Conference Publications PowerTech, 2015, pp. 1 - 6

[145] Zeineldin, H. H.: 'Optimal Coordination of Microprocessor Based Directional Over Current Relay', IEEE Canadian Conference on Electrical and Computer Engineering, 2008, pp. 1-6

[146] Zeineldin, H. H.: et al.: 'Protective Relay Coordination for Micro-grid Operation Using Particle Swarm Optimization', IEEE Large Engineering Systems Conference on Power Engineering, 2006, pp. 152 - 157

[147] El-khattam, W. and Sidhu, T.S.: 'Resolving the Impact of Distributed Renewable Generation on Directional Overcurrent Relay Coordination: A Case Study', IET, Renewable Power Generation, 2009, 3, (4), pp. 415–425

[148] Noghabi, Abbas Saberi.: 'Considering Different Network Topologies in Optimal Overcurrent Relay Coordination Using a Hybrid GA', IEEE Transactions on Power Delivery, 2009, 24, (4), pp. 1857-1863

[149] Barzegari, Mostafa. et al.: 'Optimal Coordination of Directional Overcurrent Relays Using Harmony Search Algorithm', IEEE 9th International Conference on Environment and Electrical Engineering (EEEIC), 2010, pp. 321 – 324

[150] Qu, Haibo. et al.: 'MPSO based Protective Relay Coordination for Micro-grid', IET 10th IET International Conference on Developments in Power System Protection, 2010, pp. 1 – 5

[151] Damchi, Yaser. et al.: 'Optimal Coordination of Directional Overcurrent Relays in a Microgrid System Using a Hybrid Particle Swarm Optimization', IEEE, International Conference on Advanced Power System Automation and Protection (APAP), 2011, 2, pp. 1135 – 1138

[152] Sortomme, E. et al.: 'A Differential Zone Protection Scheme for Microgrids', IEEE, Power & Energy Society General Meeting, 2013, pp. 1-5

[153] Mirazimi, S. J. et al.: 'Optimal Relay Placement in Microgrids Considering Critical Clearing Time', IEEE 7th International Power Engineering and Optimization Conference, 2013, pp. 1-6

[154] Pandya, Hemang S. et al.: 'Digital Protection Strategy of Microgrid with Relay Time Grading Using Particle Swarm Optimization', IEEE 5th Nirma University International Conference on Engineering (NUiCONE), 2015, pp. 1-6

[155] Saleh, Khaled A. et al.: 'A New Protection Scheme Considering Fault Ride Through Requirements for Transmission Level Interconnected Wind Parks', IEEE, Transactions on Industrial Informatics, 2015, 11, (6), pp. 1324-1333

[156] Zeineldin, H. H. et al.: 'Optimal Protection Coordination for Meshed Distribution Systems with DG using Dual Setting Directional Over-Current Relays', IEEE Transactions on Smart Grid, 2015, 6, (1), pp. 115-123

[157] Ghanbari, Teymoor. and Farjah, Ebrahim.: 'Unidirectional Fault Current Limiter: An Efficient Interface Between the Microgrid and Main Network', IEEE Transactions on Power Systems, 2013, 28, (2), pp. 1591-1598

[158] Redfern, M.A. and AL-Nasseri, H.: 'Protection of Micro-Grids Dominated by Distributed Generation using Solid State Converters', IET 9th International Conference on Developments in Power System Protection, 2008, pp. 1-5

[159] Laaksonen, H., Hovila, P. and Kauhaniemi, K.: 'Combined Islanding Detection Scheme Utilising Active Network Management for Future Resilient Distribution Networks', IET The Journal of Engineering, 2018, (15), pp. 1054-1060

[160] Hoshino, T., Muta, I., Nakamura, T., Salim, K.M. and Yamada, M.: 'Non-Inductive Variable Reactor Design and Computer Simulation of Rectifier Type Superconducting Fault Current Limiter', IEEE Transactions on applied superconductivity, 15, (2), 2005, pp. 2063-2066

[161] Sato, T., Yamaguchi, M., Terashima, T., Fukui, S., Ogawa, J., Shimizu, H. and Sato, T.: 'Study on the Effect of Fault Current Limiter in Power System with Dispersed Generators', IEEE Transactions on applied superconductivity, 17, (2), 2007, pp. 2331-2334

[162] Lee, B.W., Park, K.B., Sim, J., Oh, I.S., Lee, H.G., Kim, H.R. and Hyun, O.B.: 'Design and Experiments of Novel Hybrid Type Superconducting Fault Current Limiters', IEEE Transactions on applied superconductivity, 18, (2), 2008, pp. 624-627

[163] Hagh, M.T. and Abapour, M.: 'Nonsuperconducting Fault Current Limiter with Controlling the Magnitudes of Fault Currents', IEEE Transactions on Power Electronics, 24, (3), 2009, pp. 613-619

[164] Ye, L. and Lin, L.Z.: 'Study of Superconducting Fault Current Limiters for System Integration of Wind Farms', IEEE Transactions on Applied Superconductivity, 2010, 20, (3), pp. 1233-1237

[165] Jo, H.C., Joo, S.K. and Lee, K.: 'Optimal Placement of Superconducting Fault Current Limiters (SFCLs) for Protection of an Electric Power System with Distributed Generations (DGs)', IEEE Transactions on Applied Superconductivity, 2012, 23, (3), pp. 1-4

[166] Kim, Y., Jo, H.C. and Joo, S.K.: 'Analysis of Impacts of Superconducting Fault Current Limiter (SFCL) Placement on Distributed Generation (DG) Expansion', IEEE Transactions on Applied Superconductivity, 2016, 26, (4), pp. 1-5

[167] Nazari-Heris, M., Nourmohamadi, H., Abapour, M. and Sabahi, M.: 'Multilevel Nonsuperconducting Fault Current Limiter: Analysis and Practical Feasibility', IEEE Transactions on Power Electronics, 2016, 32, (8), pp. 6059-6068

[168] Nourmohamadi, H., Nazari-Heris, M., Sabahi, M. and Abapour, M.: 'A Novel Structure for Bridge-Type Fault Current Limiter: Capacitor-Based Nonsuperconducting FCL', IEEE Transactions on Power Electronics, 2017, 33, (4), pp. 3044-3051

[169] Tseng, H.T., Jiang, W.Z. and Lai, J.S.: 'A Modified Bridge Switch-Type Flux-Coupling Nonsuperconducting Fault Current Limiter for Suppression of Fault Transients', IEEE Transactions on Power Delivery, 2018, 33, (6), pp. 2624-2633

[170] Farhadi, M. and Mohammed, O.A.: 'Event-based Protection Scheme for a Multiterminal Hybrid DC Power System', IEEE Transactions on Smart Grid, 2015, 6, (4), pp. 1658-1669

[171] Mirsaeidi, S., Dong, X., Shi, S. and Tzelepis, D.: 'Challenges, Advances and Future Directions in Protection of Hybrid AC/DC Microgrids', IET Renewable Power Generation, 2017, 11, (12), pp. 1495-1502

[172] Lee, H., Byeon, G.S., Jeon, J.H., Hussain, A., Kim, H.M., Rousis, A.O. and Strbac, G.: 'An energy management system with optimum reserve power procurement function for microgrid resilience improvement', IEEE Access, 2019, 7, pp.42577-42585

[173] Dai, Z., Liu, X., Zhang, C. and Zhu, H.: 'Protection SCHEMe for DC lines in AC/DC Hybrid Distribution Grids with MMCs', IEEE International Conference on Power System Technology (POWERCON), 2018, pp. 2518-2523

[174] Manohar, M., Koley, E. and Ghosh, S.: 'Stochastic Weather Modeling-based Protection Scheme for Hybrid PV–Wind System with Immunity Against Solar Irradiance and Wind Speed', IEEE Systems Journal, 2020, DOI. 10.1109/JSYST.2020.2964990, pp. 1-10

[175] Storn, R. and Price, K.: 'Differential Evolution a Simple and Efficient Heuristic for Global Optimization Over Continuous Spaces', J. Global Optim., 1997, 11, (4), pp. 341–359

[176] Qin, A., Huang, V. and Suganthan, P.: 'Differential Evolution Algorithm with Strategy Adaptation for Global Numerical Optimization', IEEE Trans. Evol. Comput., 2009, 13, (2), pp. 398–417

[177] Freris, L., Infield, D.: 'Renewable Energy in Power Systems' (John Wile & Sons Ltd, West Sussex, UK, 2008)

[178] Lopes, F.V., Lima, P., Ribeiro, J.P.G., Honorato, T.R., Silva, K.M., Leite, E.J.S., Neves, W.L.A. and Rocha, G.: 'Practical Methodology for Two-Terminal Traveling Wave-Based Fault Location Eliminating the need for Line Parameters and Time Synchronization', IEEE Transactions on Power Delivery, 2019, 34, (6), pp. 2123-2134

[179] Palizban, O., Kauhaniemi, K., Guerrero, J.: 'Microgrids in Active Network Management – Part II: System Operation, Power Quality and Protection', Renewable Sustainable Energy Rev., 2014, 36, pp. 440–451

[180] Bountouris, P., Guo, H., Tzelepis, D., Abdulhadi, I., Coffele, F. and Booth, C.: 'MV Faulted Section Location in Distribution Systems based on Unsynchronized LV Measurements', International Journal of Electrical Power & Energy Systems, 2020, 119, pp. 1-14

[181] Basso, T.S.: 'IEEE 1547 and 2030 Standards for Distributed Energy Resources Interconnection and Interoperability with the Electricity Grid' (National Renewable Energy Laboratory, 2014)

[182] IEEE Std 2030.9-2019, Guide for Smart Grid Interoperability of Energy Technology and Information Technology Operation with the Electric Power System (EPS), and End-Use Applications and Loads, http://grouper.ieee.org/groups/scc21/ dr_shared/2030/

List of Publications from Research Work

Science Citation Index (SCI) Publications:

1. Singh, Manjeet, and Basak, Prasenjit: 'Adaptive protection methodology in microgrid for fault location and nature detection using q0 components of fault current', IET Generation, Transmission & Distribution, 2018, 13, (6), pp. 760-769
2. Singh, Manjeet, and Basak, Prasenjit: 'Identification and nature detection of series and shunt faults in a type I, III and IV wind turbine and PV integrated hybrid microgrid with fuzzy logic based adaptive protection scheme', IET Generation, Transmission & Distribution, , 2020, 14, (22), pp. 4989-4999

Revision Submitted:

1. Singh, Manjeet, and Basak, Prasenjit: 'q component-based adaptive protection coordination optimization using overcurrent relays in coordination with fuses for hybrid microgrid', IET, Generation, Transmission & Distribution - **GTD-2020-09-0049**

Conference Publications:

1. Singh, Manjeet, and Basak, Prasenjit: 'Fractionalization of microgrid protection system through detection of zero sequence component of fault current', IEEE, 7th India international Conference on Power Electronics (IICPE), India, 2016, pp. 1-5
2. Singh, Manjeet, and Basak, Prasenjit: 'Behavior of fault current in microgrid systems', IEEE, 7th India International Conference on Power Electronics (IICPE), India, 2016, pp. 1-6
3. Singh, Manjeet, Kaur, Satripleen and Basak, Prasenjit: 'An approach to adaptive protection scheme for a PV generator based microgrid', IEEE, 4th International Conference on Smart and Sustainable Technologies (SpliTech), Croatia, 2019, pp. 1-6
4. Singh, Manjeet, and Basak, Prasenjit: 'Conceptualization of adaptive relaying in protection of hybrid microgrid through analysis of open and short circuit faults based on q0 components of fault current', IET Conference on Developments in Power System Protection Conference (DPSP), Liverpool, 2020, pp. 1-6